Department of Aeronautical Engineering

# Aerodynamic analysis and optimization of Low-speed wings

Report By

**Siddhartha Yadav**

Student Number:

**P2679201**

**Supervisor**

**Dr. Weigang Yao**

**May 2023**

## Contents

# LIST OF FIGURES

# LIST OF TABLES

## ABBREVATION

UAV = Unmanned Aerial Vehicle

UA = Unitary Authorise

CFD = Computational Fluid Dynamics

CATIA = Computer Aided Three-dimensional Interactive Application

MPC = Model Predictive Control

BWB = Blended Wing Body

FW = Flying Wings

VOLT = Vertical Take-off and landing

CAD = Computer Aided Drawing

BOI = Body of Influence

DMU = De Montfort University

3D = 3-Dimensional

UPS = United Parcel Service

RPS =Remotely Piloted Vehicles

UUA = Unitarian Universalist Association

NACA =  National Advisory Committee for Aeronautics

FEM = Finite Method Element

IMU = Initial Measurement Units

PID = Proportional Integral Derivative

Re = Reynold Number

## ACKNOWLEDGEMENT

First, I want to express my gratitude to Dr Weigang Yao, a senior lecturer at De Montfort University who served as my project mentor during my study and without whom I would not have been able to complete my master's degree. His expertise and experience in the field of aeronautical engineering are very helpful to me in the dissertation. He helped me analyse my dissertation project daily, and with the support of his well-thought-out work plan, I was able to finish it on schedule.

Second, I want to thank Abhijith Moni, a PhD student in aeronautical engineering at De Montfort University. He has rectified my report and assisted me with completing all my Ansys meshing findings and teach me how to use Ansys properly during my report.

Thirdly, I would like to thank Mrs Sue Shelton, a lab technician at De Montfort University, who assisted me in improving the design and taught me how to use the Solidworks programme properly. She assisted me in printing the aeroplane model and in setting up the right conditions for the aircraft's wind tunnel testing.

Finally, I am very much to thankful to my family and friends for their unwavering love and support throughout the endeavour, especially my friend Dr Romi Yadav.

## ABSTRACT

The aviation industry has been constantly developing new and powerful aircraft. Since the recent improvement of more powerful engines as well as enhancement in the aerodynamic properties flight speed has been faster day by day. Especially, an introduction of jet engines and sweptback wings has made it feasible to achieve more speed than that of sound to the aircraft. The flow phenomena will occur depending significantly on this sonic speed, which is the rate at which very minor atmospheric pressure perturbations spread. All flow velocities around the aircraft are considerably slower than the speed of sound when travelling at low speeds.[1]

The study primarily discusses the choice, design, and FEM (Finite Method Analysis) of low-speed aircraft. The introduction of the aircraft and its brief history is covered in the first portion of the report. This is followed by a background section outlining the report's correct goal and objective. Similarly, to that, it gives the reader a solid basis so they can comprehend the goal of the entire investigation.

The result of Ansys' analysis is presented in the second section of the report. The model is similarly sent through the programme before receiving specific boundary conditions, which allow for the right set and solution to be provided. Similar testing is conducted on the model in the De Montfort University lab's wind tunnel. Finally, the study compares and discusses the findings of both the software and wind tunnel tests.



**Keywords: powerful aircraft, sweptback wings, choice, design, FEM (Finite Method Analysis), low-speed aircraft, Ansys' analysis, wind tunnel tests**

# CHAPTER-1

## 1. INTRODUCTION

From the 1920s, there are a lot of new development in the aircraft industry, many more models were introduced and most of them failed due to improper design. The following paper, the Skywalker X8 aircraft is covered with the proper selection of the airfoil and then it is designed in the Solidworks software. The Skywalker X8 aircraft with a wing size of 2.12 m, a payload of 1-3 kg and a weight is around 0.88 kg. After the design is made in the Solidworks software**,** then it is imported Ansys software for pre-processing. The paper presents the actual layout of the Skywalker X8 aircraft with proper load and performance analysis with the help of software as well as checking of static and dynamic stability of the aircraft. Furthermore, the design is imported to Prusa software for 3D Printing and then the model is tested in the wind tunnel of De Montfort University Aerodynamic lab.

During the research, they are a lot of challenges occurred. Firstly, the design selection was quite a hard task as it should fit in the wind tunnel for testing. With reference to different research, the design was developed in Solidworks. Secondly, for pre-processing in Ansys, the Solidworks file should be **.x_t** which provides proper geometry to the software. Thirdly, proper meshing in the Ansys software was a difficult task as there are around 40000 K nodes which takes longer and a higher system for getting mesh. Fourthly, the wind tunnel set-up was hard to arrange along with the noise and disturbance of the wind tunnel create some problems in the testing.

Despite these difficulties, the model was prepared with the above-given dimensions in Solidworks and then pre-processing is done in Ansys. The primary aim of the project is to design low-speed wing aircraft and calculate the physical properties like lift, drag, velocity, and angle of attack in Ansys. Similarly, the wind tunnel test in done whose results are compared with the Ansys post-processing results. Likewise, the objective of the research is to develop the proper low-speed aircraft to check its suitability for mapping. Similarly, the suitable airfoil is selected for Skywalker X8 i.e., **NACA 0009** so that proper lift and drag factors can be obtained and the software model is prepared for wind tunnel testing to get proper results.

The aim and objectives are properly covered in the research paper. Similarly, the layout of the research paper contains a brief description of the introduction, proper literature review, methodology, software analysis, wind tunnel testing, results and discussion, conclusion, and finally future scope.

## 1.1. Background

UAVs (Unmanned Arial vehicles) are aircraft where no humans on board and are operated by humans through robots with the help of an external power supply. The first human-less aircraft was designed by Britain and UUA during World War 1. [2] The gradual development of the UAV started then with the development of new advancements in technologies. The recent Global market is about USD 26.2 billion in 2022 and it will reach up to USD 38.3 billion by 2027 [3].

UAVs are either automatic or semi-automatic and is generally controlled by the remote or partially by a human with different electronic intelligence components and control system. Similarly, pilotless aircraft are divided into three types of UAV (Unmanned Arial vehicles), Remotely Piloted Vehicles (RPVs) and drones. Similarly, UAVs are divided into three categories based on their sizes i.e., small, medium, and large UAVs.

In this paper, small UAVs have been discussed with proper calculation and testing. Usually, the small UAV is greater than 50 cm and it can go up to two to three meters [4]. Several of these UAVs are hand-launched by their worker by being thrown into the air similarly to how we launch a toy glider. They have the design of a fixed-wing model aeroplane. Skywalker is a small UAV, and the description is given in Table 1.

| | |
|---|---|
| Wingspan | 2.12 m |
| Speed of Cruise | 15-30 m/s |
| Area of wing | 0.8 m2 |
| Pay Load | 1-2 kg |
| Weight | 0.89 kg |

Table 1 Description of Skywalker X8

Advancement in technologies and introduction of the new features in the UAV has made it possible to use it in different fields. Some of them are.

- Military
- Delivery
- Emergency rescue
- Agricultural
- Space Research
- Medical Sector
- 3D Mapping

- Aerial Photography

UAVs are typically self-flying UAVs that deliver food, packages, or other items to the door. In place of using supply drivers with ineffective trucks, dealers and grocery chains across the nation are switching to unmanned aerial vehicles (UAVs. Numerous major corporations, including Amazon, Walmart, Google, FedEx, UPS, and others are discovering various reiterations of delivery drones. [5]

UAVs have demonstrated their value to the agricultural sector as well, giving farmers a number of options to optimise their land for maximum output and minimal animal effort. UAVs make it easier to do field surveys, seed over fields, track livestock and estimation agricultural manufacture while also saving agriculture workers principal time. LiDAR sensors, which survey landscapes and gather detailed data that may be used to create 3D models, are equipped with LiDAR UAVs. Data from drones using LiDAR technology is much more accurate than data from drones without it. LiDAR helps drones to recognise targets in search and rescue missions, assess crops in agriculture, and more in addition to making it simpler for them to navigate different surfaces. [5]

Similarly, to this, UAVs have benefited photographers who use them to capture vast aerial photographs.  They are designed especially for photography and offer a novel way to capture some of your favourite locations from above.

## 1.2. Research Aim, Objective

### 1.2.1 AIM

The research target is to develop Skywalker X8 in Solidworks software then analysis in Ansys and the final test in the wind tunnel test.

### 1.2.2 OBJECTIVE

- To find out accurate and realistic Skywalker X8 mathematical model along with the flight stability and control.
- To calculate and verify the theoretical and numerical analysis of Skywalker X8 in software to get proper results.
- To evaluate Skywalker X8 flight stability, lift-coefficient, and drag-coefficient to match previous research.

- To produce a 3D simulation of the Skywalker X8 in the DMU lab and make it ready for wind tunnel experiment.
- To test the model in the wind tunnel and calculate the lift, drag and angle of attack of the Skywalker X8.

### 1.3 Significance of the research

This study is going to contribute to the area of developing software models for further research. The proper and fine meshing of the model gives accurate results and 2500 iterations in the solution part provide more nearby value of the model.

Hence, the calculation done by the model in the software and the calculation done in the wind tunnel should have a nearby value for accurate flight stability to the Skywalker X8.

### 1.4 Limitation

During the research, a lot of hurdles come along the way. While creating modelling, it is very difficult to select the dimensions whereas it was challenging to select the airfoil. Likewise, importing the model in Ansys from Solidworks, and selecting the proper file was challenging. Adding **BOI is a new technique** and quite confusing as enough resources were not provided in any of the previous research.

Lack of enough research papers, equipment, and time some of the calculations might be not done in this research.

### 1.5 Structure Outline

The report is divided into 7 main chapters. Chapter 1 contains an Introduction where the project's brief history and discussions are provided. Chapter 2 is about Literature Review were previous research papers with proper gaps and suggestions. The methodology is about the selection of design, development of CAD model, and FEA analysis along with the results in Chapter 3. Similarly, wind tunnel testing, Discussion and Critical Analysis, Conclusion, and recommendation if in Chapters 4,5,6 and 7 respectively.

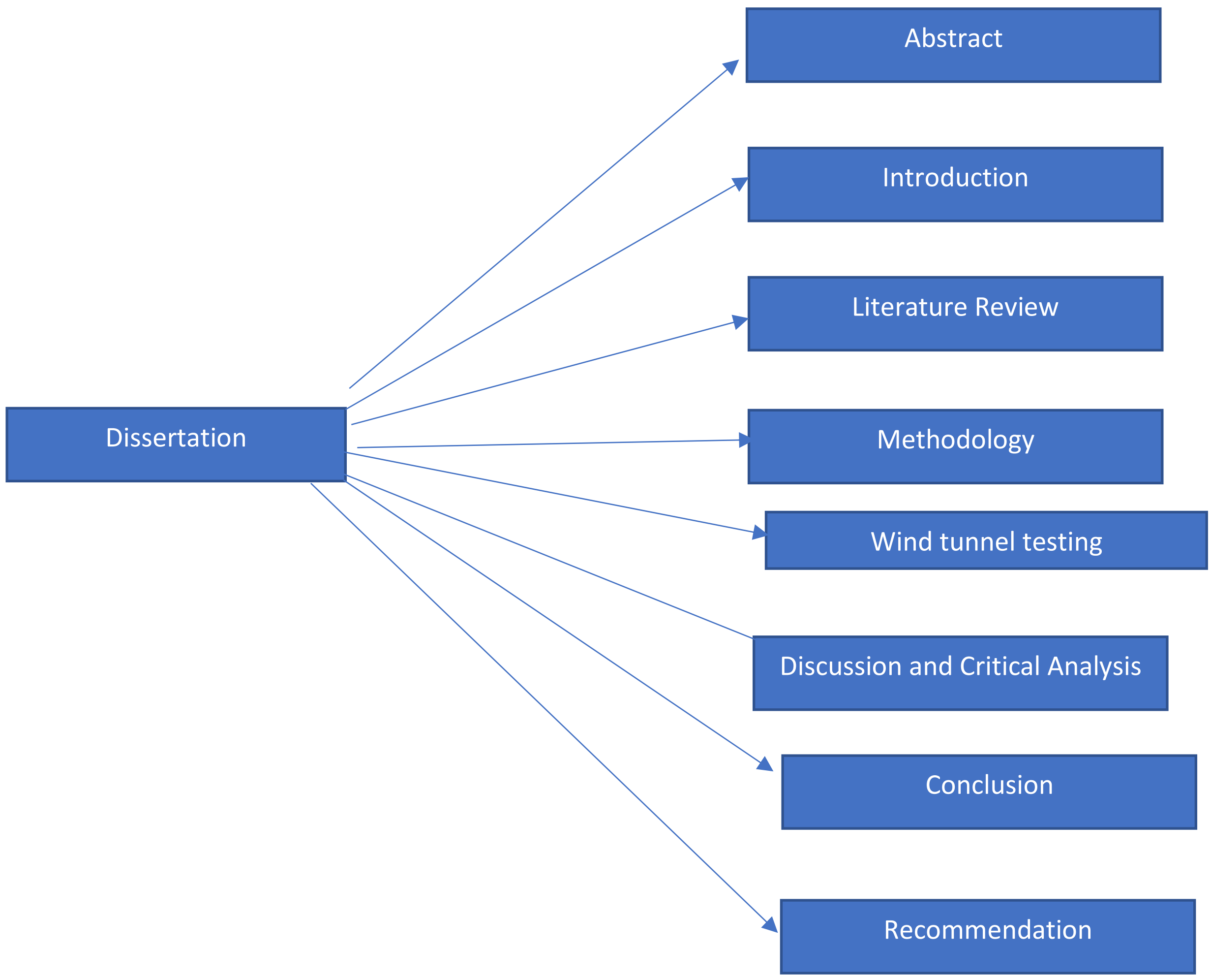


Figure 1 Structure outline of the report

# CHAPTER-2

## 2. LITERATURE REVIEW

### 2.1 Introduction

The sources review shows the design and development of the Skywalkers X8 and then analysed in the Ansys for lift-coefficient, drag-coefficient, and other results. Similarly, the models were prepared in 3D printing, and they were tested in a wind tunnel. In some of the papers, researchers tested the model and found that the Skywalkers X8 load of 4-5 kg with 2.5 wings design is capable of 40-50 minutes of flight in the air. The literature review contains a review paper between 2010-2022. It is found that some of the researchers had created code for the Skywalkers X8 aircraft in MATLAB and then tested the graph. Overall, it is still unknown which software analysis is the best for the Skywalkers X8.

### 2.2 Conceptual Design

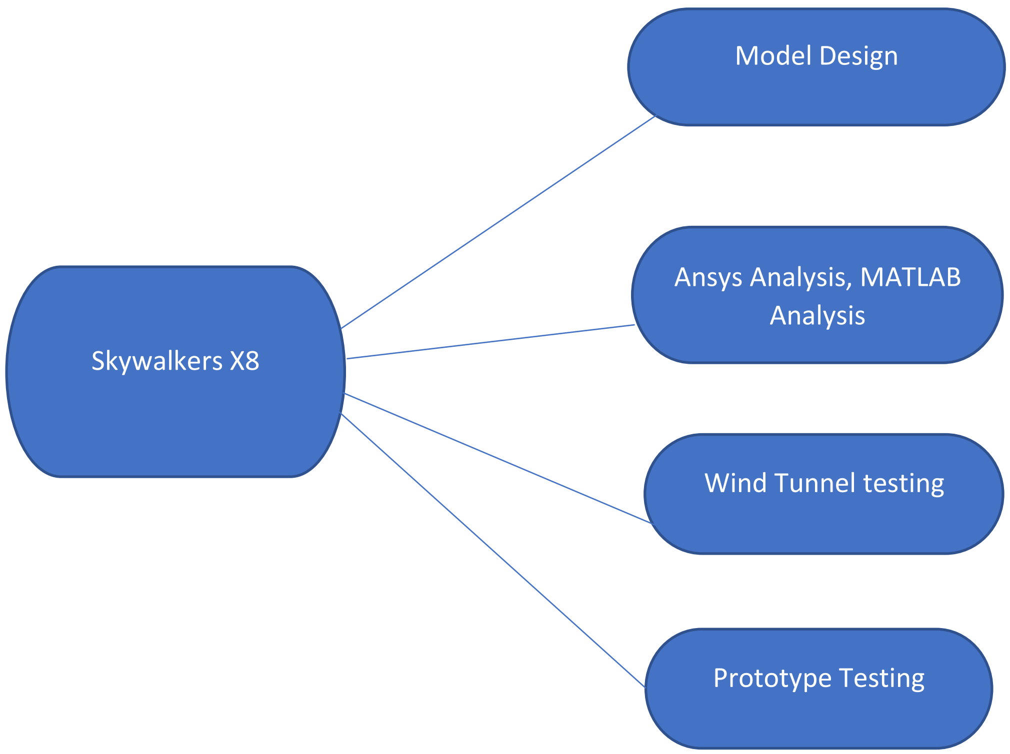


Figure 2 Conceptual work done by the researcher.

## 2.3 Pivotal Study

Skywalkers X8 is Vertical Take-off and landing (VTOL) aircraft which is designed for geographical, agricultural, and medical purposes. This aircraft is used for a short duration. Different researchers have published their ideas on Skywalkers X8.

## 2.4 Theories and model

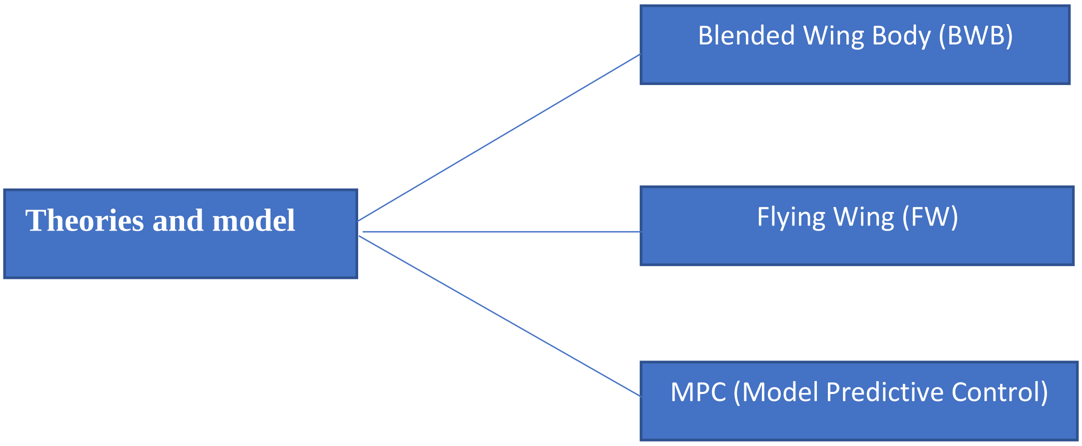


Figure 3 Conceptual theories and models by researchers

### 2.4.1 Blended Wing Body (BWB)

The aircraft with Blended Wing Body (BWB) is stable and easy to control [14]. The aircraft is examined and the function of flight, as well as design parameters, is considered to test the stability of longitudinal and lateral directions. In comparison to traditional aircraft, BWB aircraft have a larger payload capacity for the transportation of people and/or goods without having a larger ground footprint, presenting them matching with current transportation. Additionally, the larger lifting plane area yet. [16,17]

The lift-to-drag ratio rises when the total saturated area is diminished. Additionally, interference and pressure/form drag are both reduced by the streamlined geometry, which lowers fuel consumption.[18]

### 2.4.2 MPC (Model Predictive Control)

The accurate model of the aircraft is useful in the calculation of the perfect motion. Model Predictive Control (MPC), which uses the simulation to anticipate the UAV's response, enables the controller to achieve the control target with the least amount of control input possible.

Like how aerodynamic models are worked to predict the angle of attack and side-slip angle of a UAV utilised in deep stall landing, model-based estimation depends on a UAV model to propagate the estimates forward in time.

## 2.3 Review from previous work

### 2.3.1 Paper 1

**Summary:** The flying wing concept aircraft's actual layout is presented in this paper along with the project's loading, performance, software, static and dynamic stability check. It also includes the actual construction layout with any challenges that may arise, as well as the analytical process used to decide how the predicted design should be changed to better meet the requirements. **(Anug et al., 2019)**

Additionally, the expected design's performance analysis, loading impacts, static stability checks, and dynamic stability checks are calculated manually, using Microsoft Excel, and using MATLAB software. The "ANSYS FLUENT 19" software examines FEE - 004's static structural deformation and stability analysis to see whether there are any concerns. The expected design is then developed in detail using AutoCAD and Solidwork Software.

**[ Referred to Appendix 11]**

### 2.3.2 Paper 2

**Summary:** In the paper, a fixed wing for an UA aircraft that would function as a multifunctional utility tool is designed and analysed. The fixed-wing kind of UAV is chosen by the researchers because it can be used for a variety of reasons, and XFLR5 was used to compare several common aerofoils to find the optimum one. The wings of the model were created using Solid Works software using the chosen aerofoil. The final 3-dimensional model was created using a standard fuselage that was put together with designed wings using CATIA software. Using boundary conditions, one-half of the completed model was tested in a wind tunnel before being submitted to CFD analysis. **(Karthik et at., 2017)**

The CFD analysis produced favourable results for the model. To further discover the model's fundamental frequency, modal and structural analyses were used for the model. When compared to commercially available models, the developed model is more aerodynamically stable. The researchers selected two models in their report eBee and Skywalkers X8 as both have the same working principles. **[Referred to Appendix 18]**

| | eBee | Sky walker X8 |
|---|---|---|
| 1. Wing span | 0.96m | 2.12m |
| 2.Cruise speed | 11-25 $ms^{-1}$ | 15.27-30.556$ms^{-1}$ |
| 3.Wing area | 0.5$m^2$ | 0.8$m^2$ |
| 4.Pay load | Approx. 1.5kg | 1-2 kg |
| 5.Weight | 0.71kg | 0.88kg |

Table 2 Comparison between eBee and Skywalker X8

**(Source: Karthik et al, 2017)**

### 2.3.3 Paper 3

**Summary:** To develop an aerodynamic model of the Skywalker X8 aircraft, this article suggests combining wind-tunnel tests and flight experiments. A sparse damping model that discovers using flight test data and a serially threshold minimum squares approach is added to the static coefficients obtained from wind-tunnel experiments. The baseline model from the experiments has seen a major upgrade. **(Drik R., et at, 2022).**

The researcher performed automatic validation of the recognised models against the recorded wind tunnel data, yielding a favourable coefficient of determination scores that were extremely close to 1. When they contrast the accelerations determined by the force model with the performances established on flight data from Inertial Measurement Units (IMUs), the resulting score is even negative.

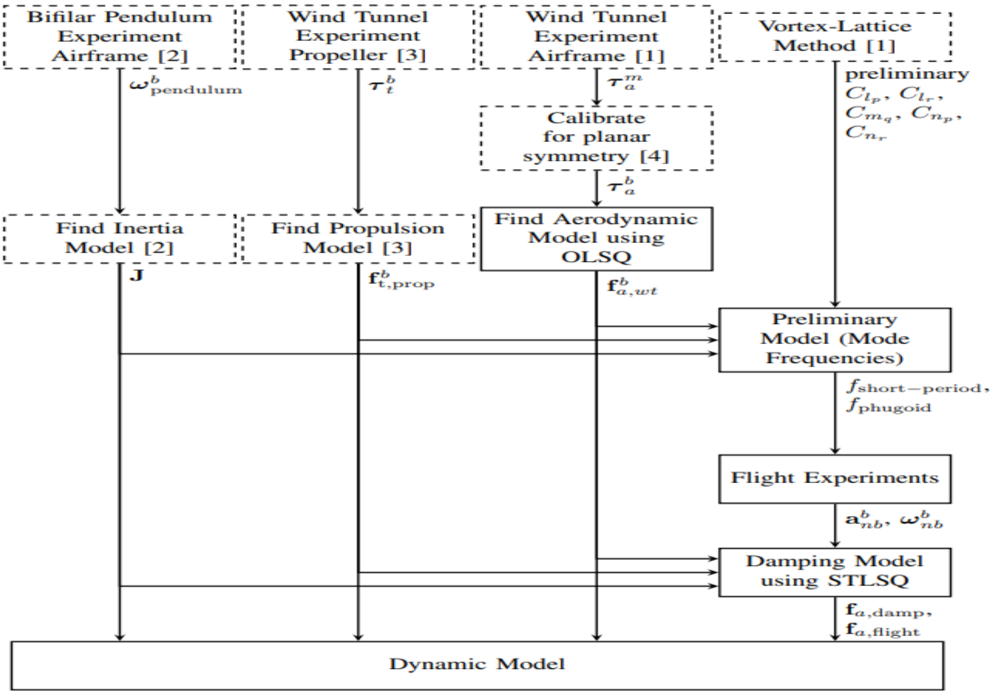


Figure 4 Working model of the Skywalker X8

**(Source: Drik R., et at, 2022)**

In the model, the occurrence point of the force vector's attack lever arm is implicit. As an alternative, they explicitly simulate the generalised forces at the aerodynamic reference point, the location of the force sensors throughout the tests, and the vector to the centre of mass using flight data. Second, they examine the portion of the data appropriate for finding aerodynamic linear coefficients associated with the side-slip angle in greater detail. Additionally, they simplify the drag model while also enhancing its fitness. the parameters determined by the wind tunnel, the outcomes of the Vortex-Lattice method (XFLR), and manual adjustments to the constraints based on knowledge gained from aircraft tests. **[ Referred to Appendix 8].**

### 2.3.4 Paper 4

**Summary:** In the study, stability, and control products of the Skywalker X8 aircraft, flight-test results are evaluated using the end product error and least square methods in conjunction with wind. To identify dynamic system of an unmanned aerial vehicle (UAV), data are gathered from padlocked-loop flight experiments with a proportional-integral-derivative (PID) controller that generated issues with data co-linearity. **(R. Mohammadi F, et al. 2018)**

By using the following techniques, one can determine a UAV's aerodynamic properties:

- wind tunnel testing,
- computational approaches,

- Using flight test data that identify the UAV dynamic system.

| Parameter | | | ZFW | SX8FW |
|---|---|---|---|---|
| Mass | $m$ | kg | 1.56 | 4.5 |
| Moment of inertia | $J_x$ | $\mathrm{kg\,m^2}$ | 0.1147 | 0.45 |
| Moment of inertia | $J_y$ | $\mathrm{kg\,m^2}$ | 0.0576 | 0.325 |
| Moment of inertia | $J_z$ | $\mathrm{kg\,m^2}$ | 0.1712 | 0.75 |
| Moment of inertia | $J_{xz}$ | $\mathrm{kg\,m^2}$ | 0.0015 | 0.06 |
| Wing area | $S$ | $\mathrm{m^2}$ | 0.2589 | 0.75 |
| Wing span | $b$ | m | 1.4224 | 2.12 |
| Mean aerodynamic chord | $c$ | m | 0.3302 | 0.3571 |
| Propeller area | $S_{\mathrm{prop}}$ | $\mathrm{m^2}$ | 0.0314 | 0.1018 |
| Air density | $\varrho$ | $\mathrm{kg/m^3}$ | 1.2682 | 1.2682 |
| Motor constant | $K_{\mathrm{motor}}$ | – | 20 | 40 |
| Propeller aerodynamic coefficient | $C_{\mathrm{prop}}$ | – | 1 | 0.5 |

Table 3 Airframe parameters of ZEW and Skywalker X8

**(Source. R. Mohammadi F, et al. 2018)**

As a result, linear models are created for the Zagi, Skywalker X8, and Aerosonde UAVs in the nonlinear simulation. For the linear standard models to estimate the aerodynamic parameters, the provided approaches are put into practice and validated. The Skywalker X8 flying wing's (SX8FW) aerodynamic coefficients are then estimated using a combination of these approaches using actual flight test data. **[ Referred to Appendix 10].**

### 2.3.5 Paper 5

**Summary:** This study analyses two popular methods for creating such aircraft , theoretical design tools, and wind tunnel testing, by outlining their benefits and probable drawbacks in a "experiences learned" fashion. An aerodynamic model with 6-degrees of freedom of the Skywalker X8 aircraft is described throughout the paper as a case study. **(Gryte, K, 2019)**

It is a well-known field to utilise numerical models to describe the motion of low-speed aircraft. A mathematical description of the motion of the aeroplane is beneficial for numerous reasons.

| | WT | XFLR5 | RMSE | $R^2$ |
|---|---|---|---|---|
| $C_{L_0}$ | 0.0867 | 0.0477 | 0.0153 | 0.996 |
| $C_{L_\alpha}$ | 4.02 | 4.06 | 0.0153 | 0.996 |
| $C_{L_{\delta_e}}$ | 0.278 | 0.7 | 0.0153 | 0.996 |
| $C_{L_q}$ | — | 3.87 | — | — |
| $C_{D_0}$ | 0.0197 | 0.0107 | 0.00262 | 0.982 |
| $C_{D_{\alpha 1}}$ | 0.0791 | $-0.00955$ | 0.00262 | 0.982 |
| $C_{D_{\alpha 2}}$ | 1.06 | 1.1 | 0.00262 | 0.982 |
| $C_{D_{\delta_e}}$ | 0.0633 | 0.0196 | 0.00262 | 0.982 |
| $C_{D_{\beta_2}}$ | 0.148 | 0.115 | 0.00234 | 0.734 |
| $C_{D_{\beta_1}}$ | $-0.00584$ | $-2.34E-19$ | 0.00234 | 0.734 |
| $C_{m_0}$ | 0.0302 | 0.00439 | 0.00576 | 0.983 |
| $C_{m_\alpha}$ | $-0.126$ | $-0.227$ | 0.00576 | 0.983 |
| $C_{m_{\delta_e}}$ | $-0.206$ | $-0.325$ | 0.00576 | 0.983 |
| $C_{m_q}$ | — | $-1.3$ | — | — |
| $C_{Y_0}$ | 0.00316 | $1.08E-08$ | 0.00326 | 0.991 |
| $C_{Y_\beta}$ | $-0.224$ | $-0.194$ | 0.00326 | 0.991 |
| $C_{Y_{\delta_a}}$ | 0.0433 | 0.0439 | 0.00326 | 0.991 |
| $C_{Y_p}$ | — | $-0.137$ | — | — |
| $C_{Y_r}$ | — | 0.0839 | — | — |
| $C_{l_0}$ | 0.00413 | $1.29E-07$ | 0.00476 | 0.953 |
| $C_{l_\beta}$ | $-0.0849$ | $-0.0751$ | 0.00476 | 0.953 |
| $C_{l_{\delta_a}}$ | 0.12 | 0.202 | 0.00476 | 0.953 |
| $C_{l_p}$ | — | $-0.404$ | — | — |
| $C_{l_r}$ | — | 0.0555 | — | — |
| $C_{n_0}$ | $-0.000471$ | $1.51E-07$ | 0.000615 | 0.98 |
| $C_{n_\beta}$ | 0.0283 | 0.0312 | 0.000615 | 0.98 |
| $C_{n_{\delta_a}}$ | $-0.00339$ | $-0.00628$ | 0.000615 | 0.98 |
| $C_{n_p}$ | — | 0.00437 | — | — |
| $C_{n_r}$ | — | $-0.012$ | — | — |

Table 4 Aerodynamic coefficient of Skywalkers X8

**(Source: Gryte, K, 2019)**

The model's accuracy imposes restrictions on the tests' application, though. Model-based control techniques require an accurate mathematical description of an unmanned aerial vehicle (UAV). Model predictive control (MPC) is a technique used in deep stall landing where the model is used to reduce the amount of control input required to achieve the control target. A UAV model is also used in model-based estimating to propagate estimates forward in time where the angle of attack and side-slip angle of a UAV is estimated using aerodynamic models. To organise the wind tunnel tests and develop an aerodynamic model, in-depth aerodynamic knowledge is required. **[ Referred to Appendix 13].**

## 2.4 Critical Evaluation

In recent days, UAVs are made more efficient to carry out various tasks like surveying, military operations, aerial mapping, rescue operations and other various purposes. [19] In this report, decided to select low-speed aircraft i.e., Skywalkers X8. In the beginning, it was difficult to select the software to design the aircraft.

So, as per the previous paper, **Solidworks** was selected. Similarly, the selection of the wing was one of the difficult tasks so various observations and research, 5 of the airfoils were selected **NACA 4412, 0009, MH60, MH45 and 5510**. All these airfoils were subjected to **XFLR5** software to compare their characteristics of them. Likewise, with proper **Cd** and **Cl** values, **NACA 0009** was decided to use in the aircraft and designed in the Solidworks.

**Karthik et al, 2017** mentioned that selecting the **half model of the aircraft** model gives proper results in CFD analysis as well as **the handling time** and power required for the calculation of the aircraft model will be **fast and more accurate**. [11] So, half of the model was subjected to Ansys software for **meshing and post-processing.** Firstly, the **enclosure** was made with **50 times** the **length of the wings** for proper analysis of the aircraft. Secondly, meshing is done with small possible elements i.e., $\mathbf{10^6}$ to make the UAV smooth for further calculation. Finally, the post-processing is done with the proper result.

**Farhadi et al.** Using aircraft data and a mix of the output-error approach and normal least squares regression, establish a lateral model of the **X8** whereas **Khouli et al.** determine the **static aerodynamic coefficients** using a computational fluid dynamics (CFD) programme that uses **Reynolds-averaged Navier-Stokes (RANS). R. Hann et al.** also offer a RANS CFD analysis and further investigate the impact of ice aggregation on the aerofoil's dynamic coefficients using time-series CFD simulations. **K. Gryte at al.** By utilising the existing wind tunnel data, improve the aerodynamic model proposed in the baseline model. Instead of using the **Vortex-Lattice approach,** which was previously used to discover the dynamic coefficients, they alter the data to increase its planar symmetry. **Aung L. et al.** found that the aircraft is statically stable with the help of **longitudinal, lateral, and directional stability.** According to them, the **pitching moment curve** is downward which gives a positive pitching moment which measures the control derivative of the **flying wing**.

## 2.5 Theory

In previous work, **XFLR5, MATLAB and Ansys software** analysis is done, and the papers were published based on their results. In some papers, researchers tested the models in the wind tunnel and then compared the results with the software analysis. The **lift coefficient, drag coefficient and angle of attack** are properly measured as **flight stability, static and dynamic stability. [6]**

But in earlier works, the **BOI (Body of Influence)** was not introduced to the geometry. In **Ansys Fluent Meshing**, BOI is a component of the **'Add local Sizing'** operation. To have a specific impact on the size of the volume mesh inside a domain, **BOI** is employed with closed 3D bodies and open surfaces. The mesh region that lies within the **BOI**'s boundary has a maximum cell size. The final computational model will not include the meshes that the BOI specify should be improved. [6]

## 2.6 Synthesis

By making the appropriate modifications, BOI (Body of Influence) aids in the resolution of issues like wakes, shear layers, and areas with significant velocity gradients in the field. The CAD model, in addition to the enclosure and BOI, can be included in the computation to aid divide velocity, sharing layers, and producing accurate meshing results. When geometry first meshed for the research, it was done without BOI and the mesh wasn't right; however, once BOI was added, the mesh was right. [6]

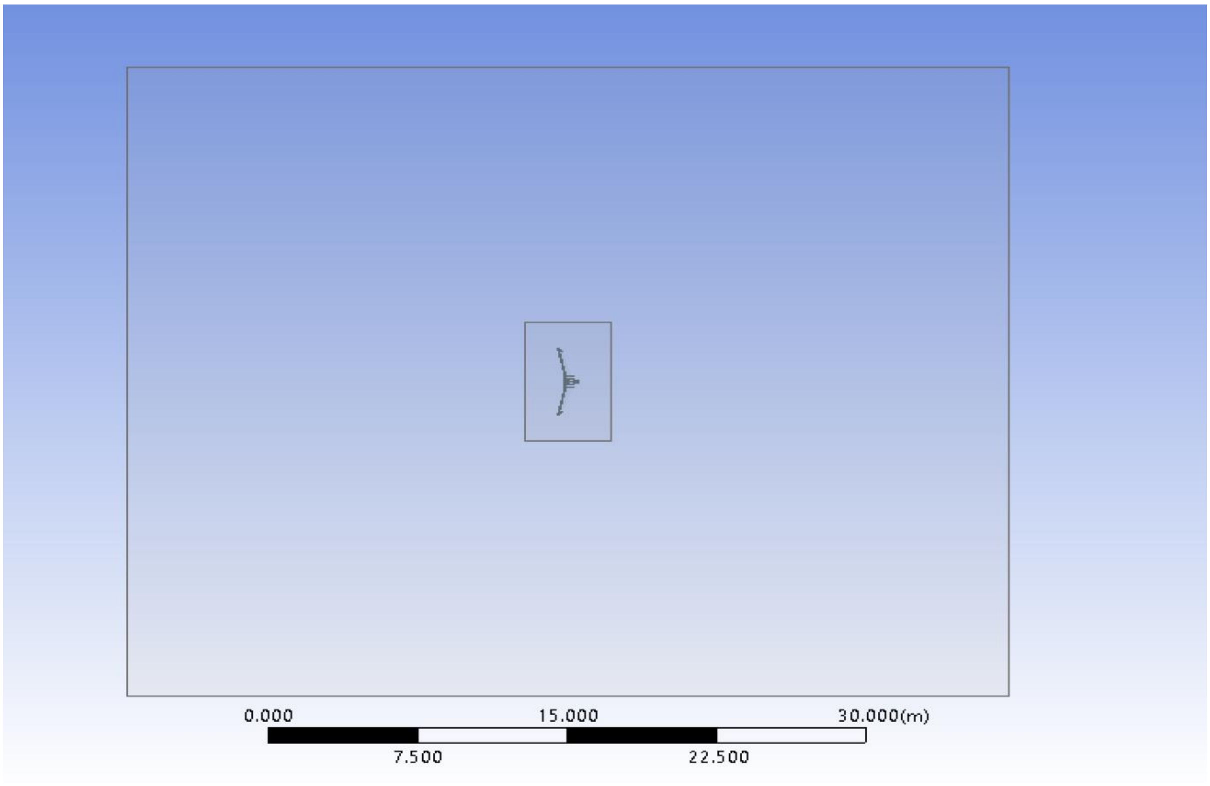


Figure 5 Geometry inside the enclosure with BOI (Body of Influence)

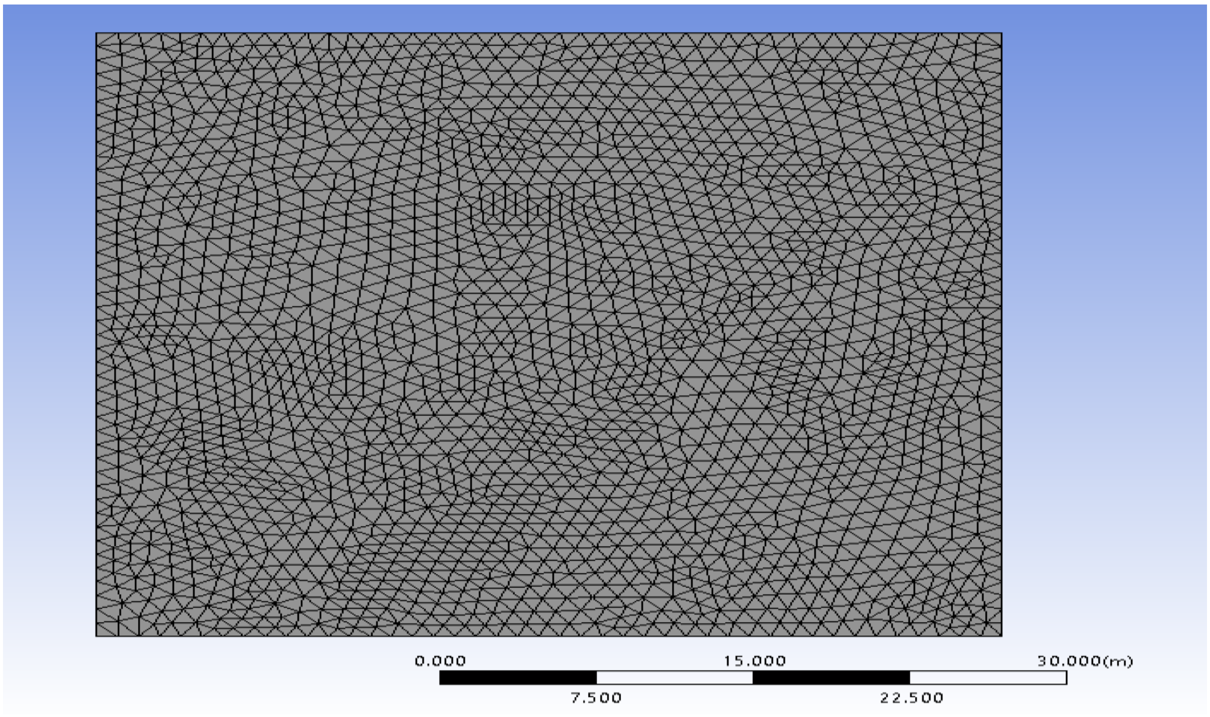


Figure 6 Mesh with BOI ((Body of Influence))

## 2.7 Gap

The research mainly focuses on the analysis of the Skywalkers X8 aircraft on software and in the wind tunnel. Here, different wings are properly analysed and then use in the aircraft to reduce any kind of lift and drag issue after manufacturing.

CFD and/or wind tunnel testing can be used to acquire precise estimates for the lateral aerodynamic derivatives. CAD tools like Ansys can be used to obtain refined inertia tensor values.[14] Latitudinal and lateral control are coupled because there are only 2 elevons. The flight model might therefore be enhanced to combine longitudinal and lateral motions, permitting the inclusion of gyroscopic phenomena, which have inherent longitudinal-lateral coupling. The aircraft model needs to be improved to take structural flexibility into account after modes analysis.[16]

Therefore, more research might involve measuring the pressure on the wing in a test tunnel or looking at the buckling stress to determine whether the wing collapses because of the pressure. An additional study might be done on alternative lightweight materials, such as basic wood, plastics, or another composite, possibly in conjunction with sandwich constructions. [18]

# CHAPTER-3

## 3. METHODOLOGY

### 3.1 Selection of design

There are several obstacles to choosing the aeroplane at the start of the project. Many different aeroplane types have been my goals. The project supervisor and I discussed the models before choosing the final design. The aeroplane is built after the design is Solidworks-approved.

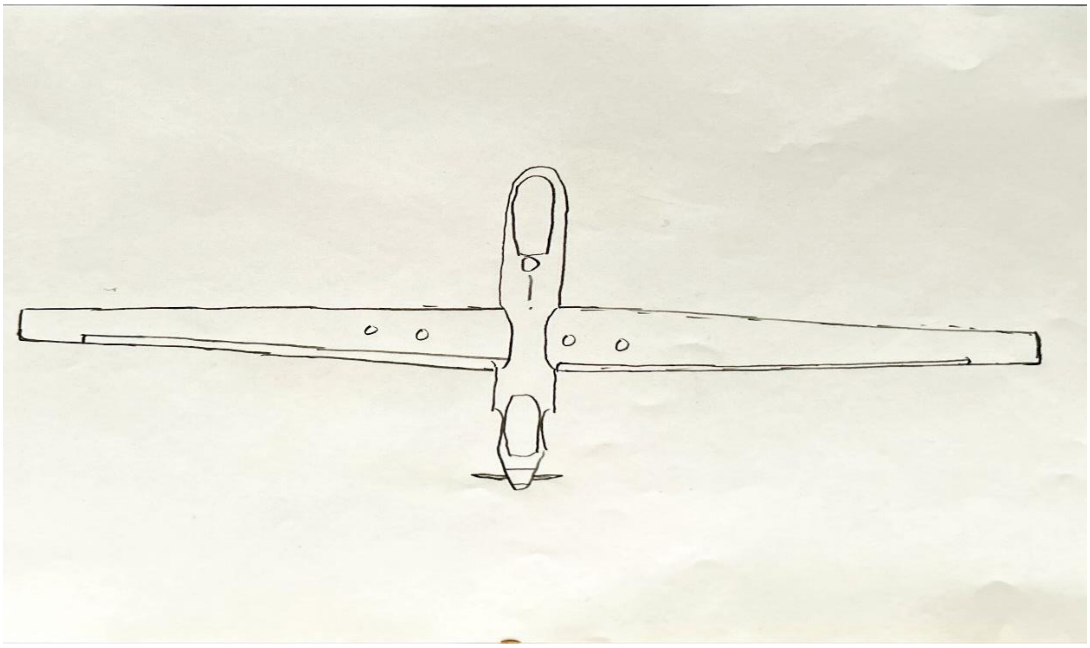

Figure 7 Short Tucano 1.0

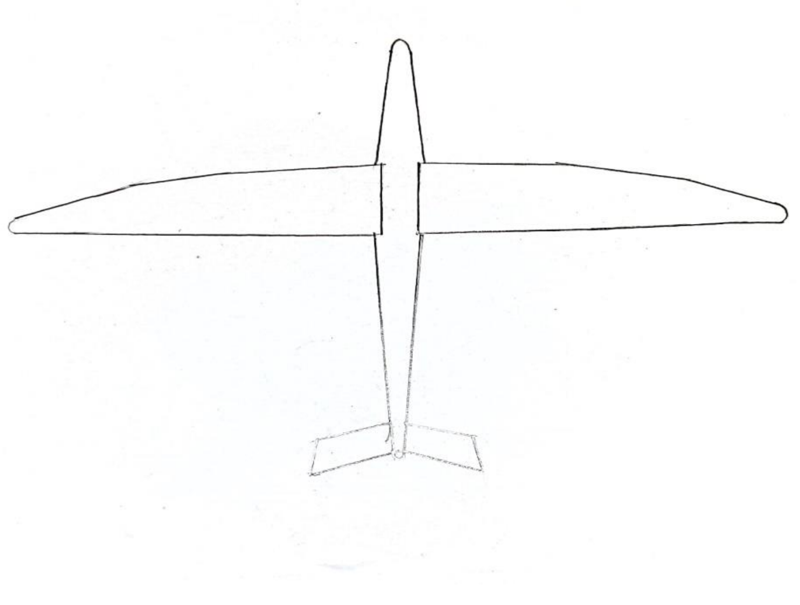

Figure 8 Atom 7

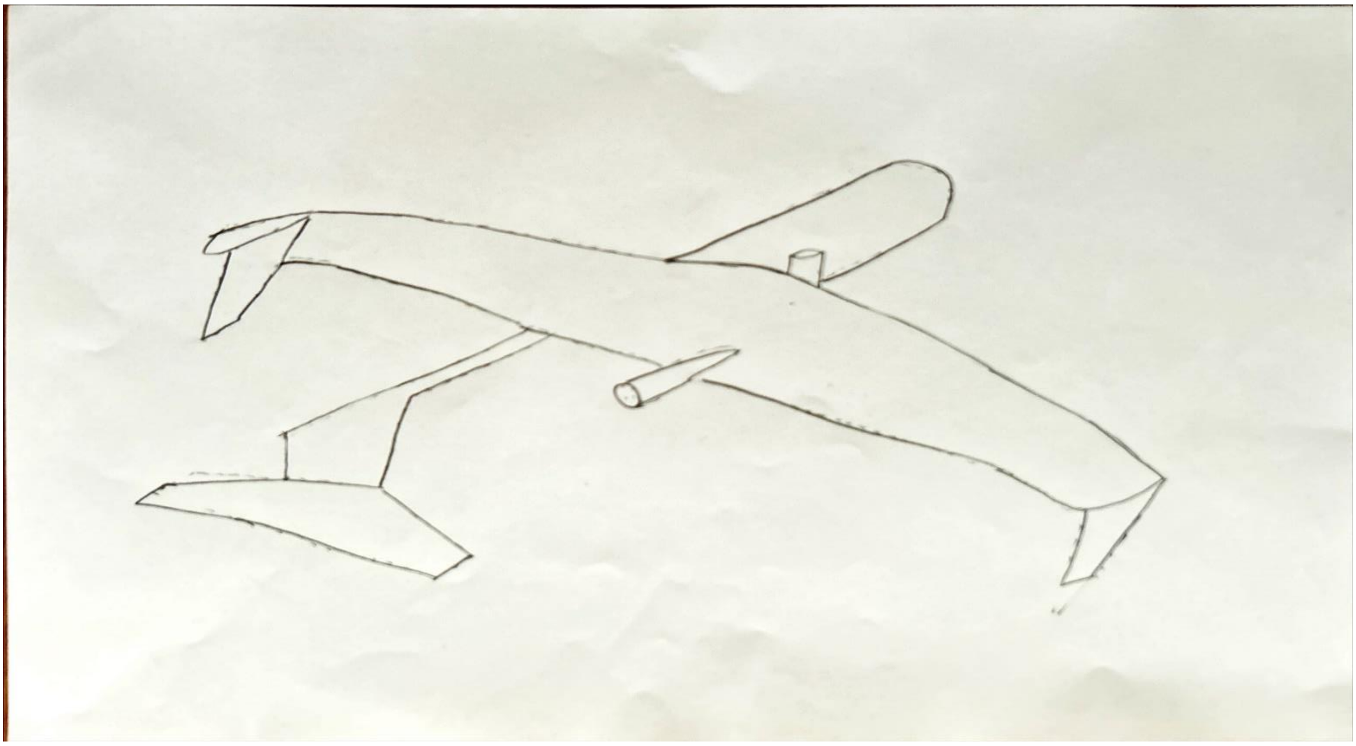

Figure 9 Cessna 172 Skyhawk 100

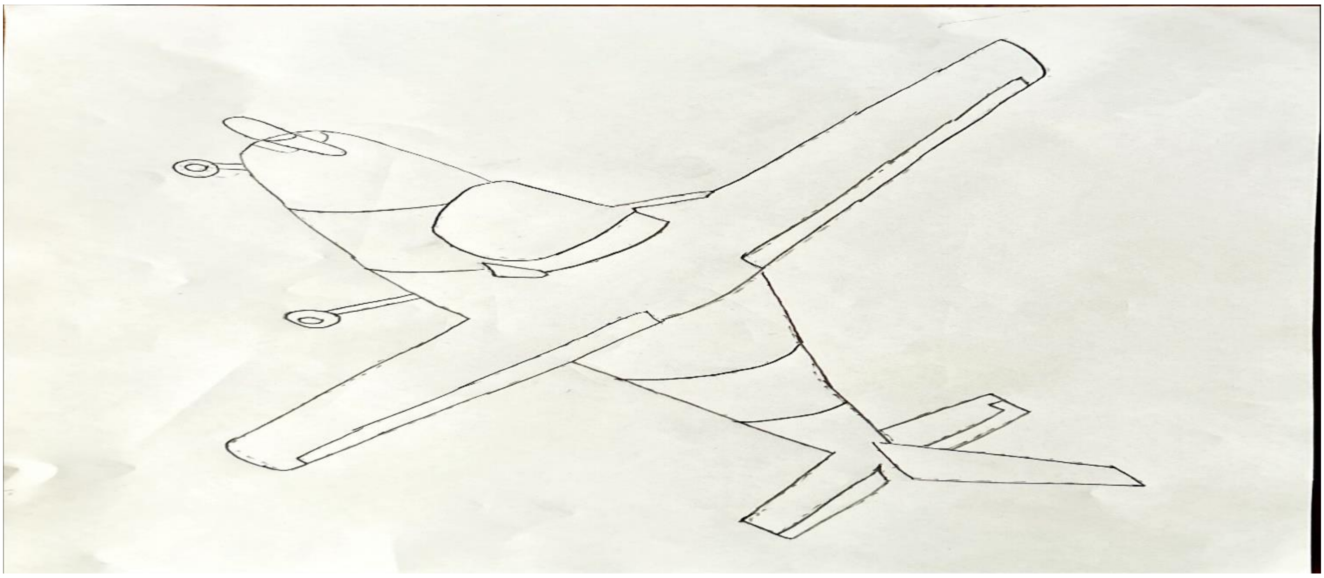

Figure 10 Fockewulf Fw-190

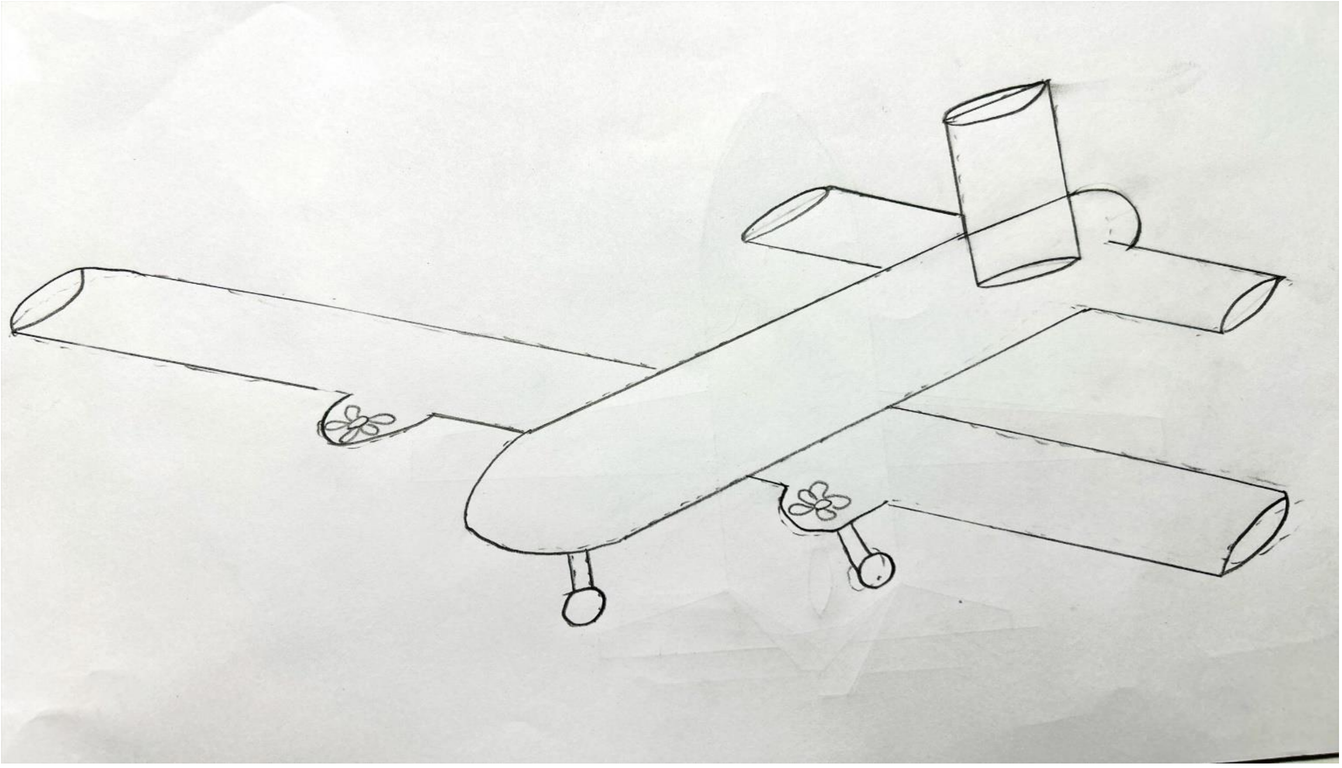

Figure 11 Boeing 727

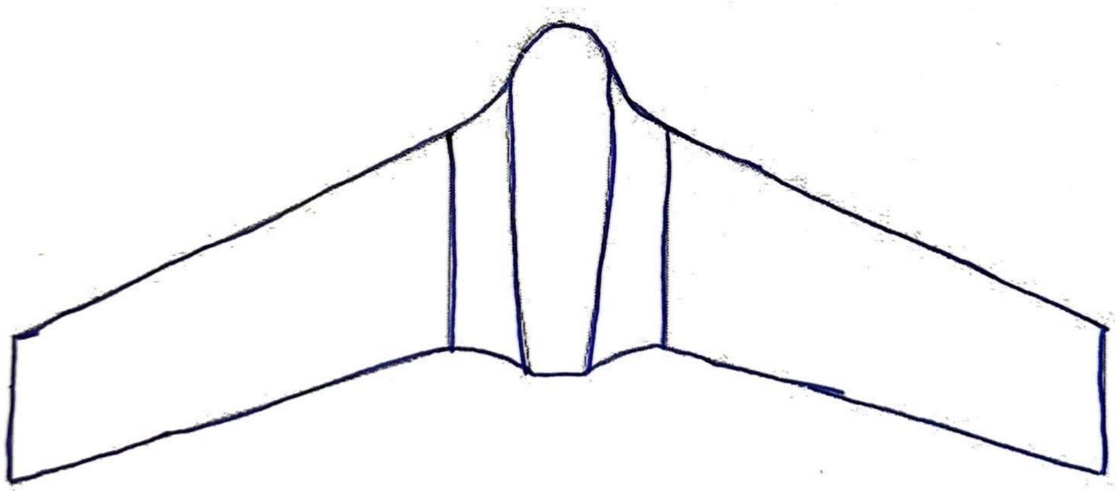

Figure 12 Skywalker X8

Here, in the project, many more models of the aircraft were purposed. Most of them are from the Royal Air Force aircraft which have a great impact on the aircraft industry. Likewise, in the report, the most significant and proper aircraft is needed for proper design and analysis.

So, the Skywalker X8 aircraft is selected for this project. This aircraft is easy to design in Solidworks software and even easier to transfer to Ansys for pre-processing and analysis. The aircraft is a 2.12 m wingspan and 72 cm to the fuselage which is easy to make the prototype in the lab.

In the De Montfort University lab, the wind tunnel is 305 mm*305 mm in diameter, so this aircraft is best for the selection. Likewise, if more time will be available for the project, then a proper model is going be prepared with the help of university funding.

## 3.2 Airfoil Selection for Skywalker X8

Deciding airfoil for the aircraft is one of the most difficult tasks in the report. A few airfoils were taken into consideration to select the proper one. All together 5 airfoils are taken, and they are analysed in the XFLR5 software for best performance. NACA 4412, 0009, MH60, MH45 and 5510 are the five airfoils which are taken for the test purpose.

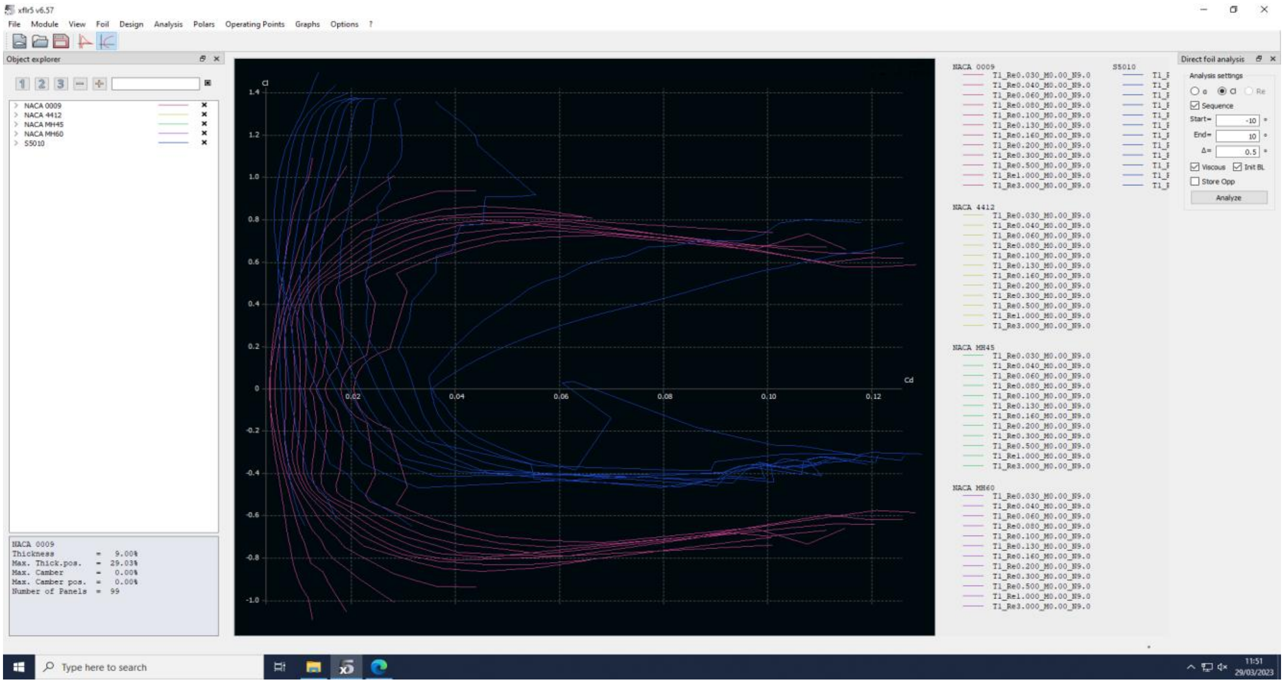


Figure 13 Cl Vs Cd graph of all the airfoils

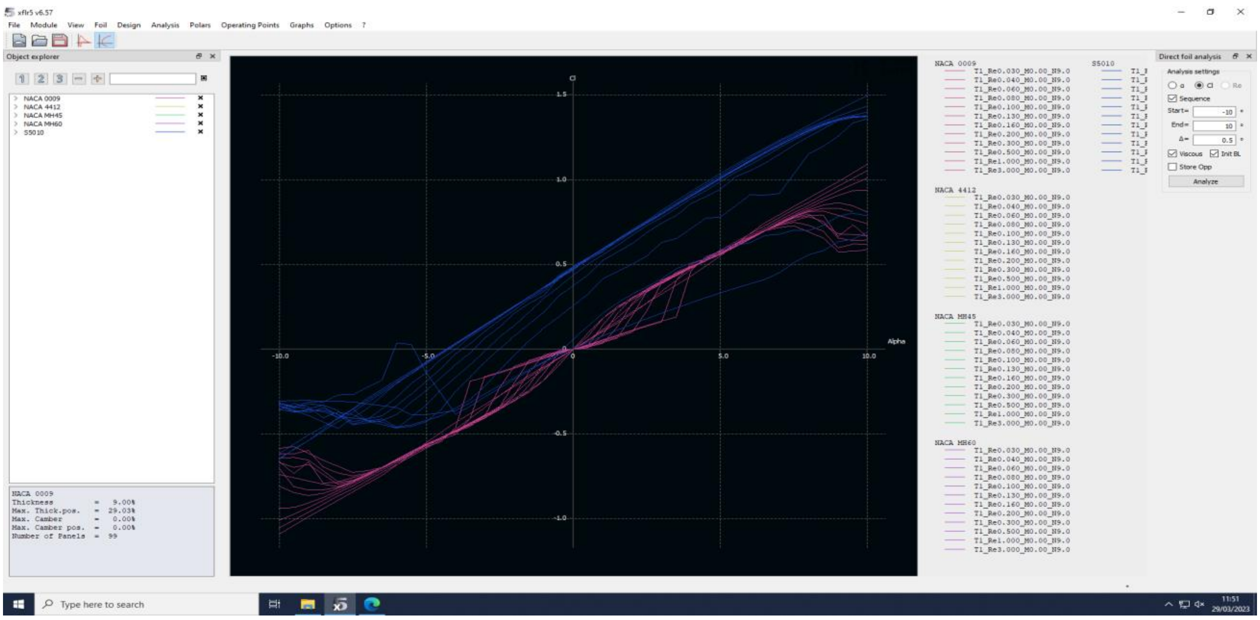


Figure 14 Cl vs Alpha graph of all the airfoils

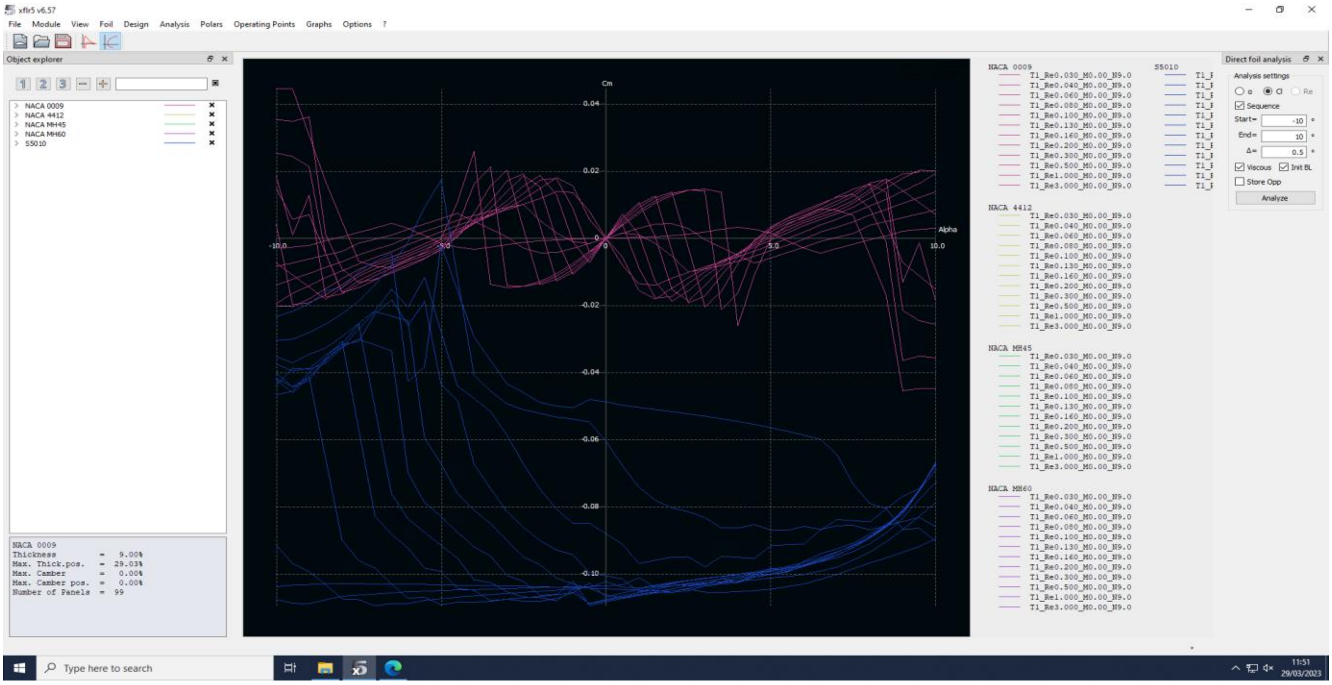


Figure 15 Cm vs Alpha of all the airfoils

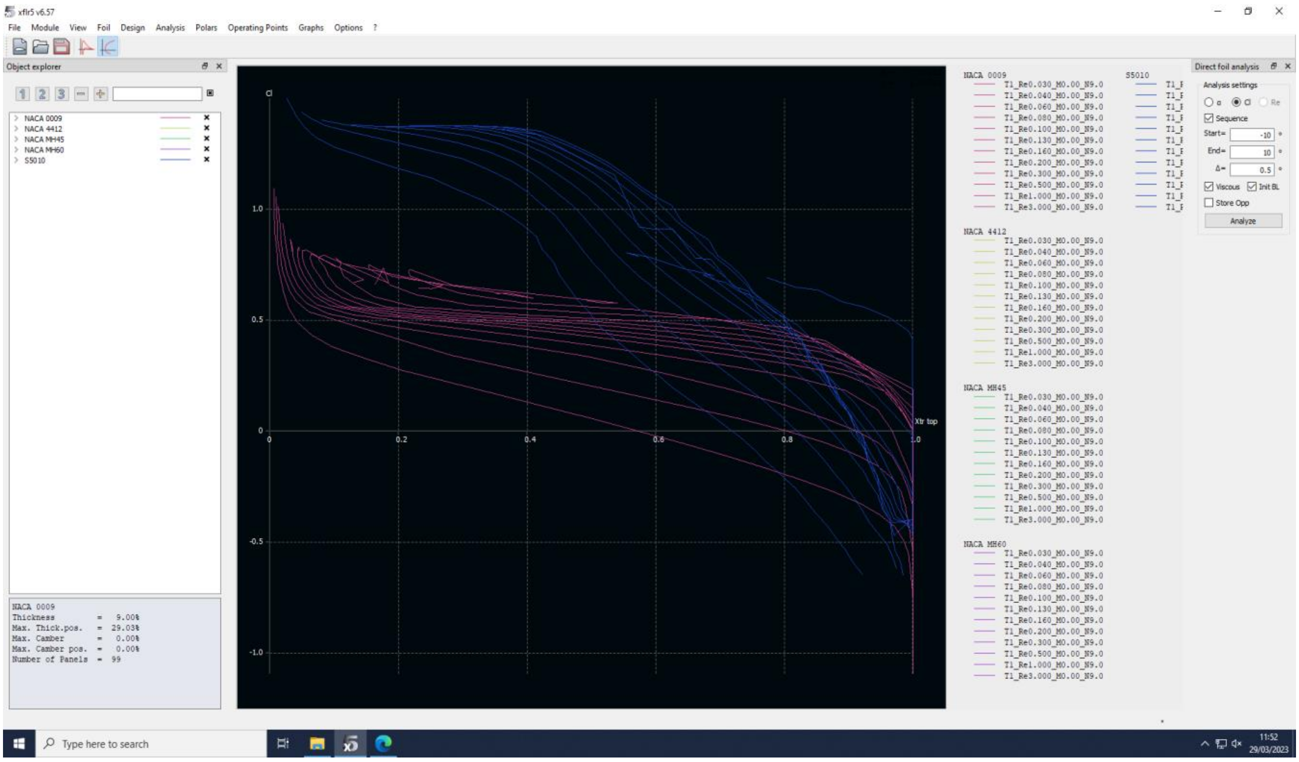


Figure 16 Cl Vs Xtr Top of all the airfoils

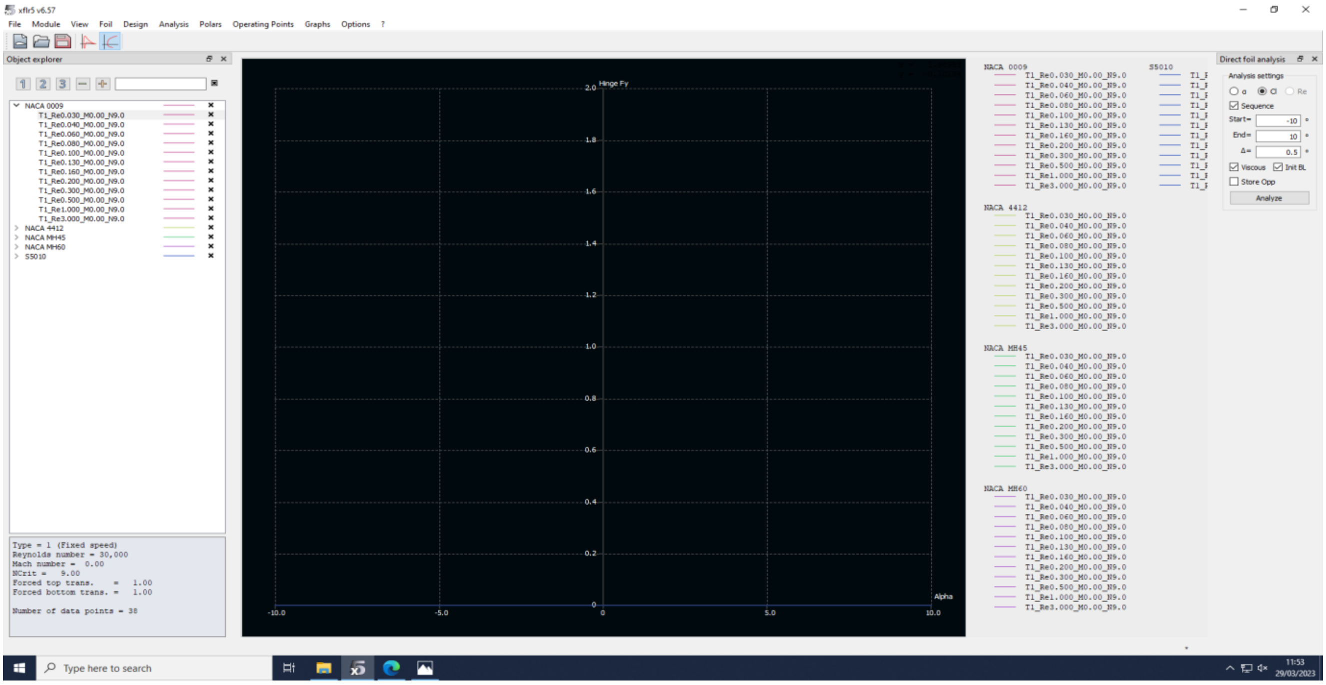


Figure 17 Hinge Fry Vs Alpha of all the airfoils

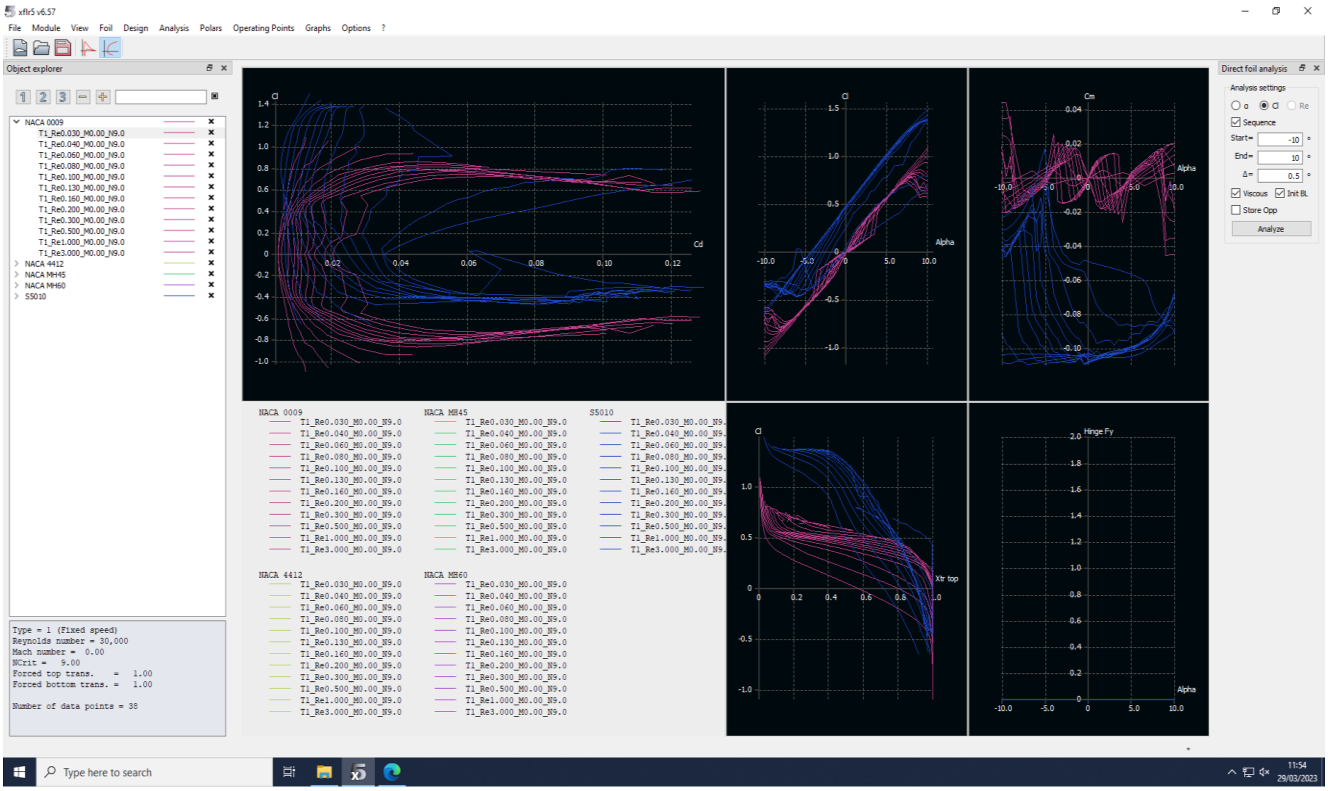


Figure 18 Analysis of all the aifoils in a single chart

The lift coefficient, Cl, and drag coefficient, Cd, are shown in the above graph as a ratio. The lift coefficient provides a measurement of the upward lift force, whereas the drag coefficient provides a measurement of the force acting in the opposite direction of the motion. It is ideal to have a high Cl/Cd ratio, meaning that the lift coefficient and drag coefficient should both be as high as possible. The graph above shows the connection between the lift coefficient and the angle of attack presented in the above figures. The angle at which the wind impacts the aerofoil is known as the angle of attack. When the angle of attack is low, the lift coefficient should be larger. The graph depicts how the lift coefficient varies along the entire aerofoil. [19]

For various angles of attack, the graph displays the variation in Cl/Cd. A low angle of attack calls for a greater Cl/Cd. In addition, the CM vs. Cl. and Cl /CD vs. Cl. comparisons of the aerofoils were made, and the relevant graphs were created. The graph above is a plot of Cm vs Cl, where Cm represents the pitching moment, which offers the lift necessary. To account for the estimated lift coefficient of 0.4, the pitching moment should be large. [16]

The NACA 0009 gives more accurate and constant results which are illustrated in the below graph.

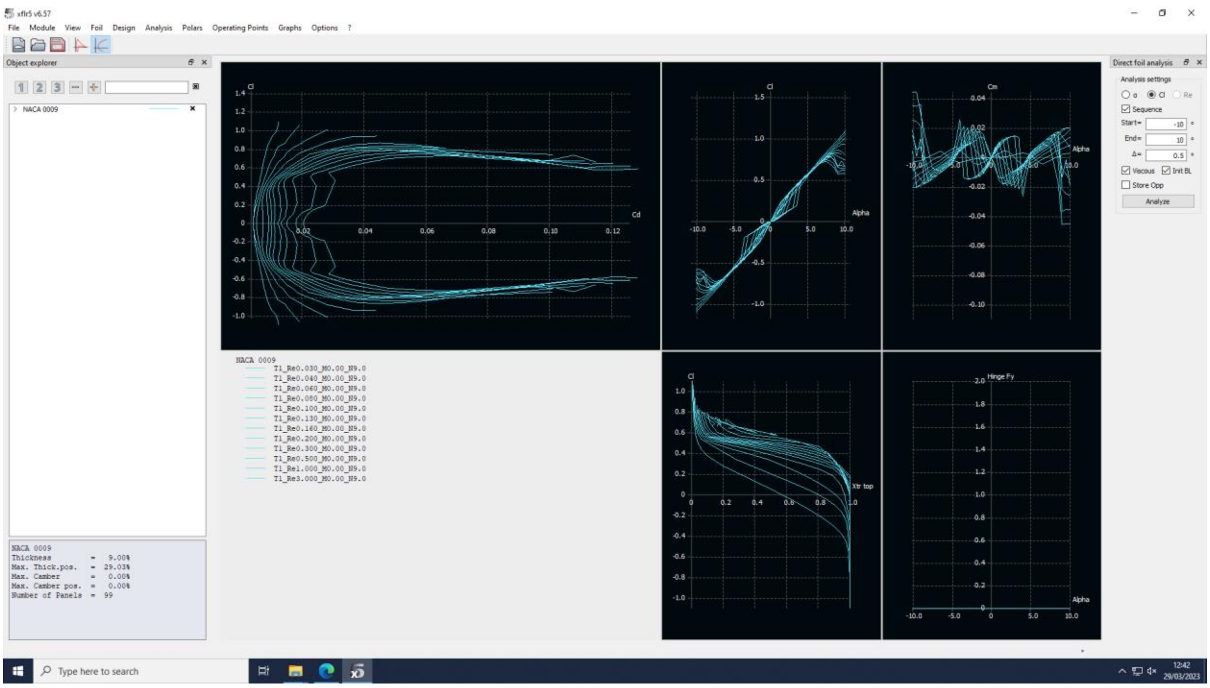

Figure 19 Cl, Cd, Cm Vs Alpha of NACA 0009

## 3.3 Design of Model

### 3.3.1 Design

The aircraft Skywalker X8 is designed in CAD software for proper analysis. In this paper, Solidworks software is selected for the design of the Model.

To build an assembly of all the parts that make up the aircraft, the Skywalker X8 design in Solidworks must first be completed. The wings, the body, the motors, the batteries, and other electronic parts will all be assembled.[26]

To produce the body's fundamental shape, the **"Extrude"** command is used. The edges are rounded off with fillets and chamfers. The aircraft's wings and body are then constructed using the **"Sketch**" tool. Using the **"Extrude"** command after the wing has been formed to give it thickness. The final step in the assembly process is to merge all the parts using the **"Assembly"** tool. [26]

Once the design is ready, materials should be added to all the parts and at the necessary joints like motors, batteries, and other electronic components to give proper aircraft.

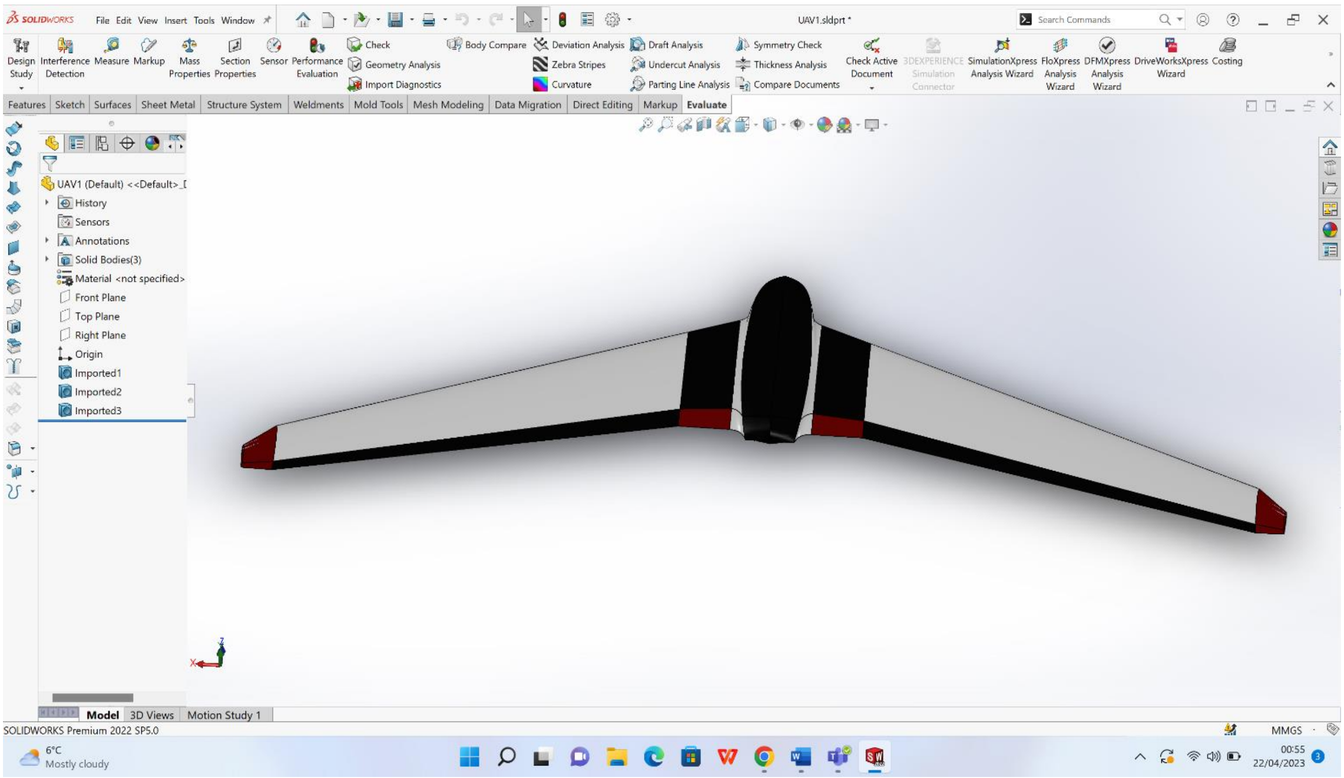


Figure 20 Design of Skywalker X8 in solidworks

In **computational fluid dynamics (CFD)** simulations and structural analysis, it is usual practice to utilise a half-model of an aircraft in the ANSYS programme. The key benefit of utilising a half model is that it requires less calculation and analysis time.

It takes a lot of work to create a complete 3D model of an aircraft, especially when simulating fluid-structure interactions and the **computational domain** is cut in half. When a **half model** is used, which considerably minimises the amount of memory and computing time needed.

The **symmetry and antisymmetric** of the aircraft structure and its aerodynamic behaviour can both be learned from a half model. This information can be utilised to spot potential structural and aerodynamic design defects or locations that could be strengthened.

It is crucial to keep in mind that using a half model requires adequate boundary conditions to faithfully simulate the behaviour of the complete aircraft. The boundary conditions must take into consideration any symmetries or ant symmetries in the model, as well as the missing half of the aeroplane. Failure to do so could result in inaccurate results and poor design choices.

The Skywalker X8 half model is used in the Ansys for pre-processing and even for wind tunnel testing.

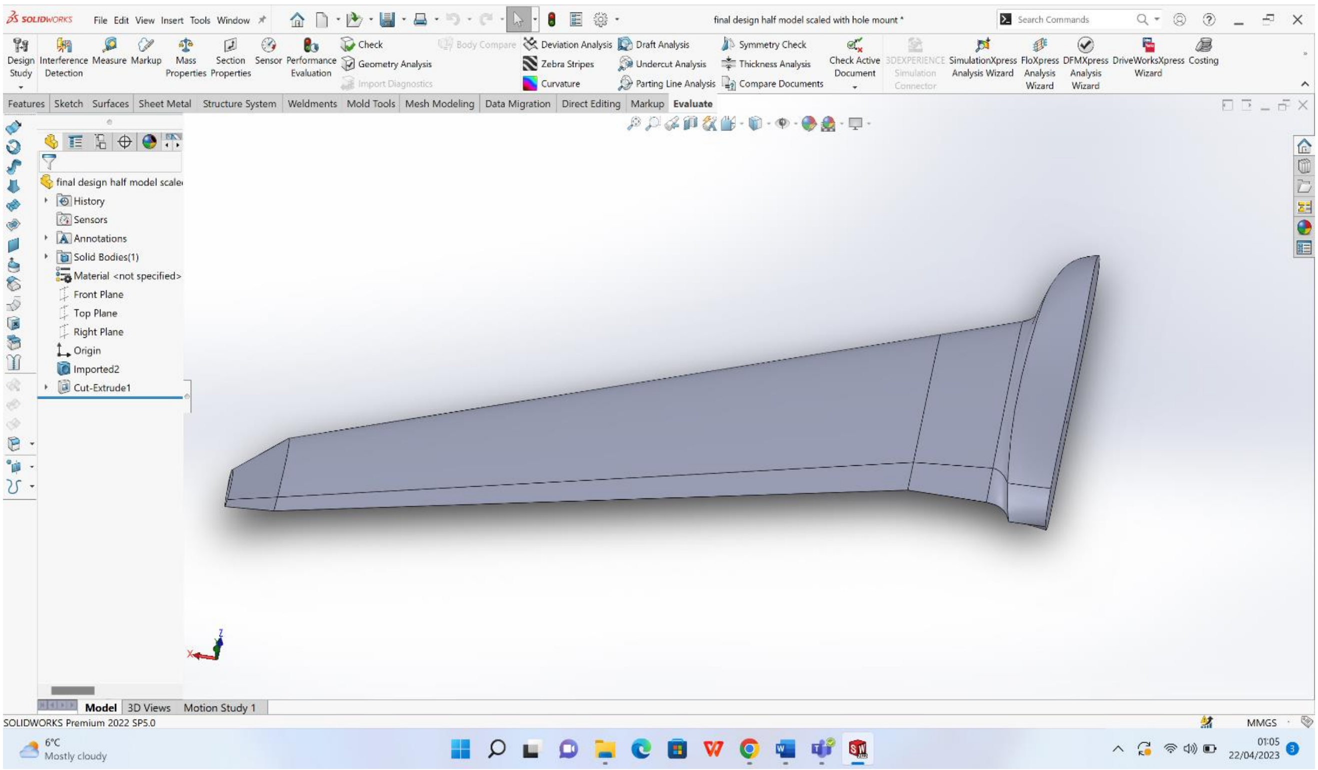


Figure 21 Half model of the Skywalker X8 in soldiworks

### 3.3.2 Aircraft Description

The Skywalkers X8 is low-speed fixed-wing aircraft which mostly used for long-endurance flights, surveillance missions, mapping, and other many activities. The aircraft's wing length is **2012 mm, the body length is 726.08 mm, the wing tip is 174.06 mm, and the weight of the aircraft is approximately around 2-3 kg.**

Mostly, the aircraft is constructed from durable and lightweight materials like **EPO form and carbon fibre.** These materials are helpful in their **robustness and resistance** to damage and the prevention of harsh weather conditions. The Skywalkers X8 is simple in design so it is easy to assemble and disassemble. The aircraft model is easy to transport and maintain. [16]

With **a top speed of about 100 km/h and a top altitude of 5,000 metres,** the Skywalker X8 is capable of both. A high-resolution digital camera, an infrared camera, and a video transmitter are among the sensors and cameras it is outfitted with for surveillance and reconnaissance missions.

With the use of remote control or a pre-programmed flight plan, the aircraft can be flown manually. It's extended endurance and steady flight qualities make it suitable for a range of tasks, such as mapping and surveying, environmental monitoring, search and rescue, and border enforcement.[19]

| | |
|---|---|
| **Wing length** | **2012 mm** |
| **Wing Tip** | **174.06 mm** |
| **Body** | **726.08 mm** |
| **Weight** | **2-3 kg** |
| **Top Speed** | **100 km/hr** |
| **Top Altitude** | **5000 meters** |

Table 5 Specification of skywalkers X8

### 3.4 CAD Model

After the model is prepared in Solidworks, it is saved in the **x.t format** and then it is imported to **Ansys software** for further calculation. The **Skywalker X8's CAD** model in ANSYS would be a **three-dimensional depiction** of the actual plane made up of a variety of surfaces and solid volumes. The model would probably include precise geometry for the wings, fuselage, and other parts of the aircraft, as well as any interior systems or structures. The model would be broken up into finite elements, which are concise sections of the model that may be examined separately. [14]

A variety of analyses, including **structural, aerodynamic, thermal, and fluid-structure interaction analyses,** can be carried out on the CAD model once it has been imported into ANSYS. Through these assessments, the design of the aircraft can be changed for **increased performance and safety** and can reveal how the aircraft behaves in various operational scenarios.

In general, the CAD model of the Skywalker X8 in ANSYS would be a **highly realistic and complete reproduction** of the actual aircraft, enabling a thorough investigation of its performance and behaviour.[12]

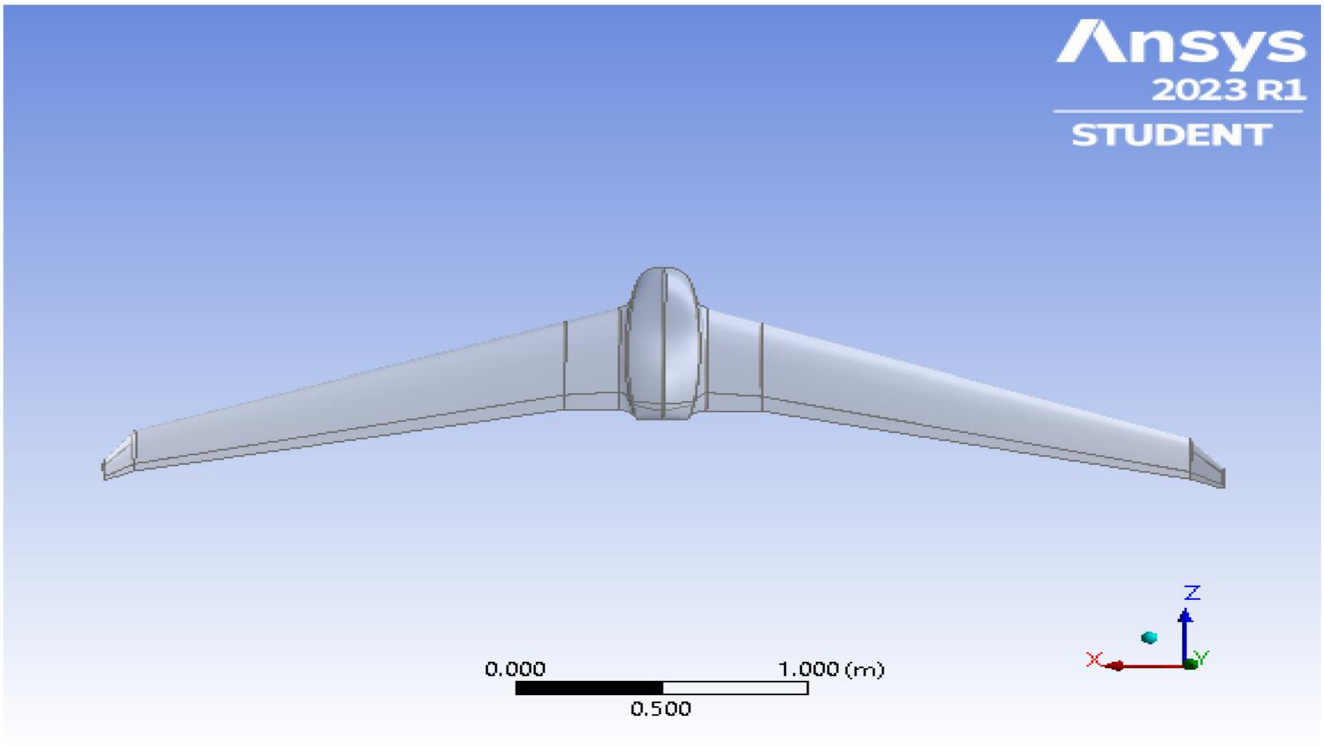


Figure 22 Skywalkers X8 imported in Ansys.

### 3.4.1 Engineering Analysis

With the use of computer software and FEA (Finite Element Analysis), the engineering analysis performed for this report calculates the performance of the aerodynamic analysis and structural analysis of the Skywalker X8. This research evaluates CFD analysis using Ansys software.

### 3.4.2 CFD Analysis

The numerical analysis of the interactions between fluids and non-fluids in any engineering product is known as CFD analysis. These programmes provide most engineering problem solutions prior to product manufacturing. These programmes support the examination of a variety of product attributes, including thermal properties, pressure resistance, flow dynamics, etc. There are many different software programmes available on the market that can carry out these tasks. The Skywalker X8 aircraft's aerodynamics have been examined in this research using Ansys Fluent. Five separate steps of aerodynamic analysis have been carried out by the software. To conduct the evaluation, the following processes are carried out: geometry, meshing, setup, solution creation, and lastly result in a verification.

### 3.4.3 Problem Statement

The project's research is conducted in three steps. The aeroplane model was initially chosen, created in Solidworks, transferred to Ansys for pre-processing, and then the final model was completed. After being verified in the programme, the model is printed on a 3D printer for wind tunnel testing. The report follows the same procedure, and after the wind tunnel testing is finished, the graph is compared with the software and wind tunnel result.

The original Skywalker X8 design in Solidworks is a 3D CAD with NACA 0009 airfoil model which is shown in the figure [22]. The aircraft has a wingspan of 2.12 meters and a maximum altitude of 2000 meters with a maximum speed of 100-120 km/h.

The major goal of the study is to develop a Skywalkers X8 with the proper wing structure using the prior design as a guide and to satisfy the requirements for the issue. The weight of the aircraft must be kept to a minimum to withstand the stress caused by the wing's aerodynamic load.

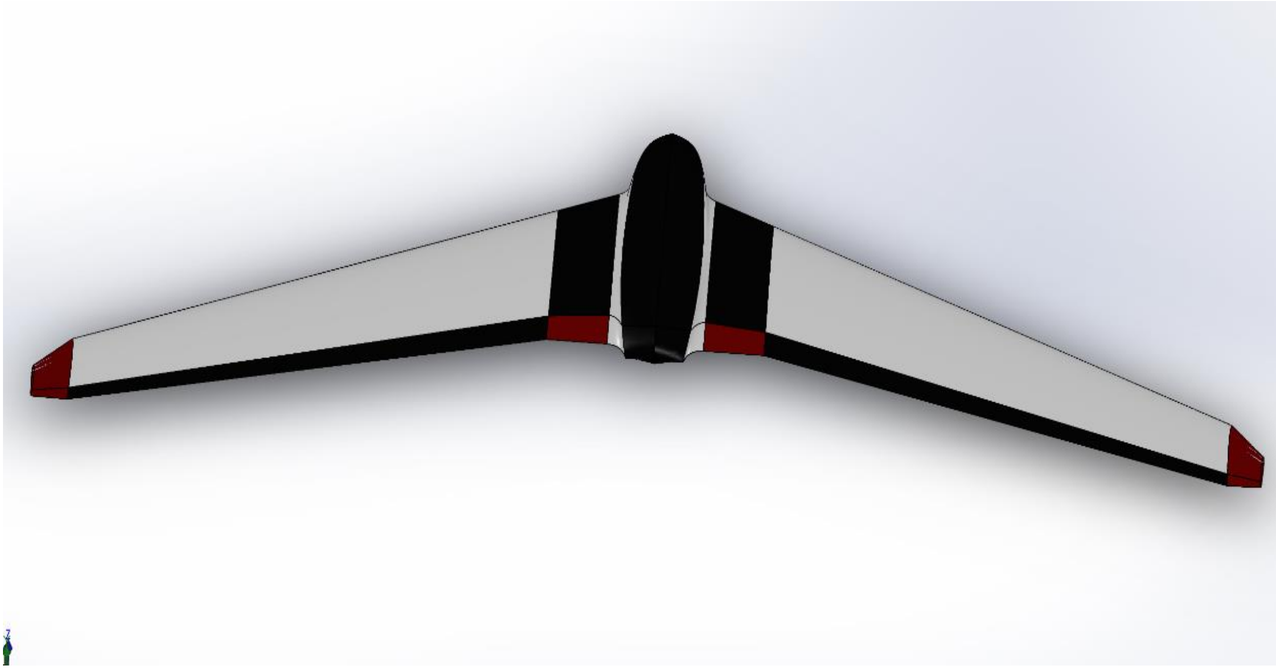

Figure 23 The original Skywalkers X8 design in the Solidworks [27]

## 3.5 Mathematical Model

There are several formulas that describe the Mathematical Model of the Skywalker X8 aircraft. Some of the equations are: -

- Navier-stokes Equation.
- Continuity Equation
- Lift and drag Equation.
- Structural Equation

### 3.5.1 Navier-stokes Equation.

Navier-stokes Equations include the motion of the fluid around the aircraft and are used to determine basic aerodynamic simulations mostly in Ansys software. In this equation partial differential equation play a particular role which describes the conservation of mass, momentum, and energy of the fluid. The Navier-stokes Equation can be written as

$$\rho\,(\partial u/\partial t + u\nabla u) = -\nabla p + \mu\nabla^2 u + f$$

$$\nabla \cdot u = 0$$

where:

- $\rho$ is the density of the fluid
- u is the velocity vector of the fluid
- p is the pressure of the fluid
- $\mu$ is the dynamic viscosity of the fluid
- f is the body force acting on the fluid (such as gravity)
- $\nabla$ is the gradient operator.
- $\nabla^2$ is the Laplacian operator.

The first equation asserts that the total of the external forces acting on the fluid equals the rate of change of momentum in a control volume, which is how momentum is conserved. The term "u" refers to the fluid acceleration known as convective acceleration, which is caused by the movement of other fluid particles. The force produced by the internal friction of fluid particles is known as the viscous force and is denoted by the symbol 2u. The force that fluid pressure applies to fluid particles is shown by the pressure gradient, or -p. The second equation mandates that the velocity field's divergence be zero and indicates the conservation of mass.[28]

These equations are employed in ANSYS to simulate the fluid flow around the Skywalker X8 and to determine the aerodynamic forces acting on the aircraft. Finite element analysis and other computer techniques are used to solve the equations numerically. The Skywalker X8's shape, the boundary conditions, and the intended outcomes will all affect the simulation's specifics. [6]

### 3.5.2 Continuity Equation

The continuity equation is the extended form of Navier-stokes Equations which describe the conservation of the mass inside the fluid around the aircraft.

$$\nabla \cdot u = 0$$

- where:
- u is the velocity vector of the fluid
- ∇ is the gradient operator.

The divergence of the velocity field must be zero according to his equation, which indicates that the rate of change of mass in a control volume is equal to the net flow rate of mass into or out of the control volume. Mass is thus conserved in the fluid. [7]

The continuity equation is applied as a constraint in ANSYS to simulate fluid flow around the Skywalker X8. To make sure that mass is conserved, and the fluid flow is physically consistent, the equation is often calculated jointly with the Navier-Stokes equations. The geometry of the Skywalker X8, the boundary conditions, and the desired outcomes will all affect the specifics of the simulation.[28]

### 3.5.3 Lift and Drag Equation

To determine the lift and drag forces acting on the Skywalker X8, ANSYS use the lift and drag equations. The aircraft's geometry, the fluid's velocity and density, and the angle of attack—the angle formed by the chord line of the aircraft and the relative wind—all factor into these equations. The equations for lift and drag's generic forms are as follows:

Lift: $L = 1/2 * \rho * V^2 * S * Cl$

Drag: $D = 1/2 * \rho * V^2 * S * Cd$

- where:
- L is the lift force
- D is the drag force
- ρ is the density of the fluid
- V is the velocity of the fluid relative to the aircraft
- S is the reference area of the aircraft
- Cl is the lift coefficient, which depends on the angle of attack and the shape of the airfoil
- Cd is the drag coefficient, which depends on the angle of attack and the drag-producing features of the aircraft, such as the fuselage and the wings.

Tests in a wind tunnel, simulations of computational fluid dynamics (CFD), or other experimental techniques are used to determine the lift and drag coefficients Cl and Cd. Typically, these coefficients are supplied as simulation input parameters in ANSYS. The equations can be used to compute the lift and drag forces if the coefficients are known. To analyse the Skywalker X8's performance and improve its design, these forces can be used.[28]

### 3.5.3 Structural Equation

The precise materials and geometry utilised in the aircraft's construction determine the structural equations that are employed in ANSYS to model the Skywalker X8. However, in general, the equations used to analyse the structural mechanics of the Skywalker X8 are based on the ideas of solid mechanics. Stress and strain, load and displacement and Failure criteria are examples of Structural equations. [7]

In ANSYS, these equations are used to analyse the structural mechanics of the Skywalker X8 and to improve its design. To test and improve the design before creating actual prototypes, engineers can use ANSYS to model how the structure would behave under various loads and situations. The shape, components, and boundary conditions of the Skywalker X8, as well as the desired outcomes, will determine the specifics of the simulation. [28]

### 3.6 Computational Domain

Once the model is prepared in Solidworks it is ready for transferring into Ansys for further processing. But the model is cut into half by using **Extrude command** so that it will be easy to calculate and avoid unnecessary complications. The testing of the half-model body is easy to analyse and plot the graphs.

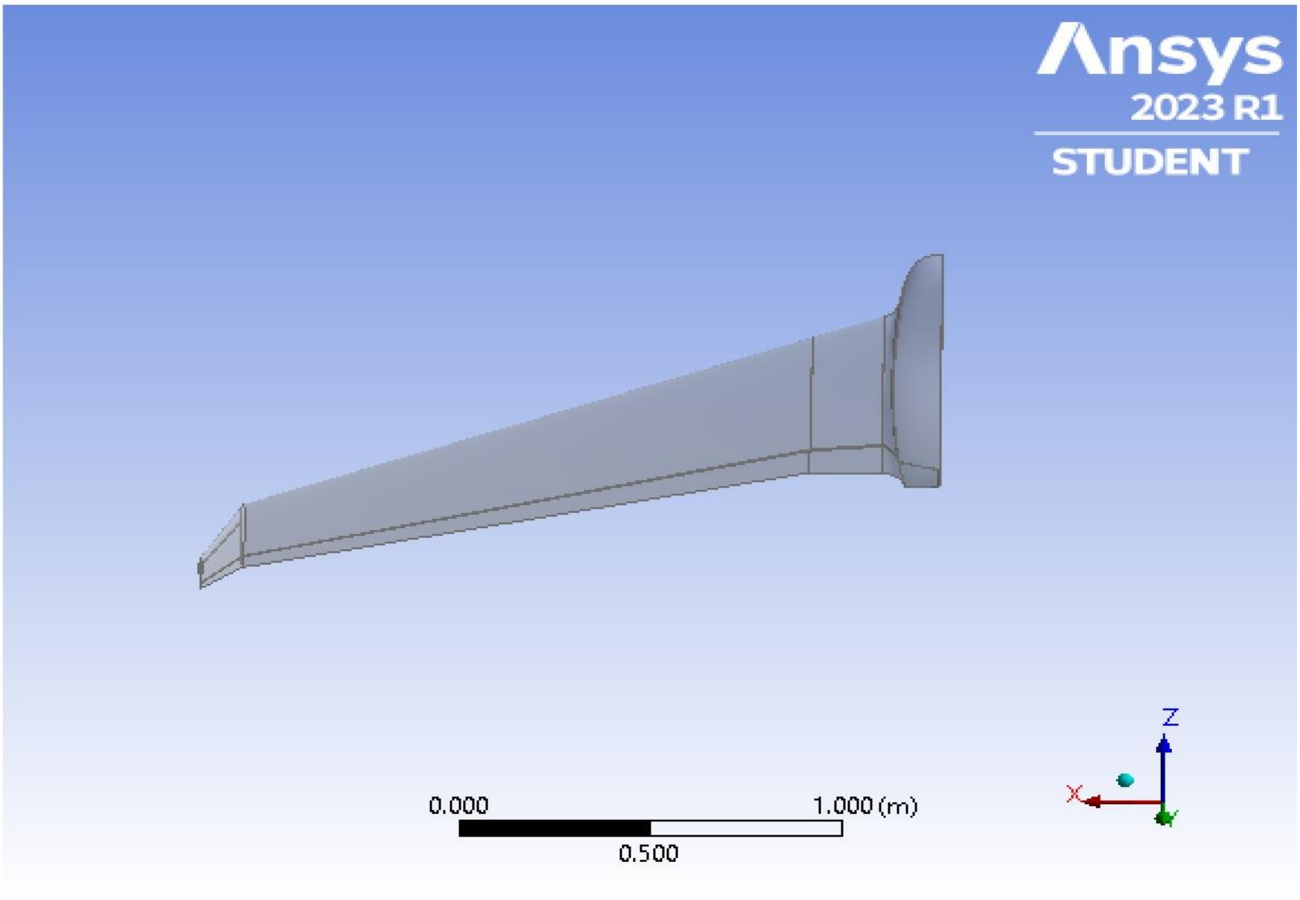


Figure 24 Half model of the Skywalkers X8 in Ansys

The model is imported into Ansys from the solidwork then **Enclosure** is created. It is necessary to create an enclosure to the geometry to determine the fluid flow rate and other physical phenomena. It is one of the most important in the CFD which defines the boundary condition of the fluid domain and helps the solver to solve the flow behaviour properly. By creating an enclosure around the geometry, it is easy to analyse shape, size, and volume.

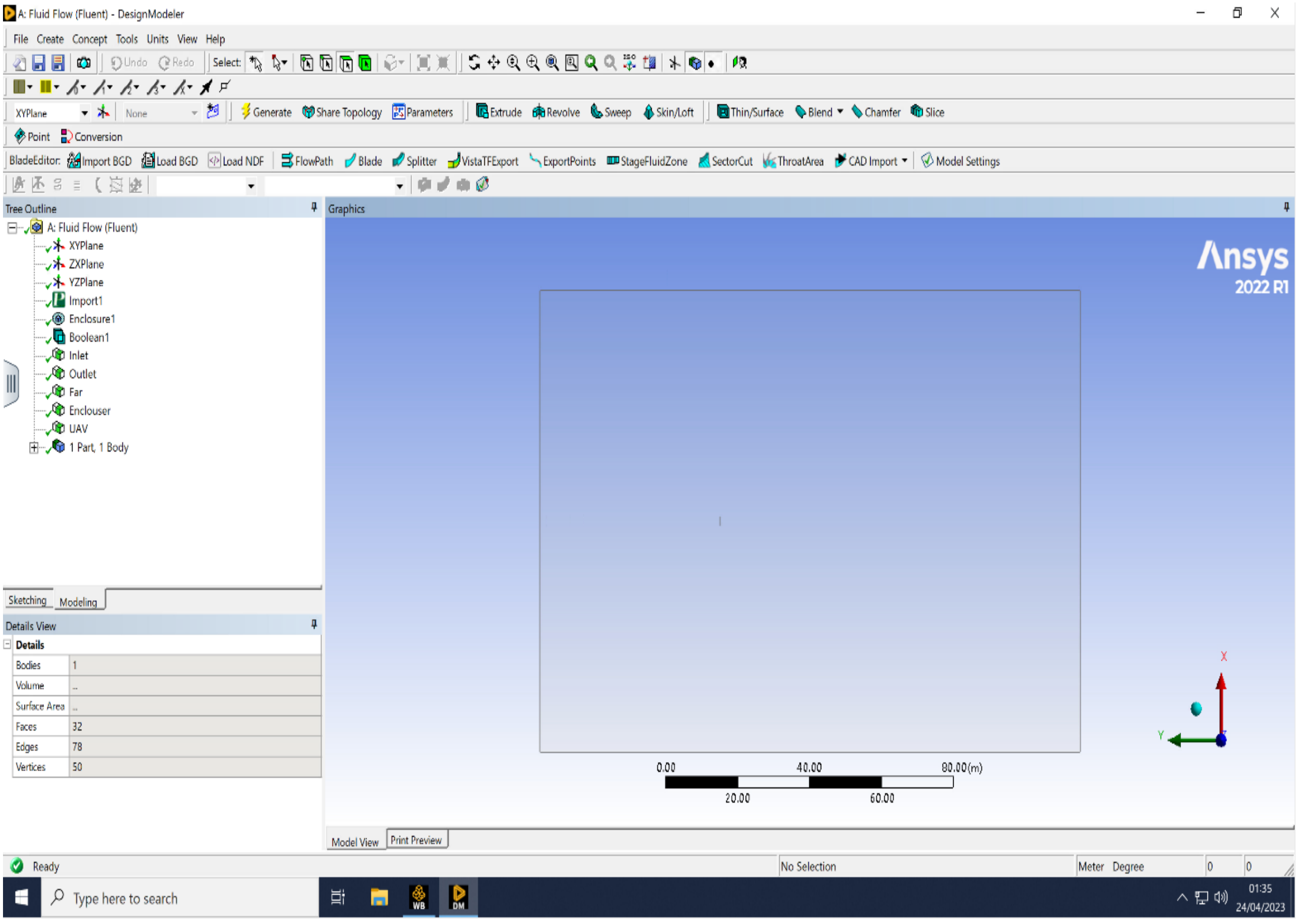


Figure 25 Skywalker X8 model with Enclosure

| Axis | +X-Axis | -X-Axis | +Y-Axis | -Y-Axis | +Z-Axis | -Z-Axis |
|---|---|---|---|---|---|---|
| **Diameter (meter)** | **50** | **50** | **50** | **100** | **50** | **50** |

Table 6 Enclosure Diameter

Once the enclosure is created, the **UAV and enclosure** should be separated. Boolean operation is used to separate the UAV and enclosure by using **Subtract** from the **diagonal box**. After the enclosure is created next process is the **naming section**. **Inlet, outlet, Far and UAV** is named which can be later used in the **meshing section**. [6]

## 3.7 Mesh

For further examination, the geometry is transmitted to the meshing. Mesh creation is crucial to validate the FEA study. The mesh involves mesh region creation, mesh size determination, and mesh generation.[7] To ensure that the meshing process is functioning properly, the mesh is coarse at first. Following mesh creation, the geometry is fine-meshed.

### 3.7.1 Course mesh

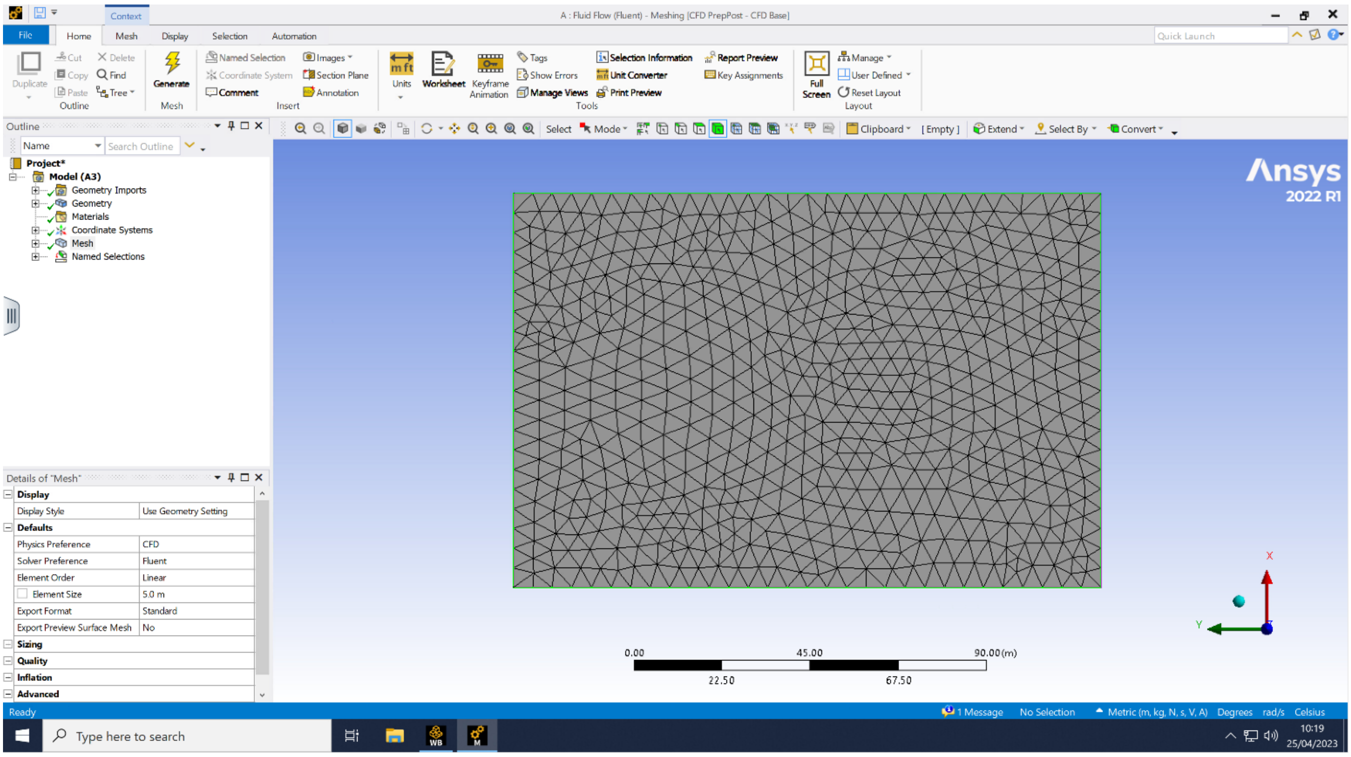


Figure 26 Course mesh of Skywalkers X8

In the above figure, the mesh size is 10 m, and the sizing is 1 m which is just a course mesh. And the result is shown in the below table.

| | |
|---|---|
| **Nodes** | **16880** |
| **Elements** | **91144** |

### 3.7.2 Fine mesh 1

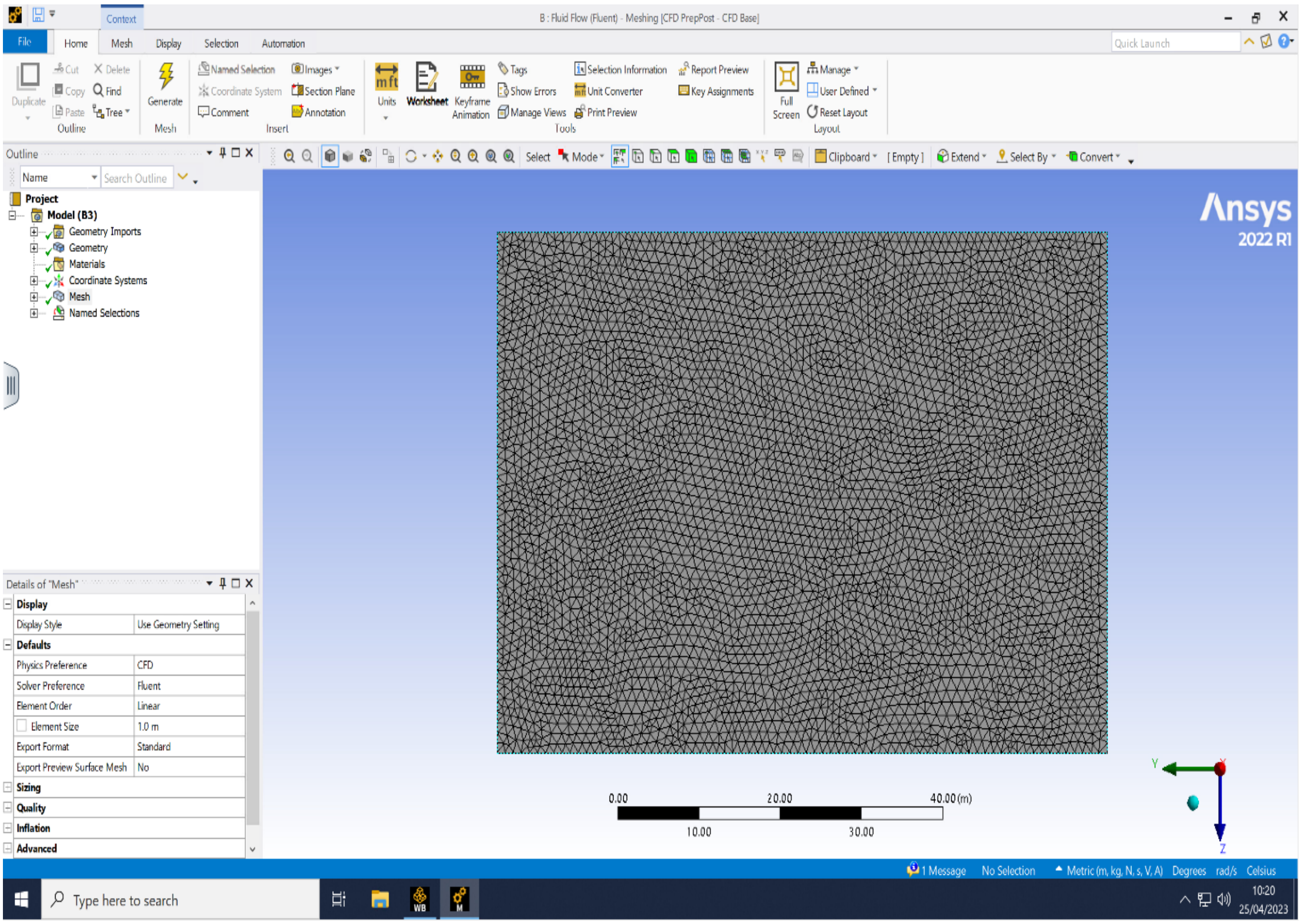


Figure 27 The fine mesh of Skywalker X8

In the above figure, the mesh size is 1m, and the sizing is 0.10 m which is just a course mesh. And the result is shown in the below table.

| | |
|---|---|
| **Nodes** | **206209** |
| **Elements** | **1125675** |

### 3.7.3 Fine Mesh 2

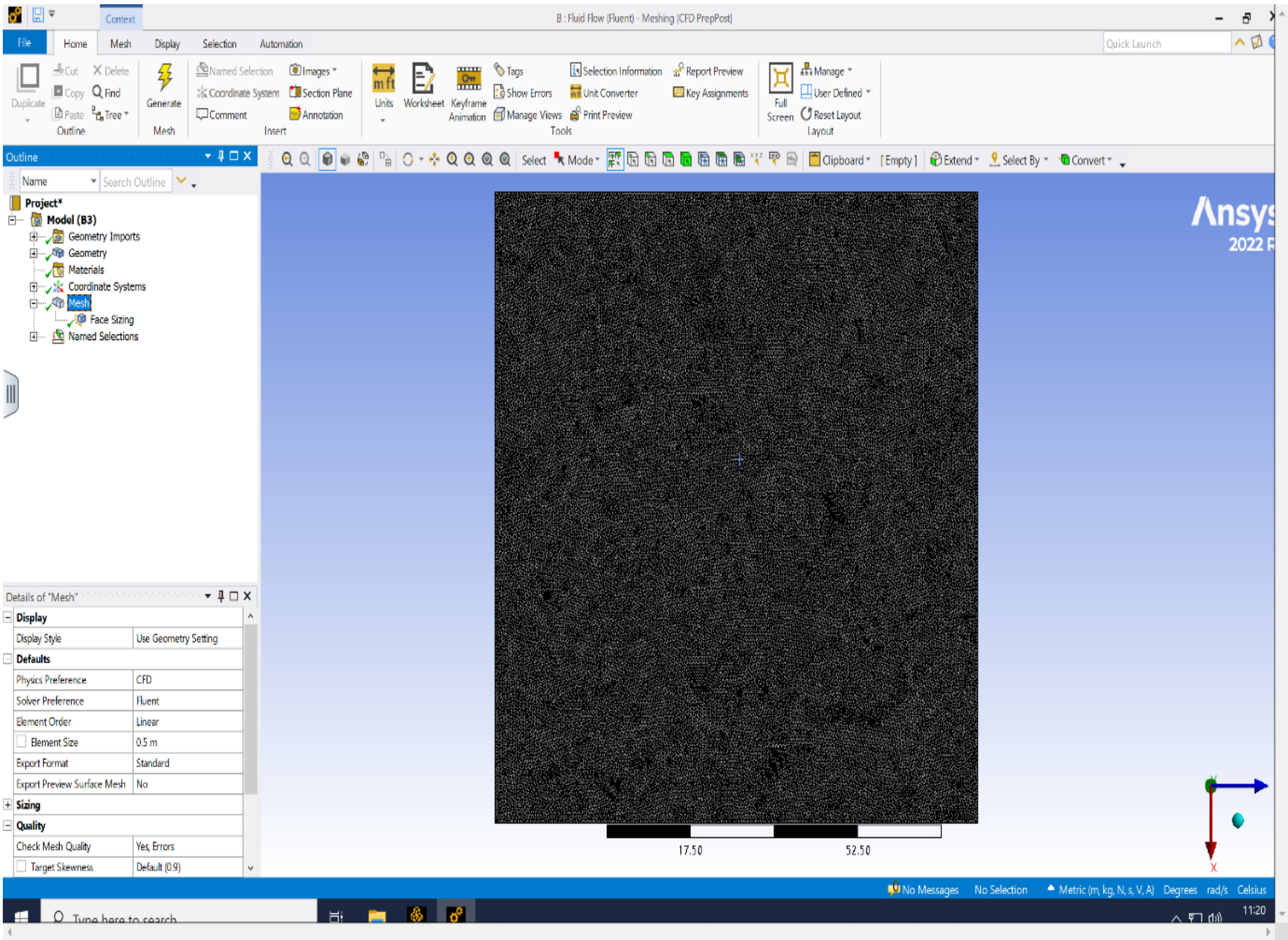


Figure 28 Finest mesh of Skywalker X8

In the above figure, the mesh size is 0.1 m, and the sizing is 0.001 m which is just a course mesh. And the result is shown in the below table.

| | |
|---|---|
| **Nodes** | **3664264** |
| **Elements** | **20745290** |

## 3.8 Boundary Condition

The **boundary condition** is chosen for additional computation following meshing. First, the **material** for this report that is **fluid** as **air** is chosen. Calculations for the boundary are displayed after the material has been chosen. **Initialised values** for the **intake** and **outlet** velocities are **19m/sec and 0,** respectively.

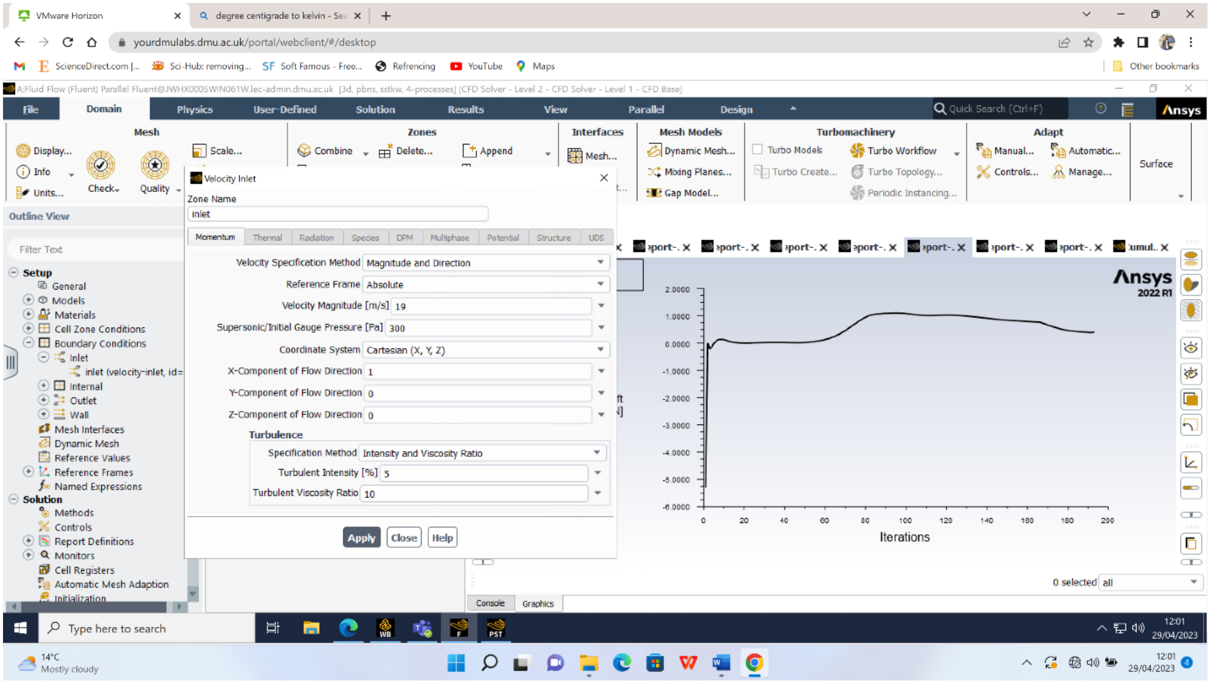


Figure 29 Inlet boundary condition of report Definition

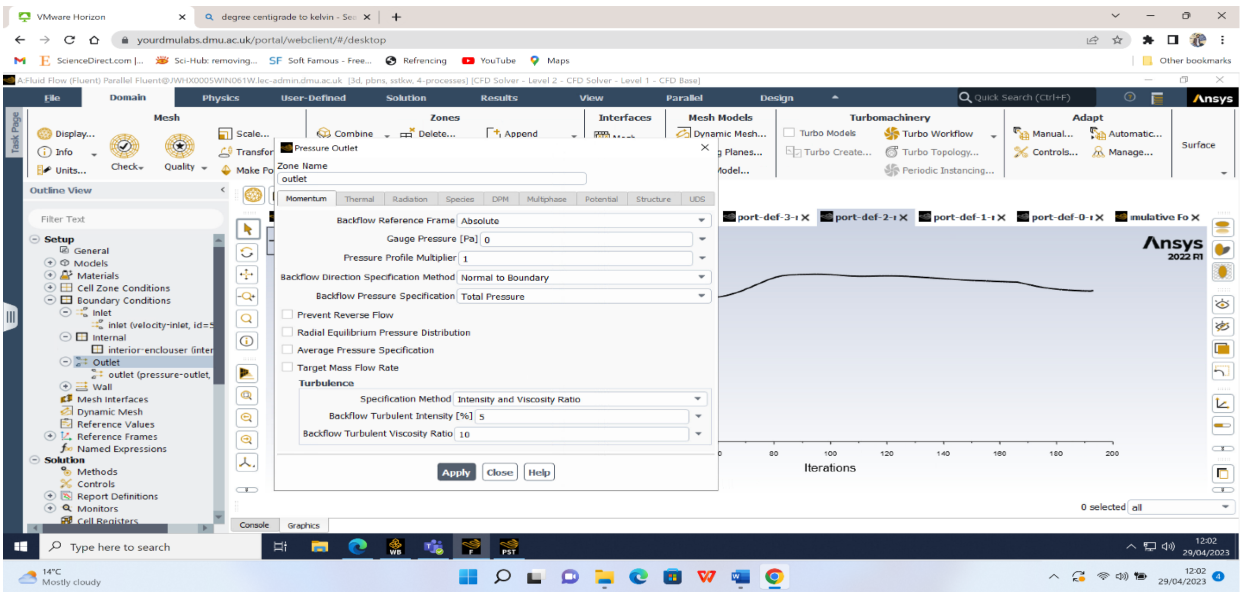


Figure 30 The outlet boundary condition of Skywalkers X8 for results

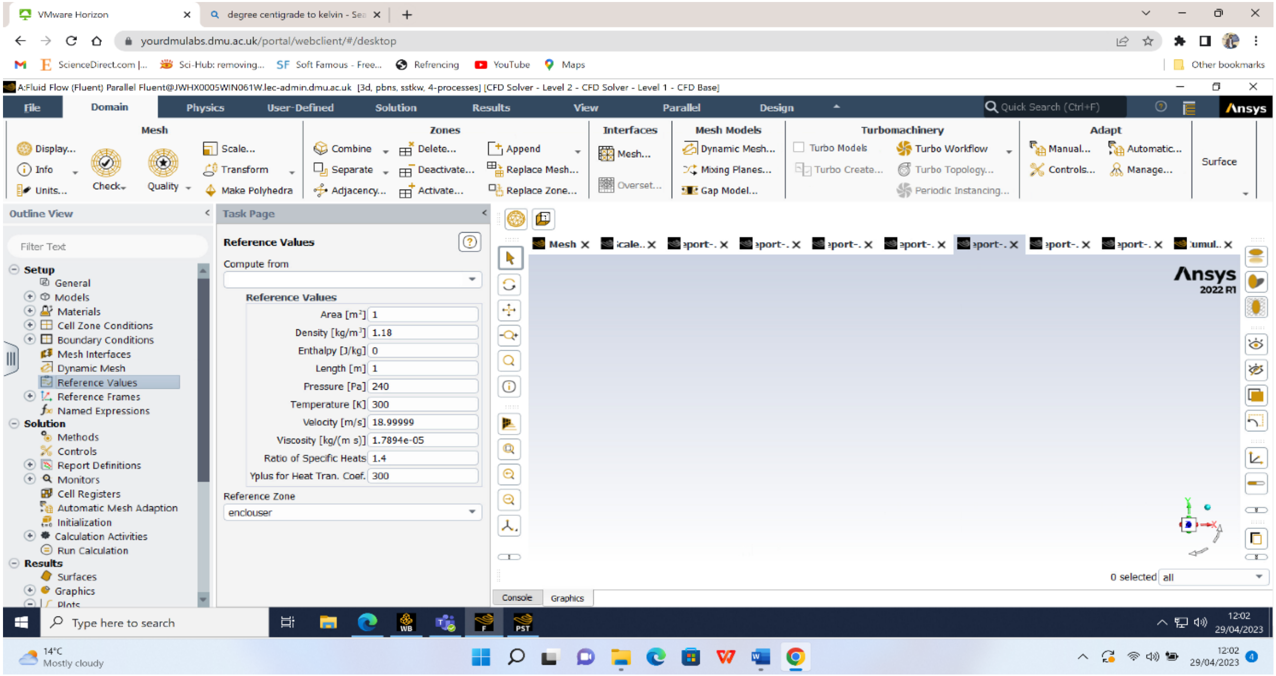


Figure 31 Reference values of Skywalkers X8 for results

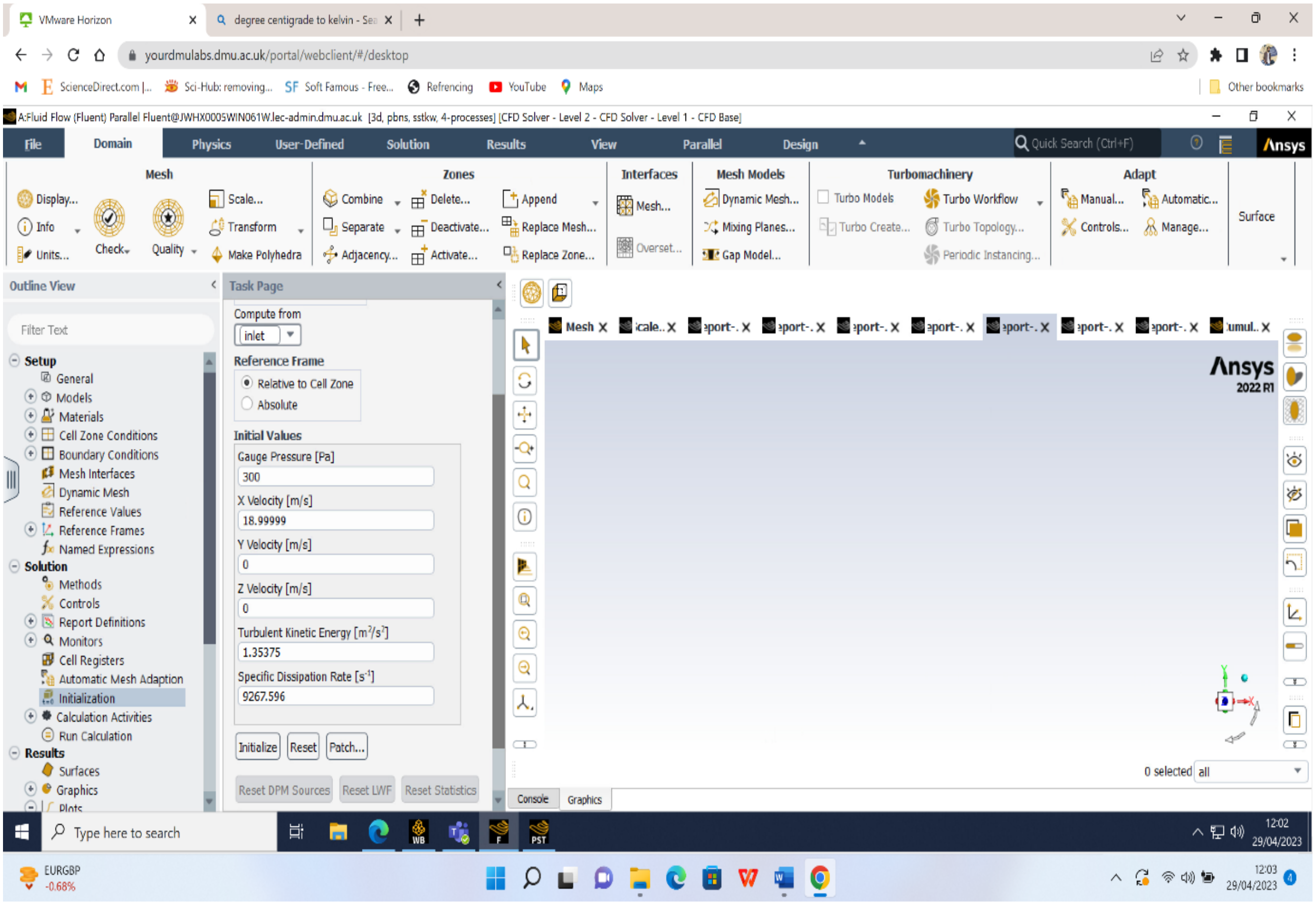


Figure 32 Initialization of Skywalkers X8 for results

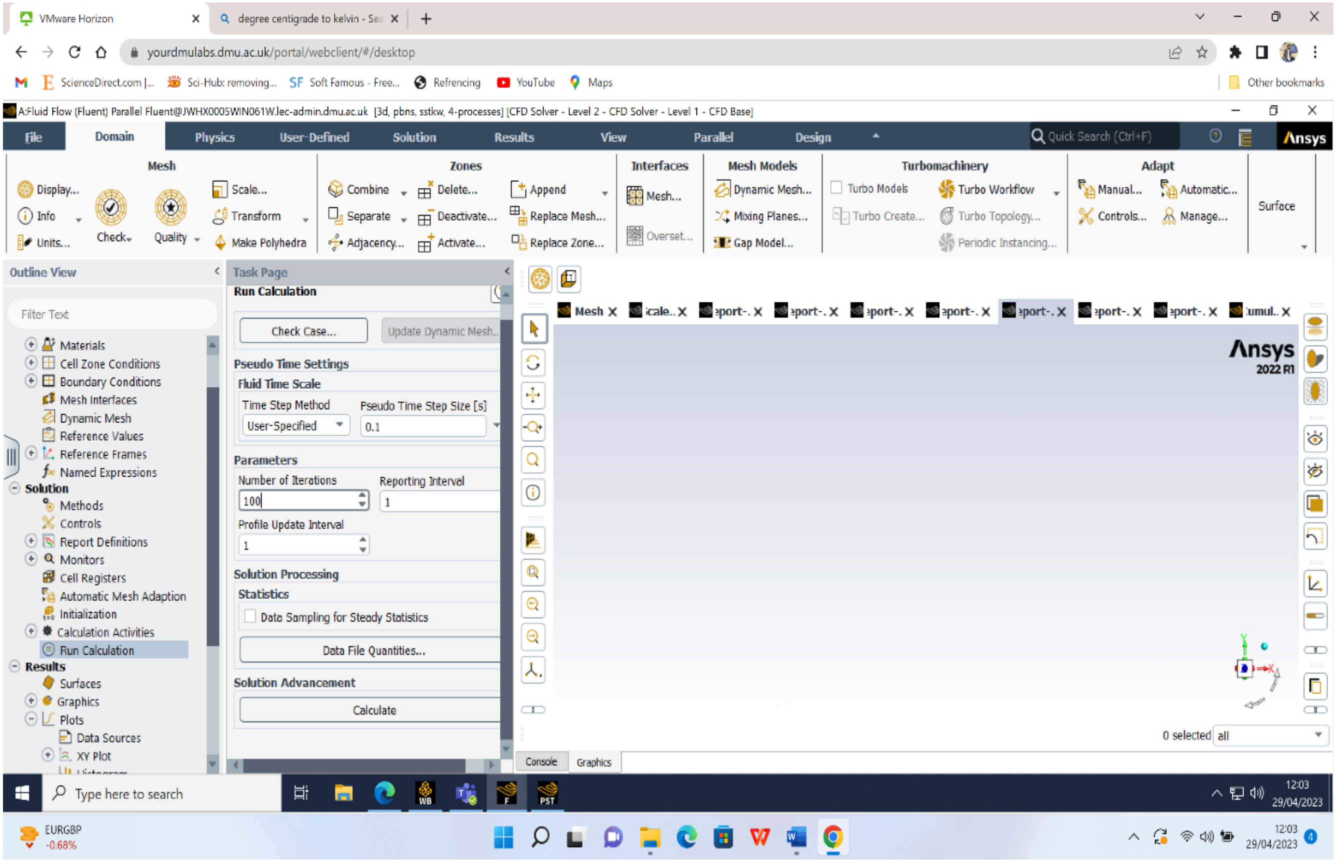


Figure 33 Run calculation of Skywalkers X8 for results.

## 3.9 Set up.

The setup is done with the boundary condition as follows: -

| | |
|---|---|
| **Angle of Attack** | **$0^0$** |
| **Area [$m^2$]** | **1** |
| **Density [$kg/m^3$]** | **1.18** |
| **Enthalpy [J/kg]** | **0** |
| **Pressure [Pa]** | **240** |
| **Temperature [K]** | **300** |
| **Velocity [m/s]** | **18.999** |
| **Viscosity [kg/ (m s)]** | **$1.7894*10^{-5}$** |
| **The ratio of Specific Heats** | **1.4** |

The report is broken down into the following categories: **drag, drag coefficient, lift, lift coefficient, force, moment, and moment coefficient, with initialization occurring after 200 iterations**. The calculation is then completed, and the graph of the results is displayed in the image below.

The results shown in the below graph are used for the post-processing.

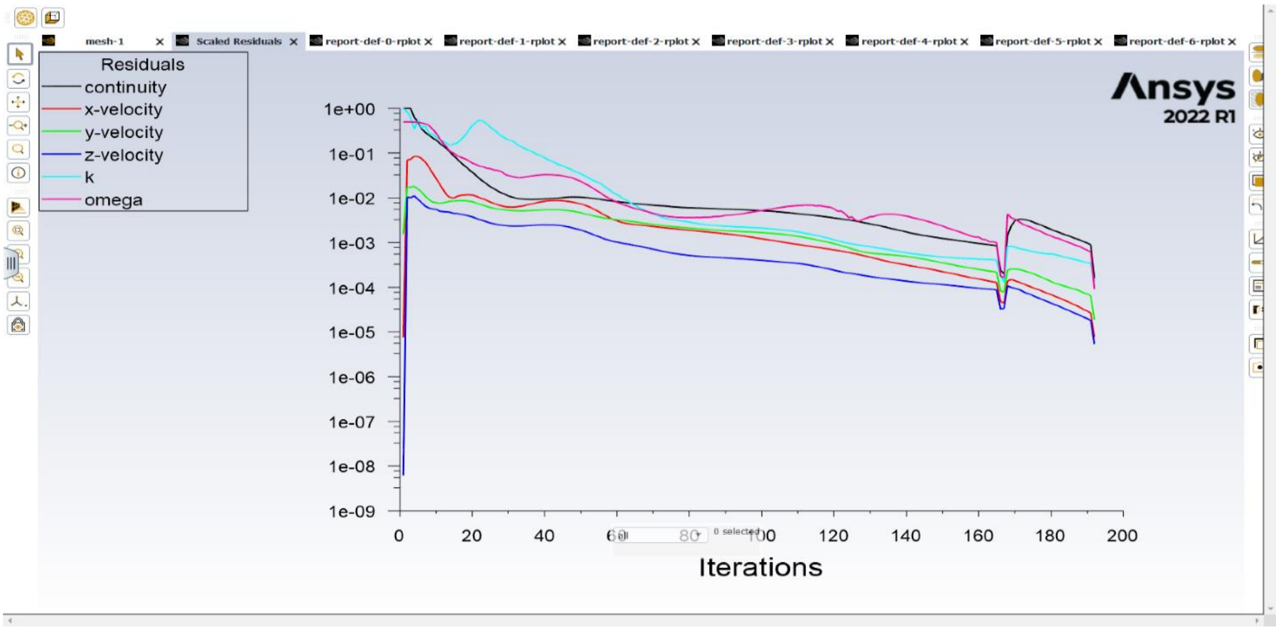


Figure 34 Scaled Residuals of Skywalkers X8

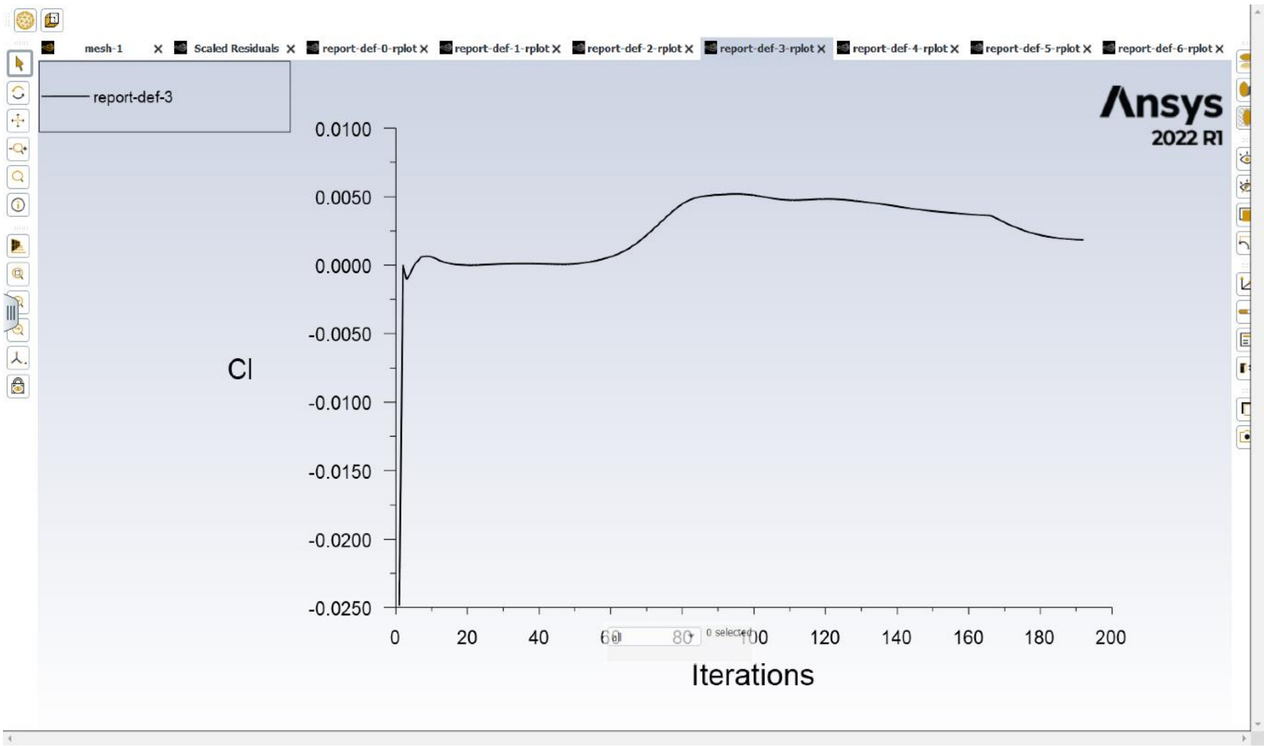


Figure 35 Lift coefficient of Skywalkers X8

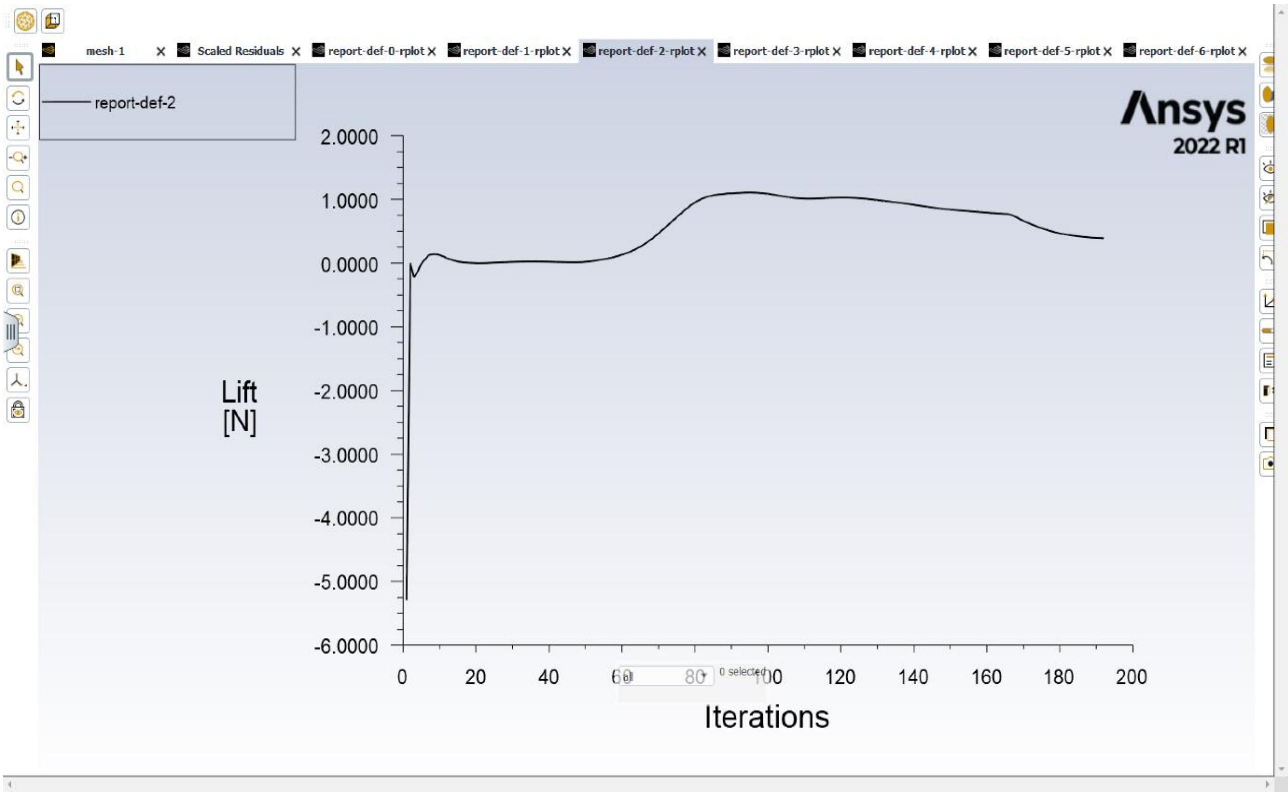


Figure 36 Lift of Skywalkers X8

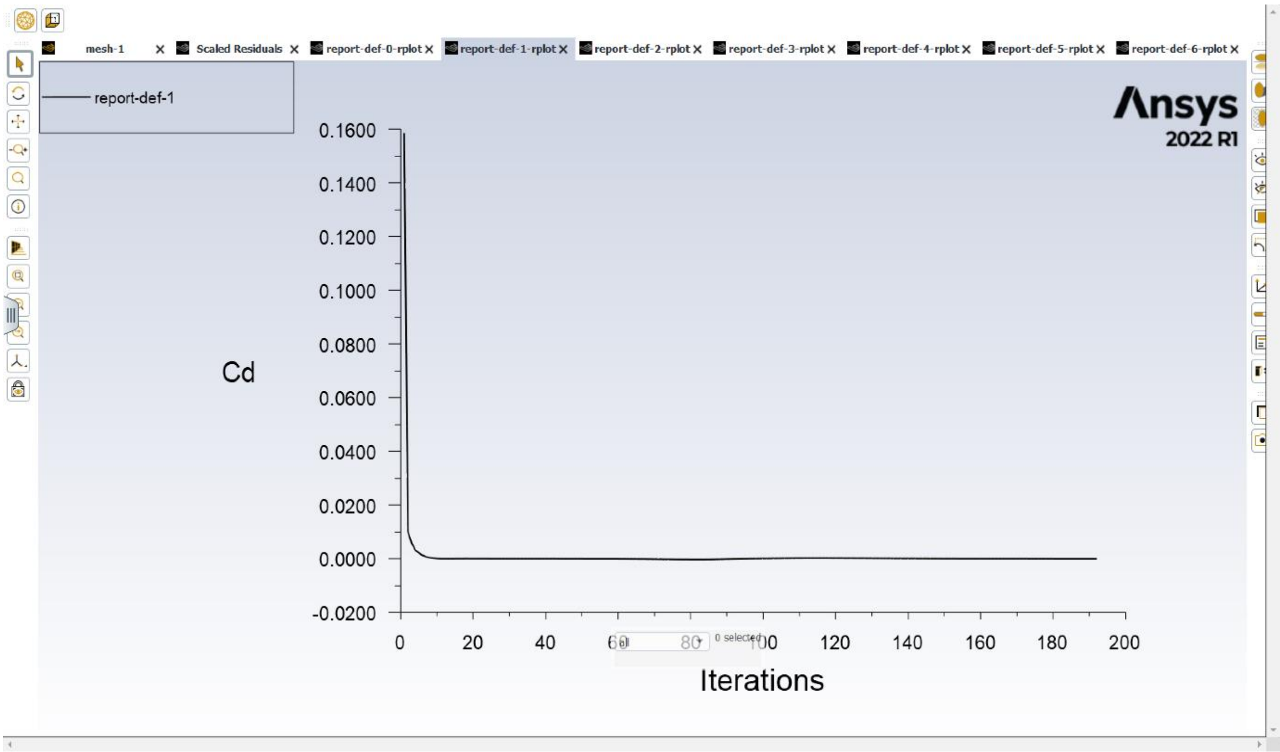


Figure 37 Drag coefficient of Skywalkers X8

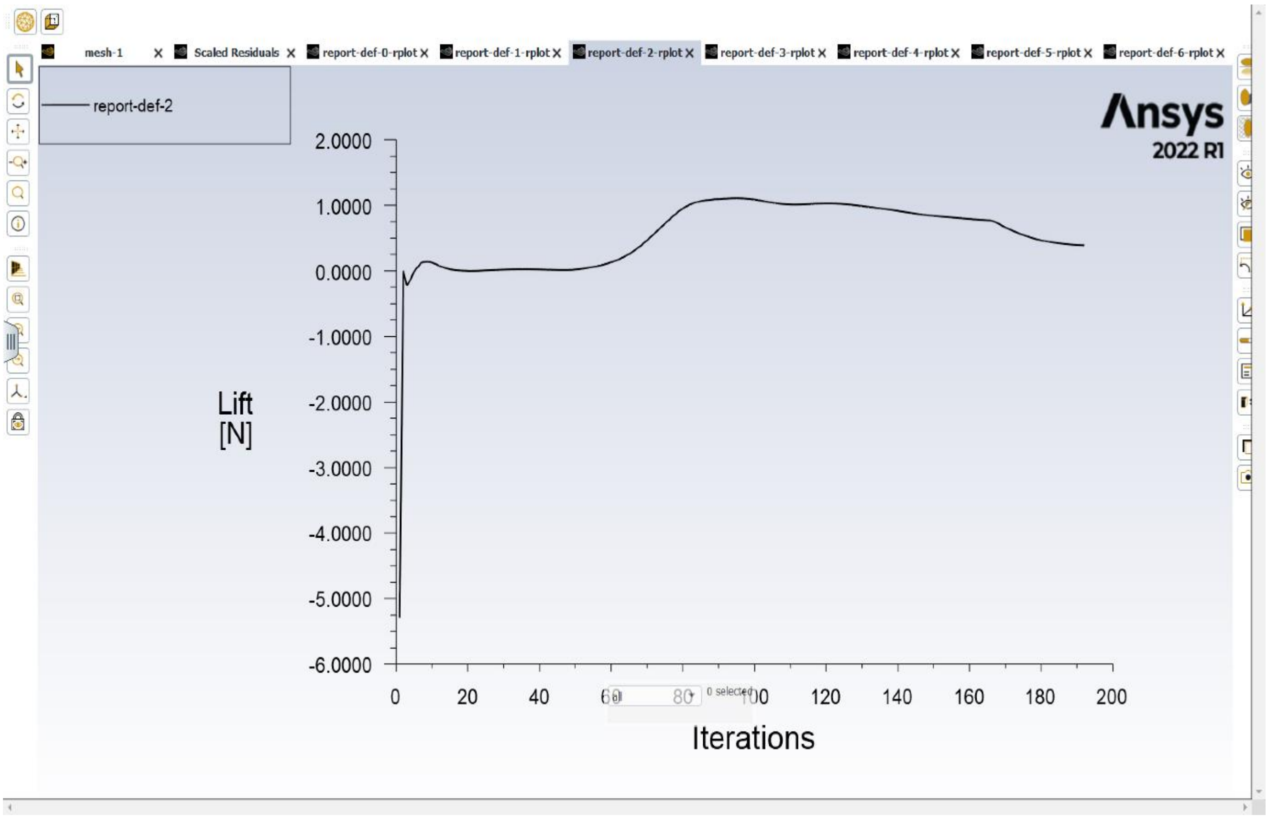


Figure 38 The drag of Skywalkers X8

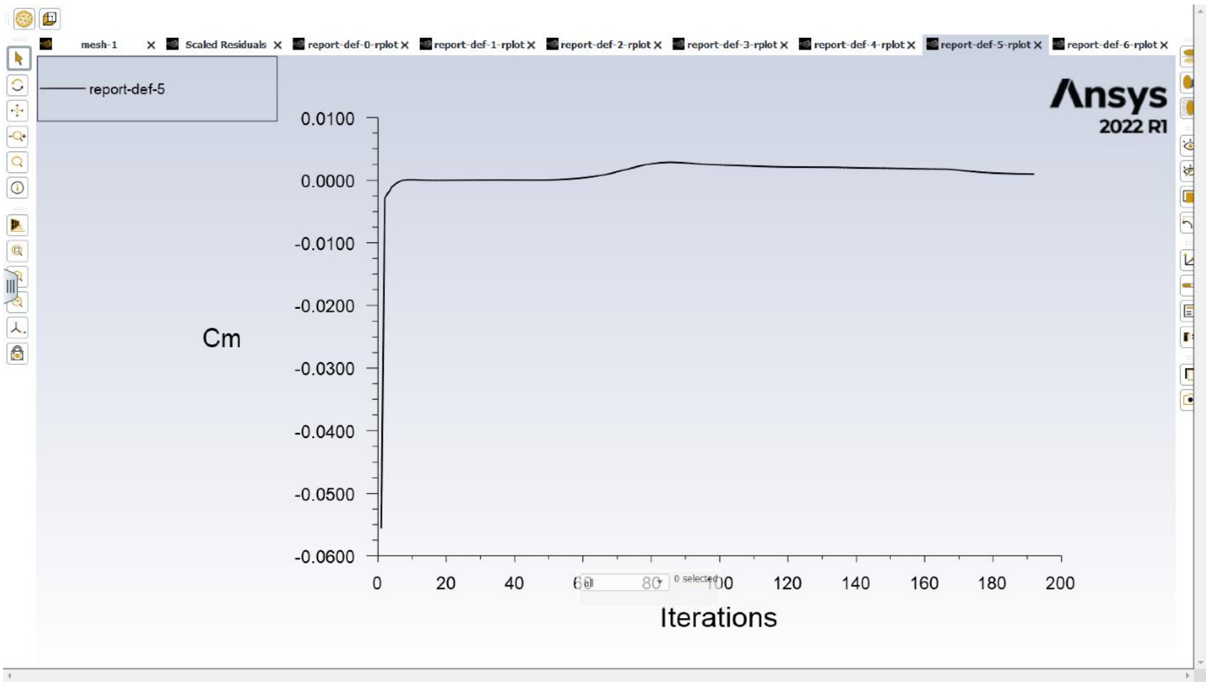


Figure 39 Moment-coefficient of Skywalkers X8

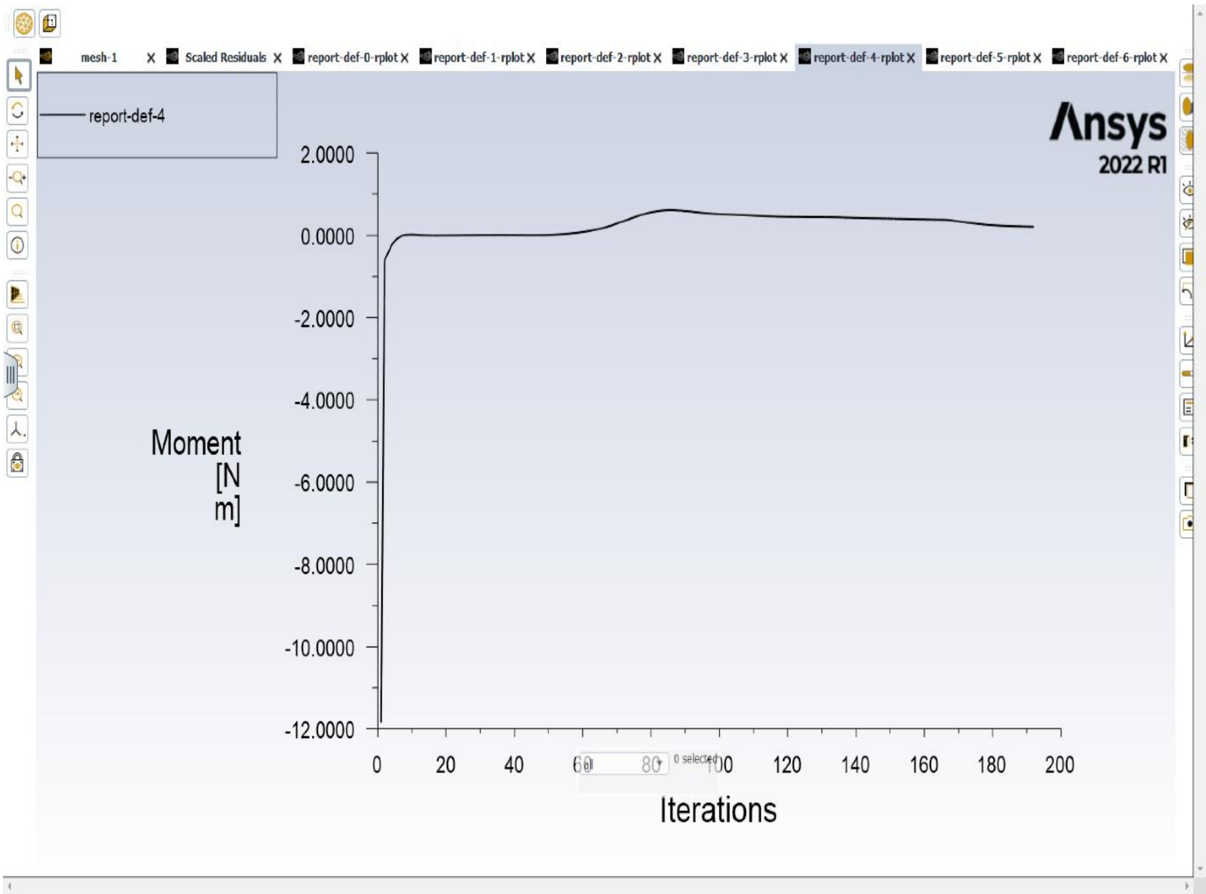


Figure 40 Moment of Skywalkers X8

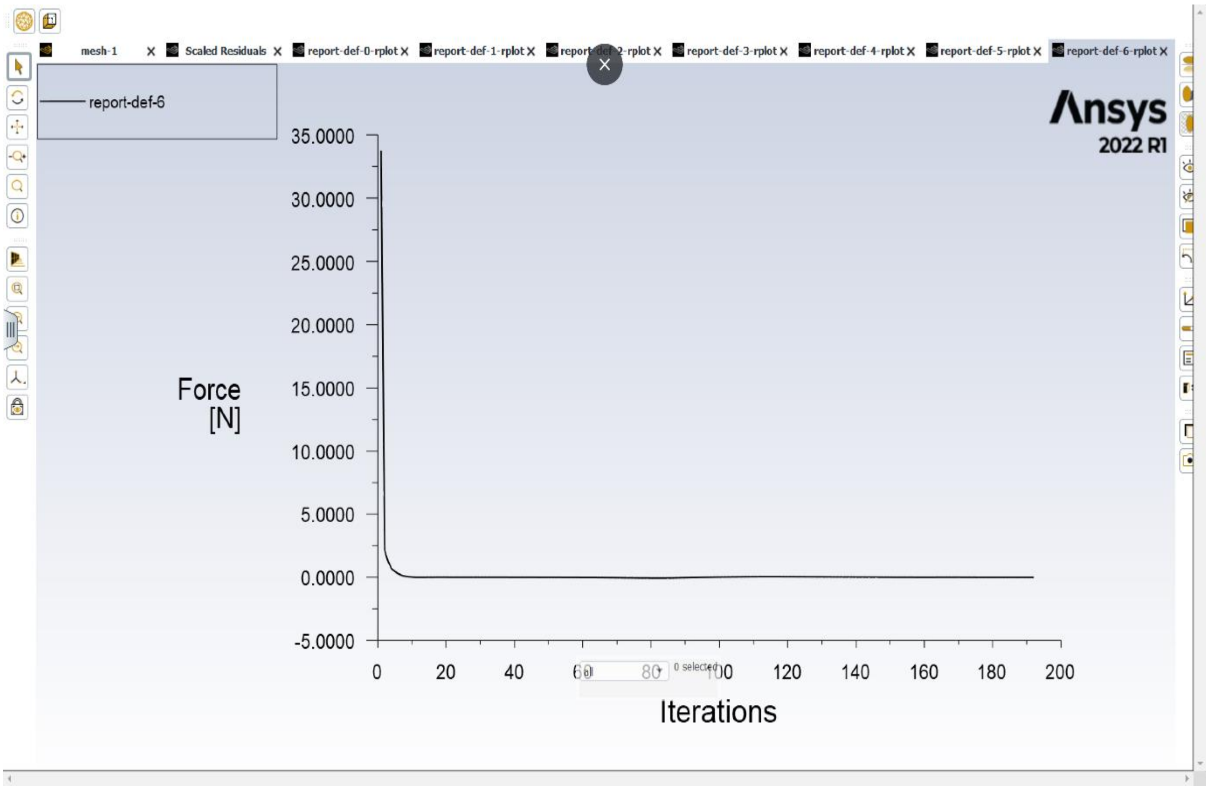


Figure 41 Force of Skywalkers X8

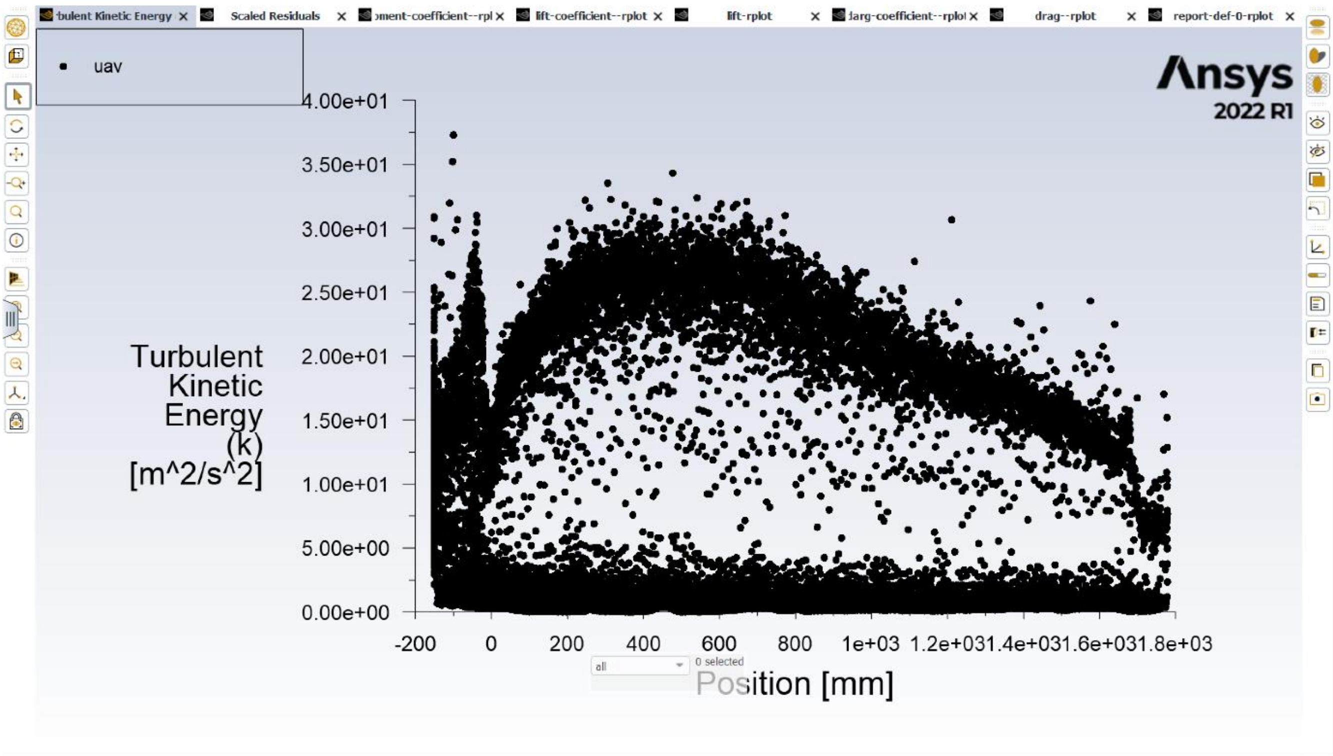


Figure 42 The turbulent kinetic energy of Skywalkers X8

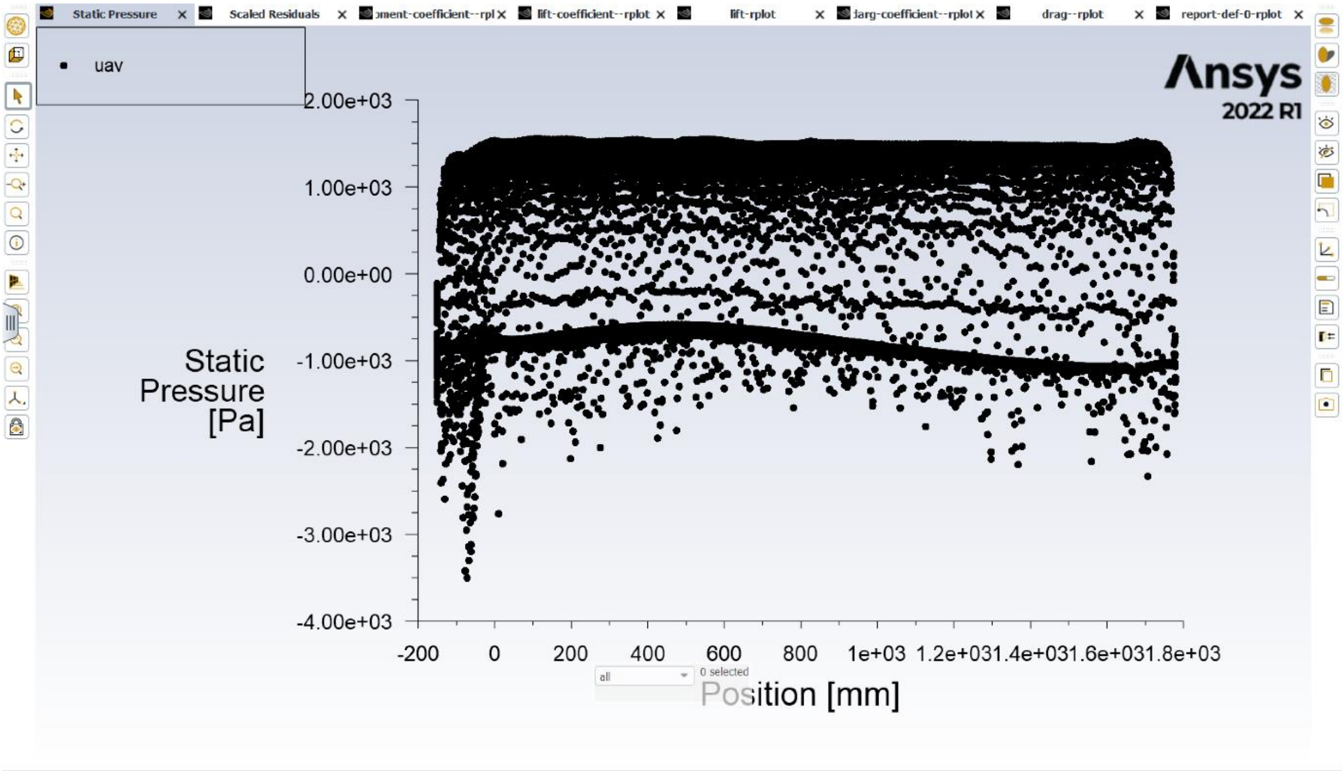


Figure 43 The static kinetic energy of Skywalkers X8

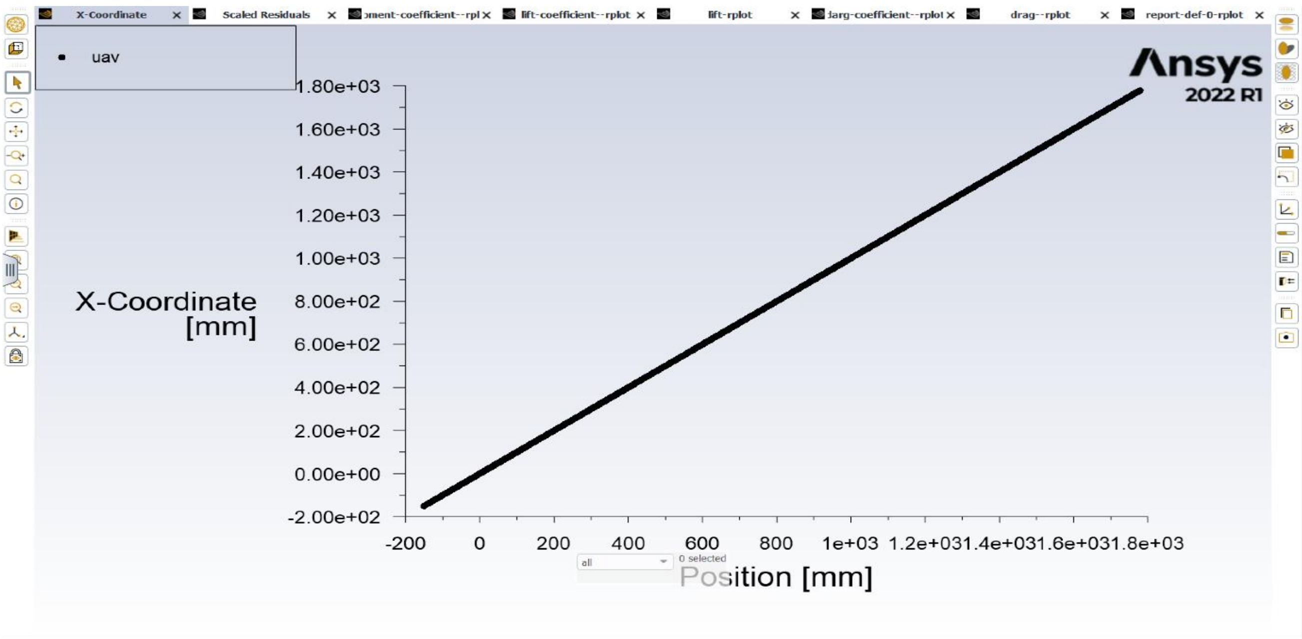


Figure 44 Meshing result of Skywalkers X8

The (34) graph shows Residual operation where continuity, x-velocity, y-velocity, z-velocity, and k-omega are calculated with 200 iterations. It is shown that the continuity equation is $10^{-3}$ which is a proper and good result.

| **Forces** | **L (lift)** | **Cl (co. of lift)** | **D(Drag)** | **Cd (C0. of Drag)** | **Cm (Co. of Moment)** | **F (Force)** |
|---|---|---|---|---|---|---|
| **Value** | **-0.08** | **0.001** | **0.004** | **0.006** | **0.009** | **0.001** |

Table 7 Value of different forces

## 3.10 Results

Once the set-up results are done then it is calculated for results. In the results, streamlined velocity is calculated which shows that the how fluid flow in the enclosure. This shows how aircraft will encounter the flow of the air when it is flying.

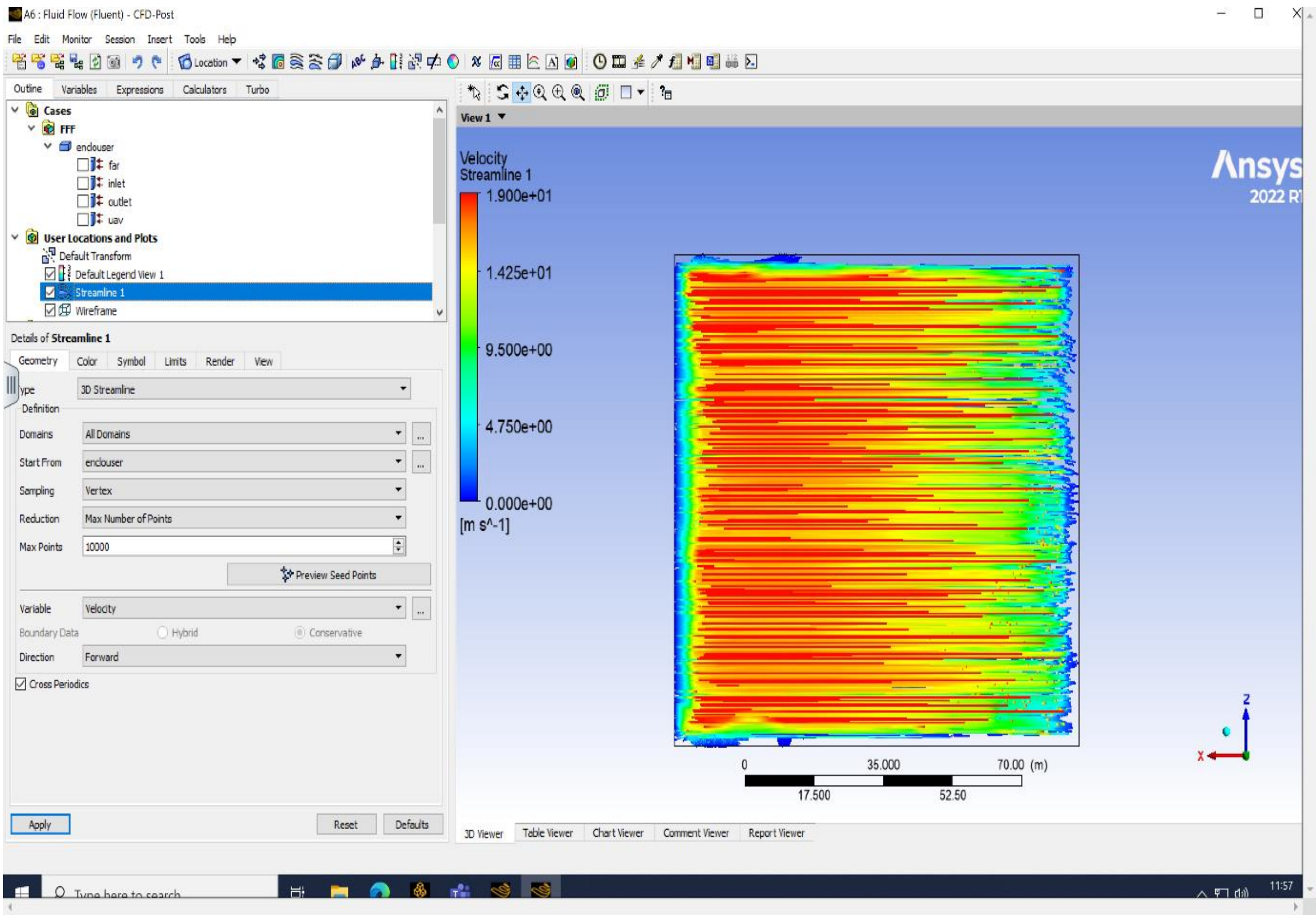


Figure 45 Velocity streamline of Skywalkers X8

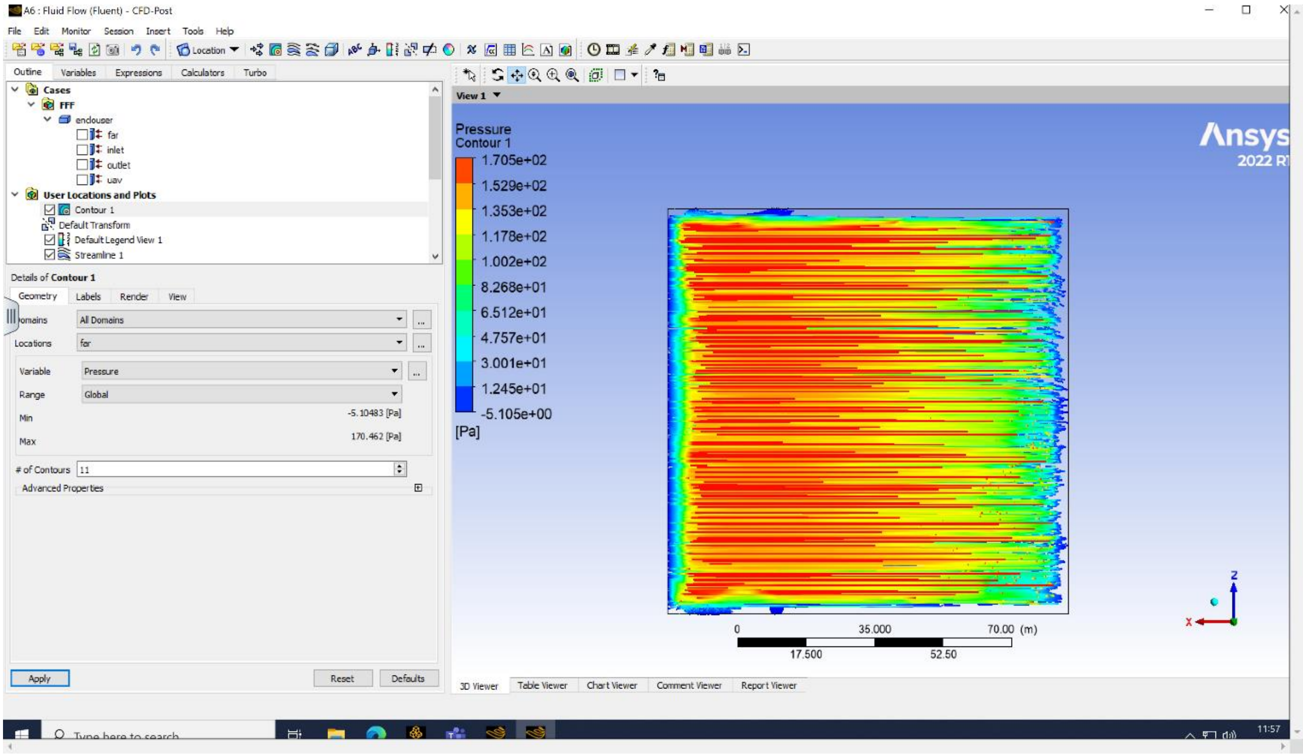


Figure 46 Pressure contour of Skywalkers X8

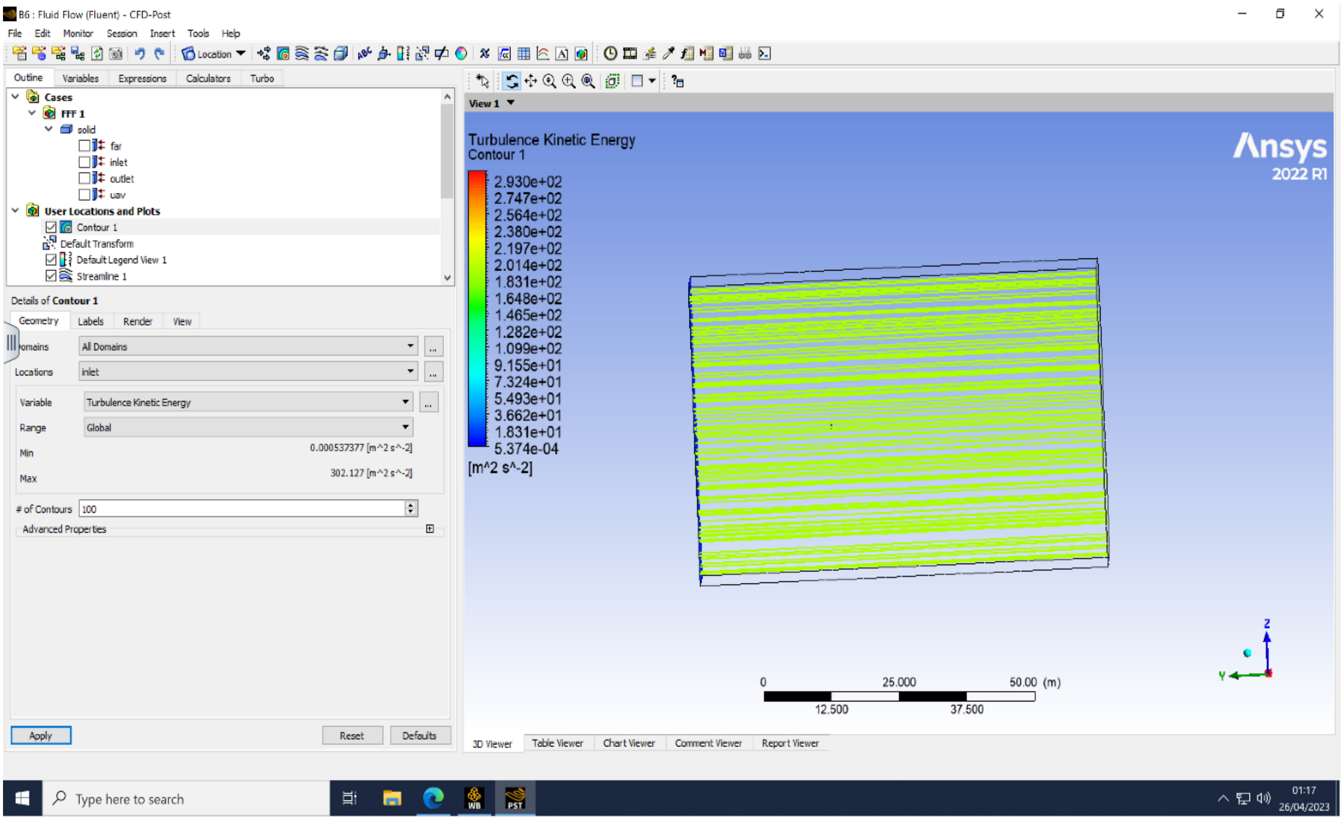


Figure 47 Turbulence kinetic energy contour of Skywalkers X8

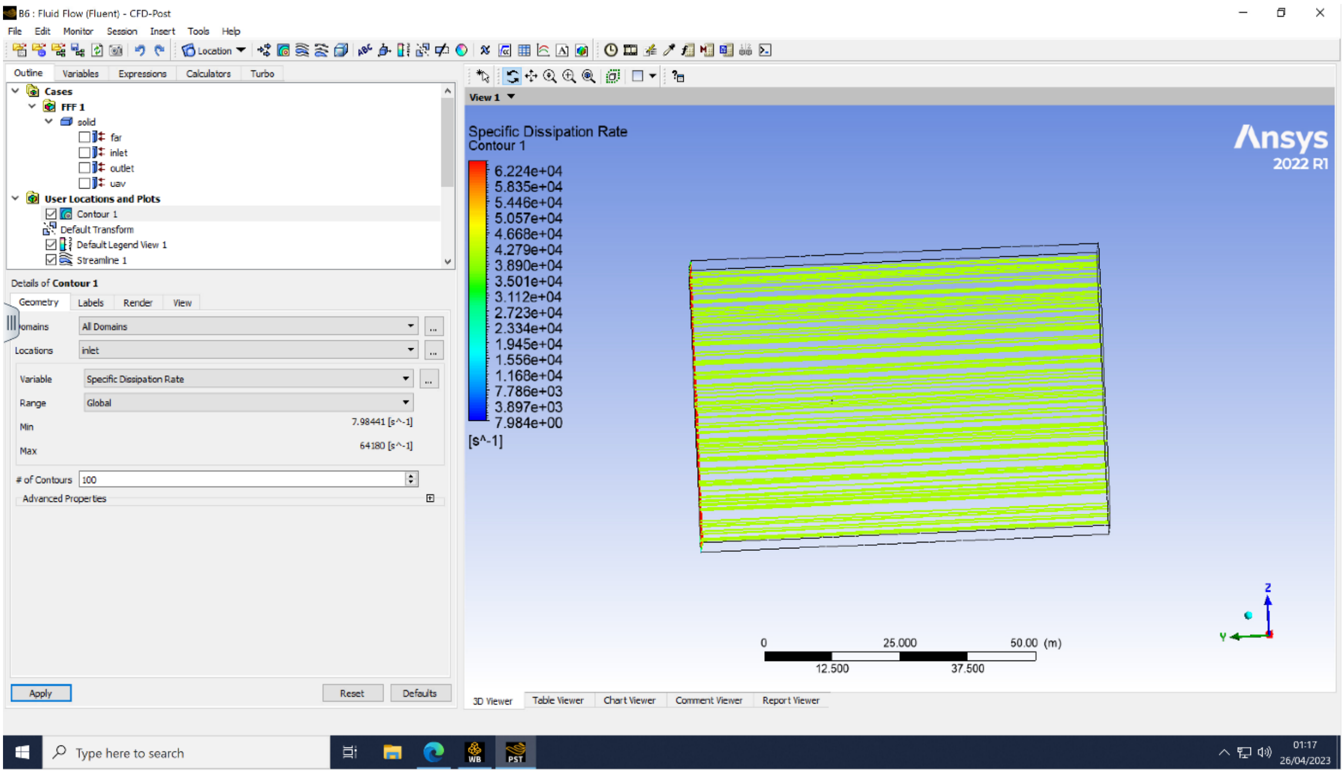


Figure 48 Specific Dissipation Rate Contour of Skywalkers X8

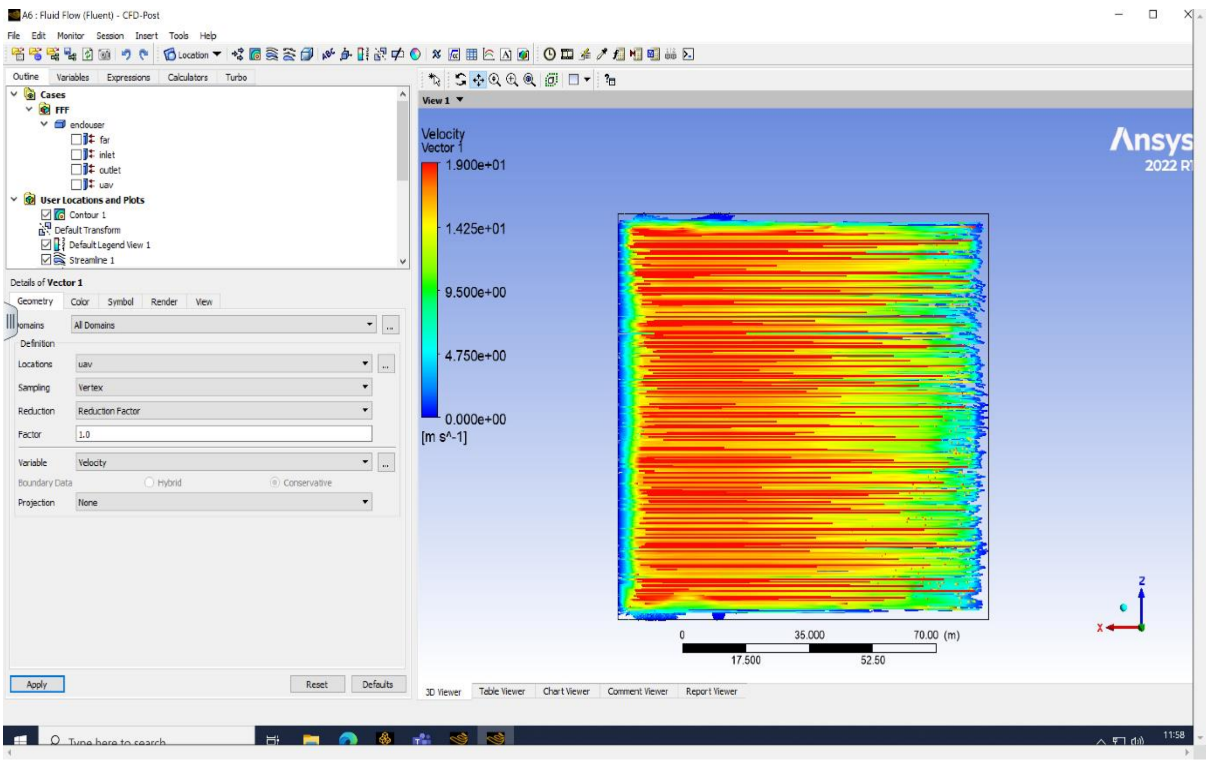


Figure 49 Velocity Contour 1 of Skywalkers X8

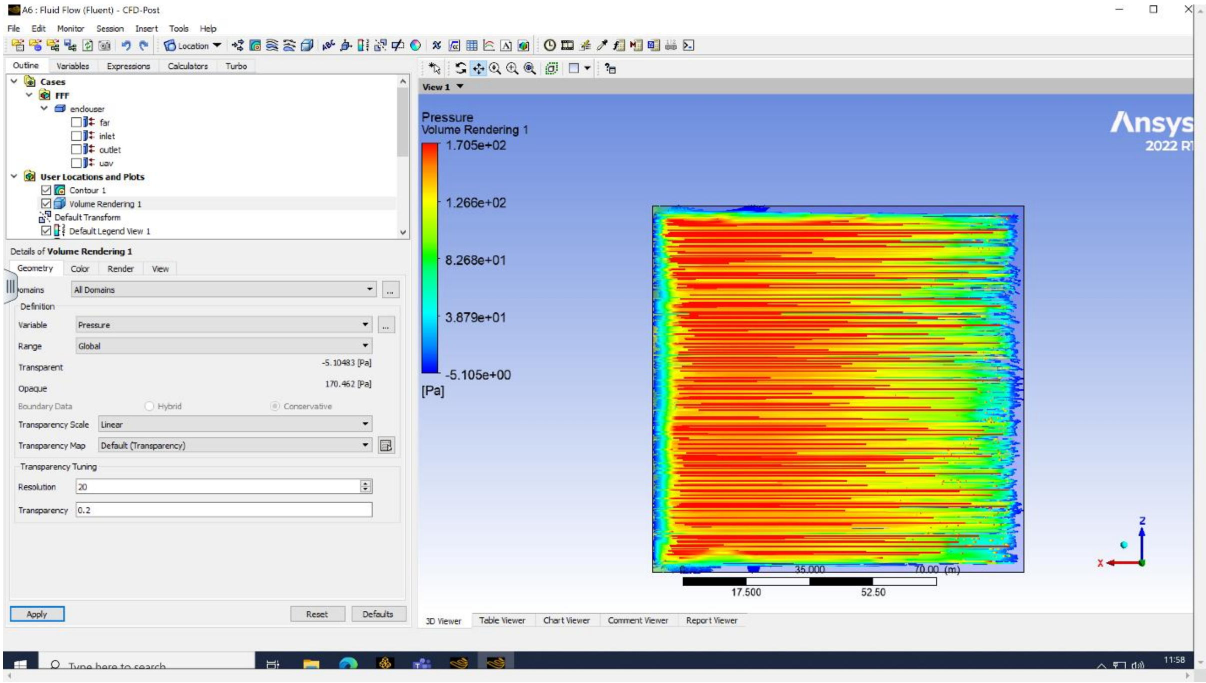


Figure 50 Pressure-Volume Rendering of Skywalkers X8

The aircraft’s centre experiences a stagnation situation, and the velocity contour shows that the aircraft's tip has the highest velocity of any other area. The pressure contour, on the other hand, shows a higher-pressure concentration across the leading surface of the aircraft and low pressure is noted at the tip of the propellers where flow separation occurs.

| | |
|---|---|
| **Velocity streamline** | **190 m/s** |
| **Pressure contour** | **$1.75*10^2$ Pa** |
| **Turbulence kinetic energy contour** | **$2.903*10^3$ $m^2/s^2$** |
| **Specific Dissipation Rate Contour** | **$6.2*10^4$ /s** |
| **Velocity Contour 1** | **190 m/s** |
| **Pressure-Volume Rendering** | **$1.705*10^2$ Pa** |

## 3.10. FEA Analysis

By breaking complicated structures and systems down into tiny, linked pieces, finite element analysis (FEA) is a computer method used to analyse them. Aerial photography, surveying, and mapping are prominent uses of the Skywalker X8 aircraft. A collection of linked pieces that each represent a minor portion of the aircraft can be used to simulate the aeroplane in FEA.

There are various steps to do FEA analysis.

### 3.10.1 Selection of Geometry

The first step is to create the geometry in Solidworks, or any CAD software and it should be accurate and proper in shape and size. Similarly, the force and torque are applied to the geometry by using the Simulation command in Solidworks. A force of 100 N is applied to the structure to calculate the remaining task.

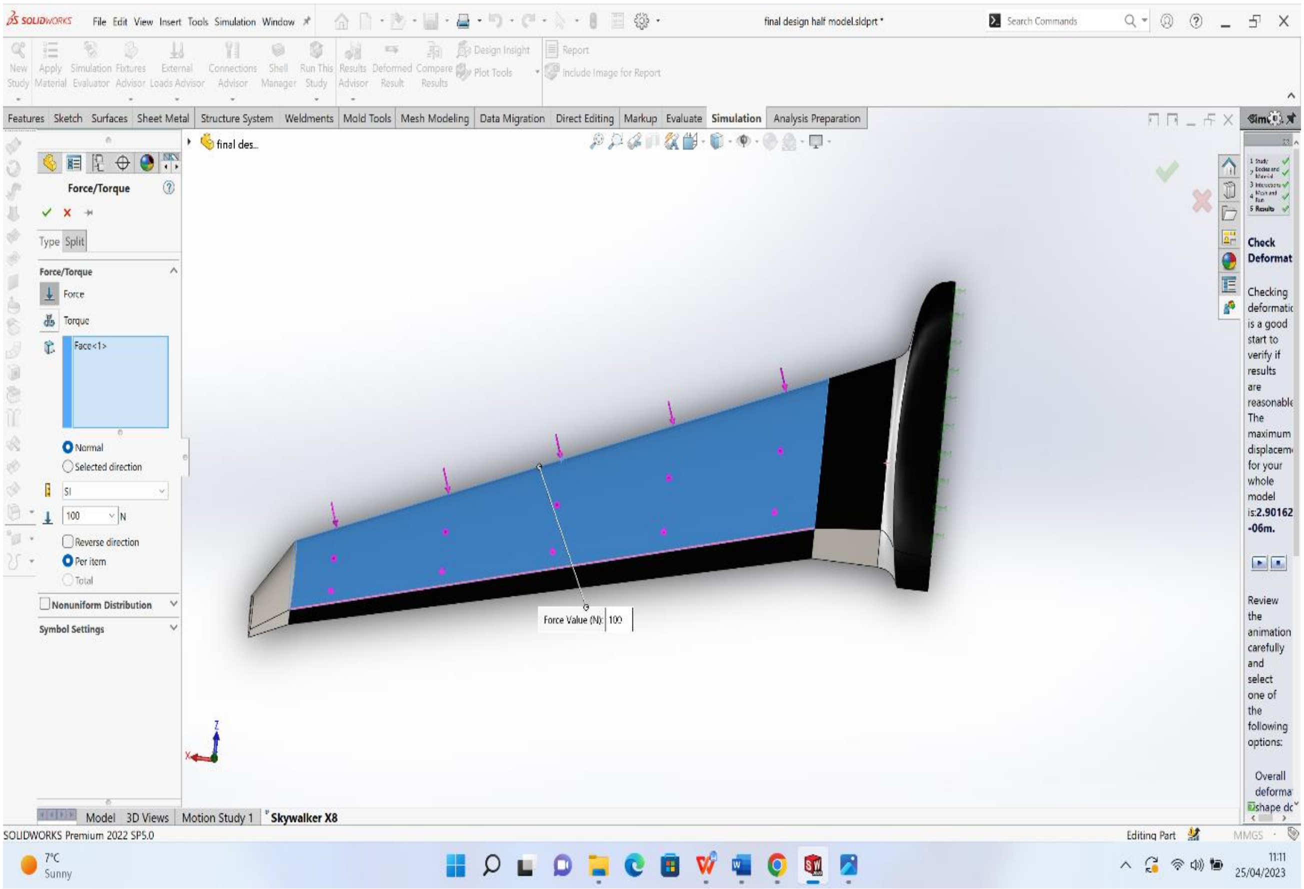


Figure 51 Force and torque applied to the Skywalker X8

### 3.10.2 Generating Mesh

Once the force is applied the geometry is subjected to the meshing process where the model is broken down into small parts which are shown in the figure (52).

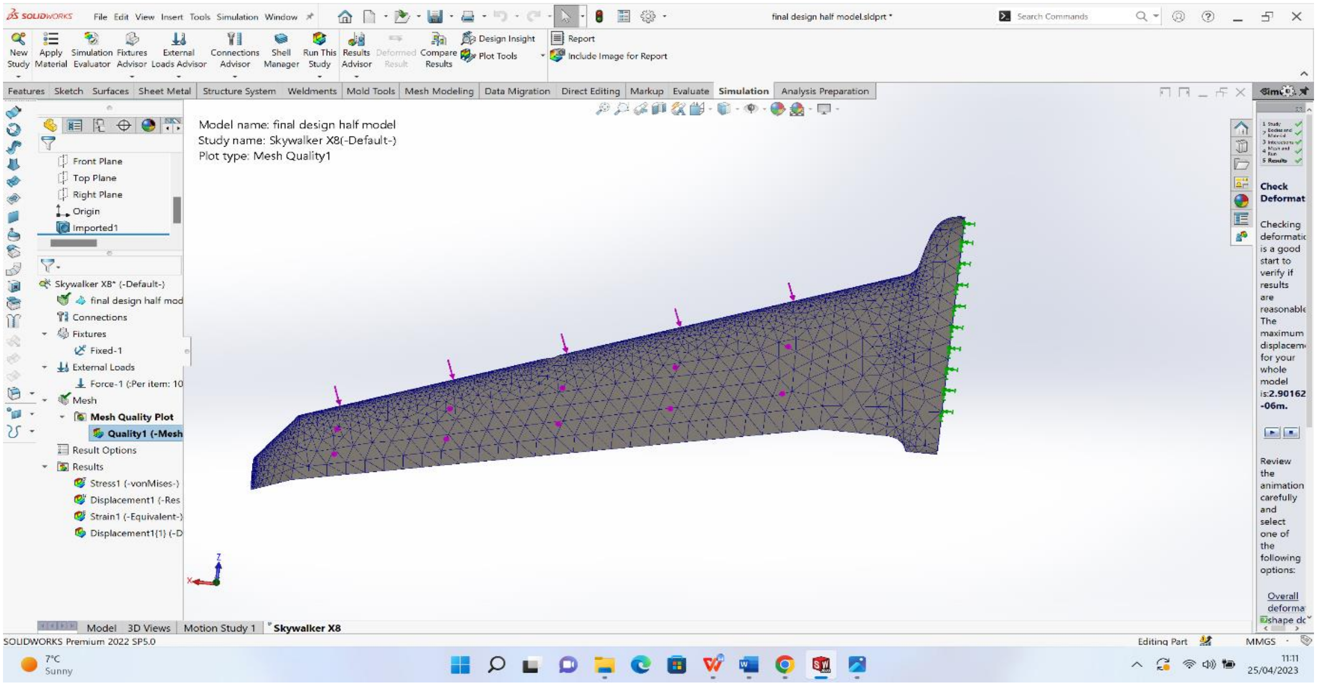


Figure 52 The meshing of the Skywalker X8

### 3.10.3 Boundary condition and FEA analysis

The loads that the aircraft will encounter during flight, including aerodynamic forces, gravitational forces, and thrust, are defined as part of the boundary conditions for the study.

To calculate the deformation, stress, and strain in each component of the model, the FEA programme solves a set of equations. Colour-coded maps or contour plots can be used to display the results.

To ensure that the study was accurate, the FEA findings are contrasted with experimental data or analytical solutions. The model may be improved by using any inconsistencies between the FEA and the experimental data to increase the precision of upcoming studies.

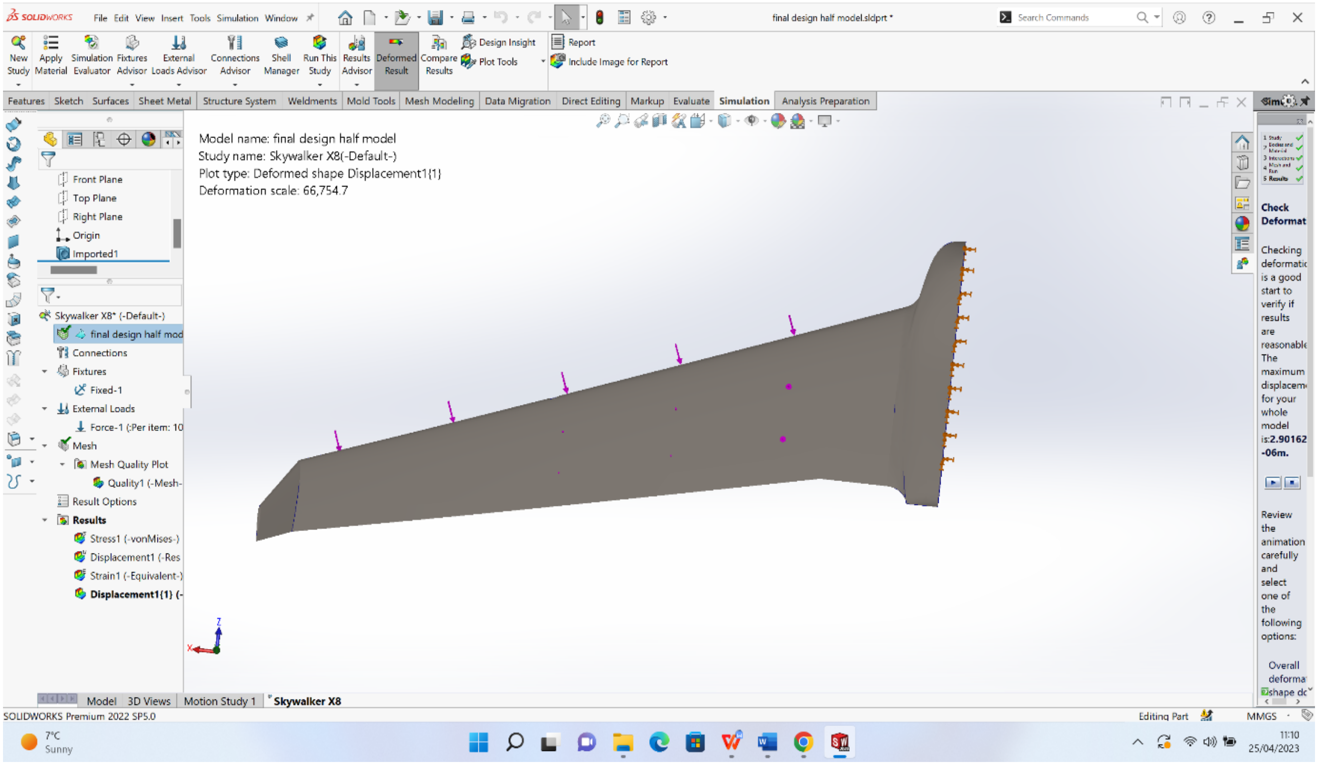


Figure 53 Deformed shape displacement of Skywalker X8

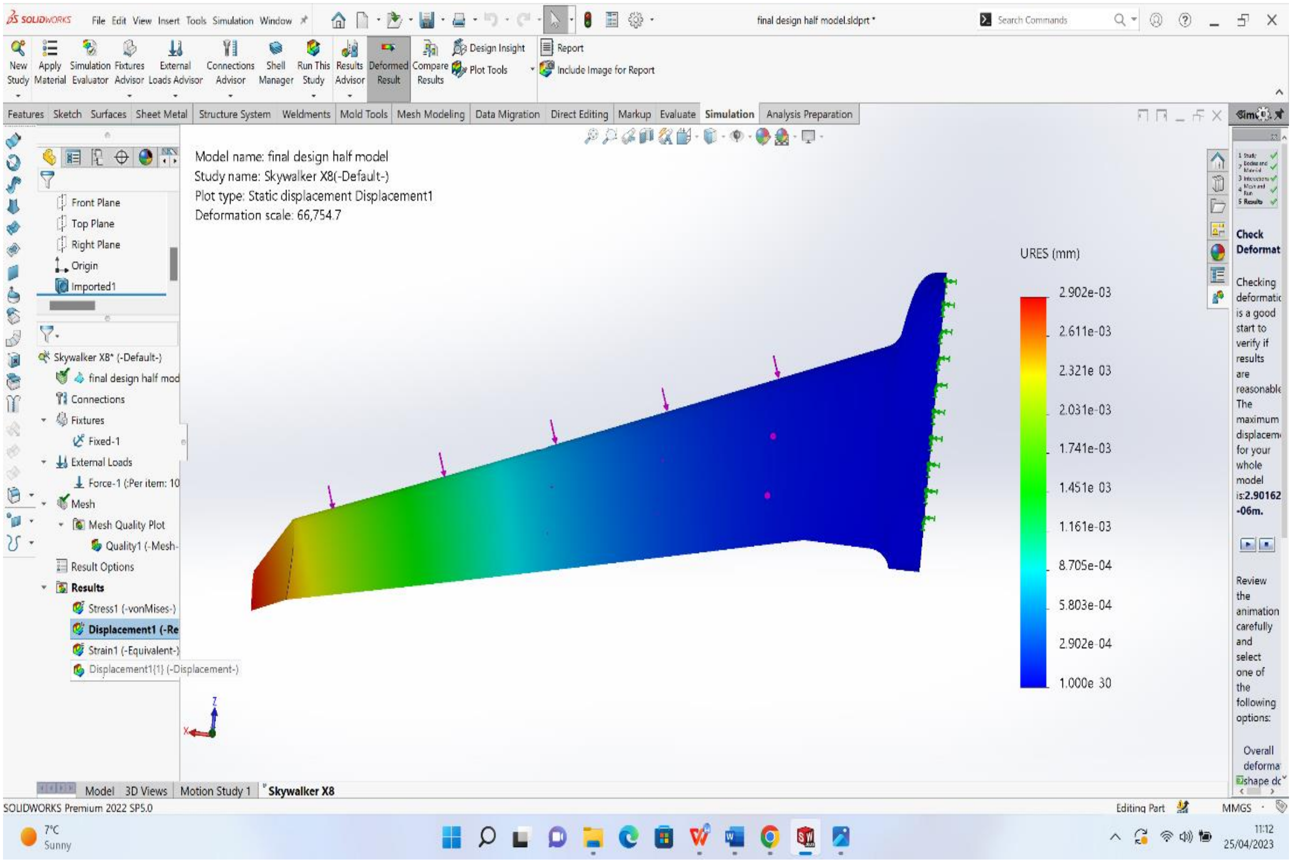


Figure 54 Static displacement of Skywalker X8

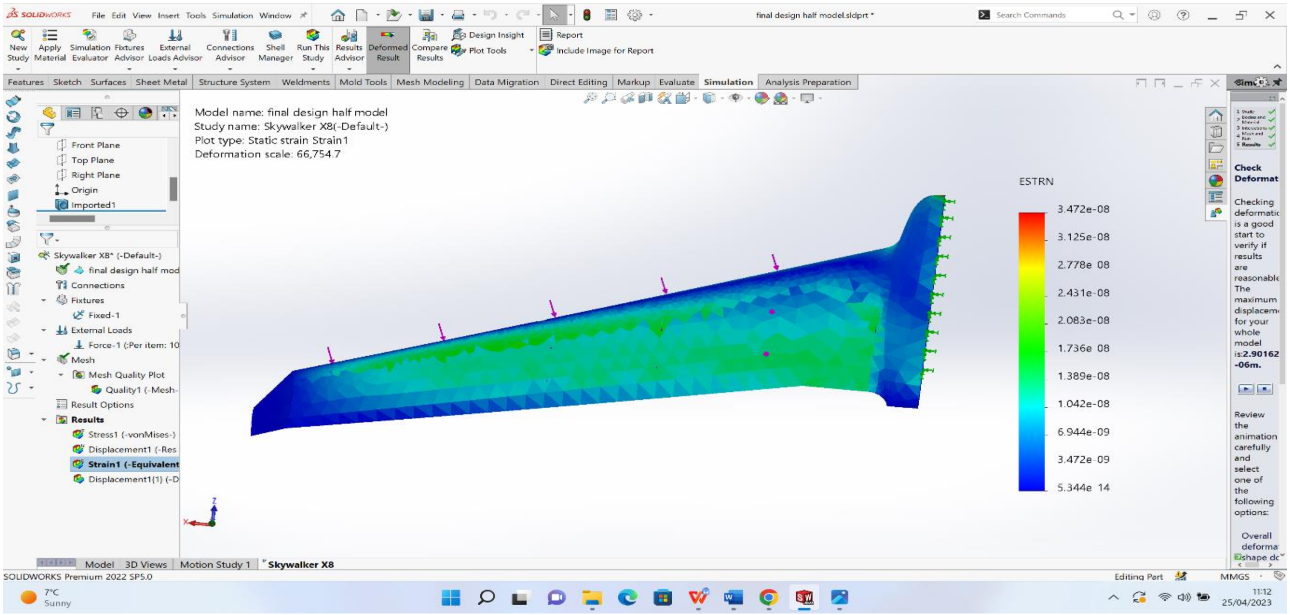


Figure 55 Static strain displacement

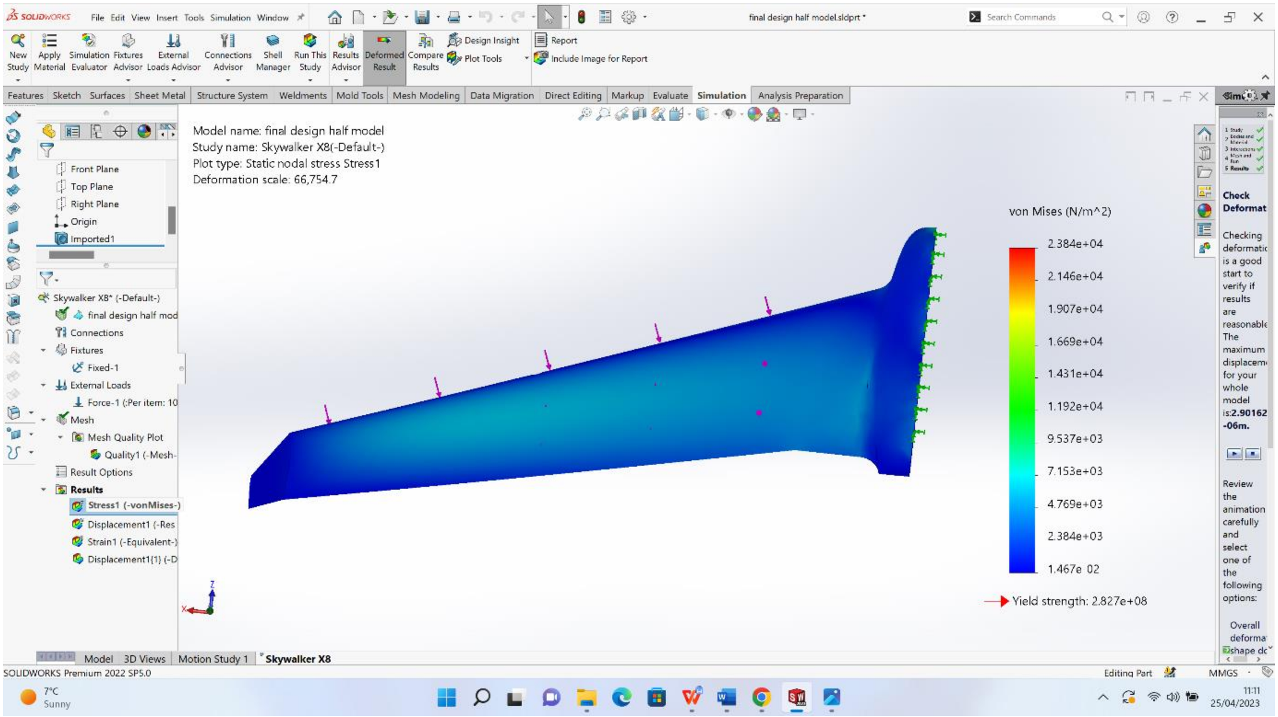


Figure 56 Static nodal stress

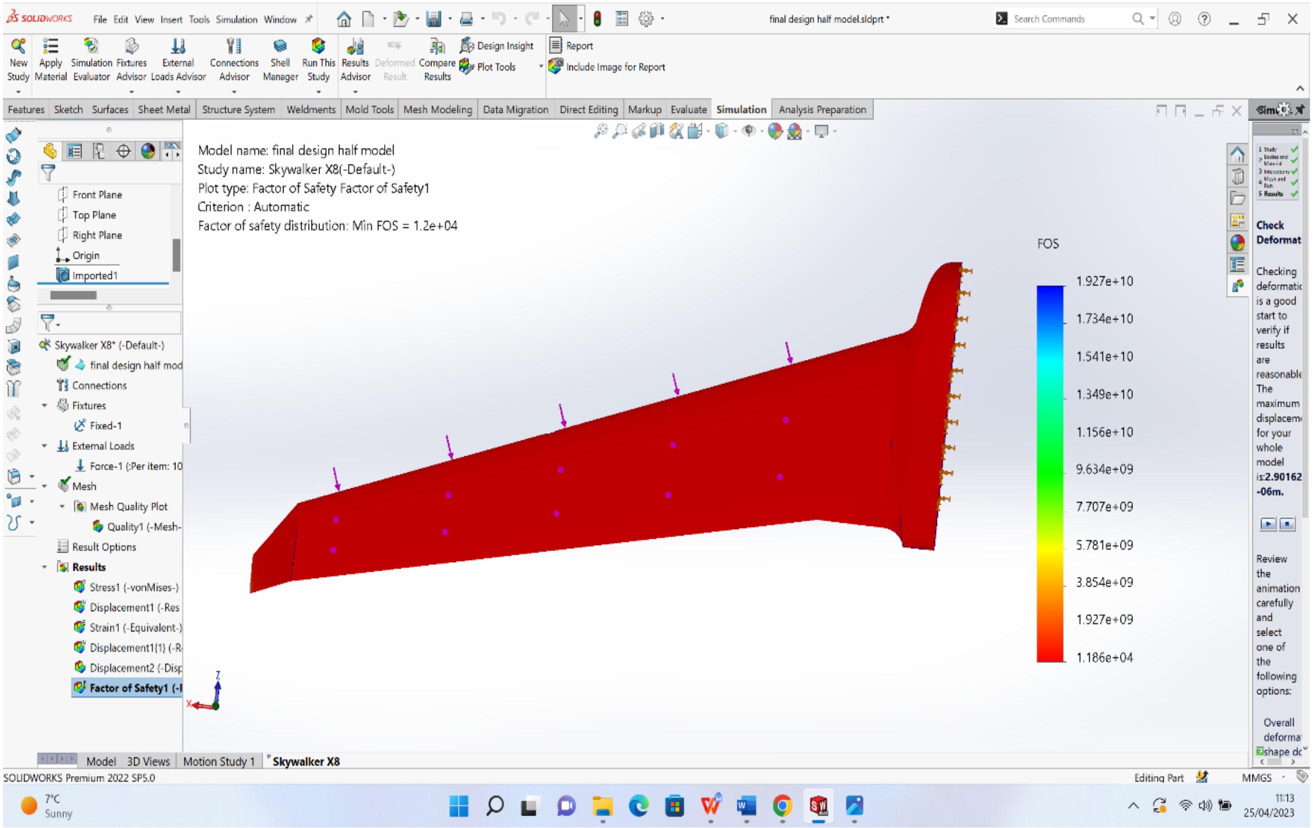


Figure 57 The factor of safety of the Skywalker X8

The industry norm for the "a factor of safety" for aircraft is 1.5. The importance of weight in aviation is exemplified by the thin factor of safety. Additionally, it indicates that a lot more time, engineering analysis, and testing have been invested in determining the maximum load and the characteristics of the components on the plane.[38] Here, in this report the FOS is around 1.9 which shows that the aircraft is suitable to use.

# CHAPTER -4

## 4.1 WIND TUNNEL TESTING

The mass balance's precision determines how accurate the records from a wind tunnel testing are. As a measurement of the minimal load for the mass balance, this accuracy is often expressed, so the nominal load should accurately represent the assumed loads in the experiment.

Since small UAVs direct at lower Reynolds numbers (Re)1 than larger aircraft, for which most wind tunnels are designed, this presents a challenge when testing them in wind tunnels. As a result, there is very little impact that UAVs have on the mass balance. There are two obvious alternatives, each with a flaw, to maximise the signal-to-noise ratio of the forces surveyed in the experiment.

Using a mass balance that is intended for monitoring small forces is the first way to reduce noise. As such, mass balances tend to be more expensive and have a smaller range. The alternative method is to increase the UAV's forces on the mass balance to the point where the precision of the mass balance is minimal in contrast. As a result, the tests must be run at larger Reynolds numbers because force and Reynolds numbers are directly related. Increasing the airspeed is the most practical way to increase the Reynolds number, followed by employing a larger model of the UAV and lowering the viscosity. This method's disadvantage is that the UAV will be subjected to a greater structural load.

If the servos are unable to handle the bigger moment brought on by the higher airspeed, the UAV may suffer structural damage as well as a change in the deflection of its control surfaces. Furthermore, for actual flight conditions, the Reynolds numbers ought to be representative.

## 4.2 Wind Tunnel Specification

The wind tunnel device is present in the report where the test is conducted in present in **De Montfort University, United Kingdom**. A gap was cut in the back of the fuselage to allow the mass-balance to be securely fastened inside before the UAV was mounted so that it could be flown through the wind tunnel. The forces as well as moments exerted on the UAV are determined using this on the inside mounted strain gauge mass balance. outlines the wind tunnel's basic specifications, including its nominal forces, moments, and accuracy. The mass balance is also connected to a perpendicular rod that can be adjusted longitudinally and laterally to alter the angle of attack and the side-slip angle, respectively.

## OPERATING CONDITIONS

**OPERATING ENVIRONMENT:**

Laboratory

**STORAGE TEMPERATURE RANGE:**

–25°C to +55°C (when packed for transport)

**OPERATING TEMPERATURE RANGE:**

+5°C to +40°C

**OPERATING RELATIVE HUMIDITY RANGE:**

80% at temperatures < 31°C decreasing linearly to 50% at 40°C

## SPECIFICATION – WIND TUNNEL (AF1300)

TecQuipment is committed to a programme of continuous improvement; hence we reserve the right to alter the design and product specification without prior notice.

**NETT DIMENSIONS AND WEIGHT (ASSEMBLED):**

3700 mm x 1065 mm x height 1900 mm and 293 kg

**APPROXIMATE PACKED VOLUME AND WEIGHT:**

4.9 $m^3$ and 450 kg

**SPACE NEEDED:**

Solid, level floor – allow at least 2 m of free space around the inlet and 4 m at the outlet

**WORKING SECTION:**

305 mm x 305 mm, and 600 mm long.

Air velocity: 0 to 36 $m.s^{-1}$

**NOISE LEVELS:**

80 dB(A) at operators ear level.

**ELECTRICAL SUPPLY (THREE PHASE):**

220 VAC to 240 VAC 50 Hz/60 Hz (20 A) or

380 VAC to 440 VAC 50 Hz/60 Hz (16 A)

## ANCILLARY AND EXPERIMENT SPECIFICATIONS

For specifications of included and optional ancillaries and experiments please see their individual data sheets.

Figure 58 Detail specification of the Wind tunnel


Figure 59 Wind tunnel AFI300 SUBSONIC

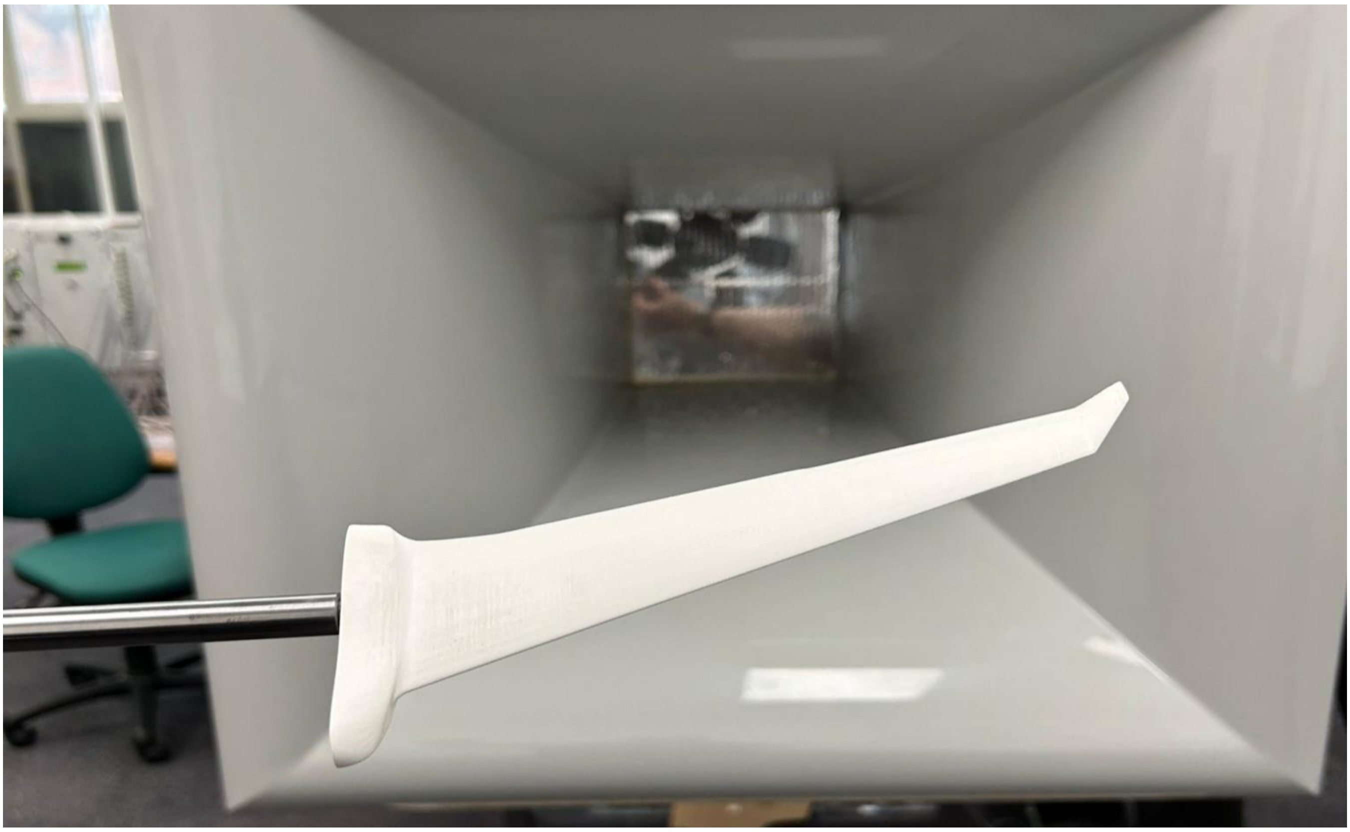

Figure 60 Aircraft before testing

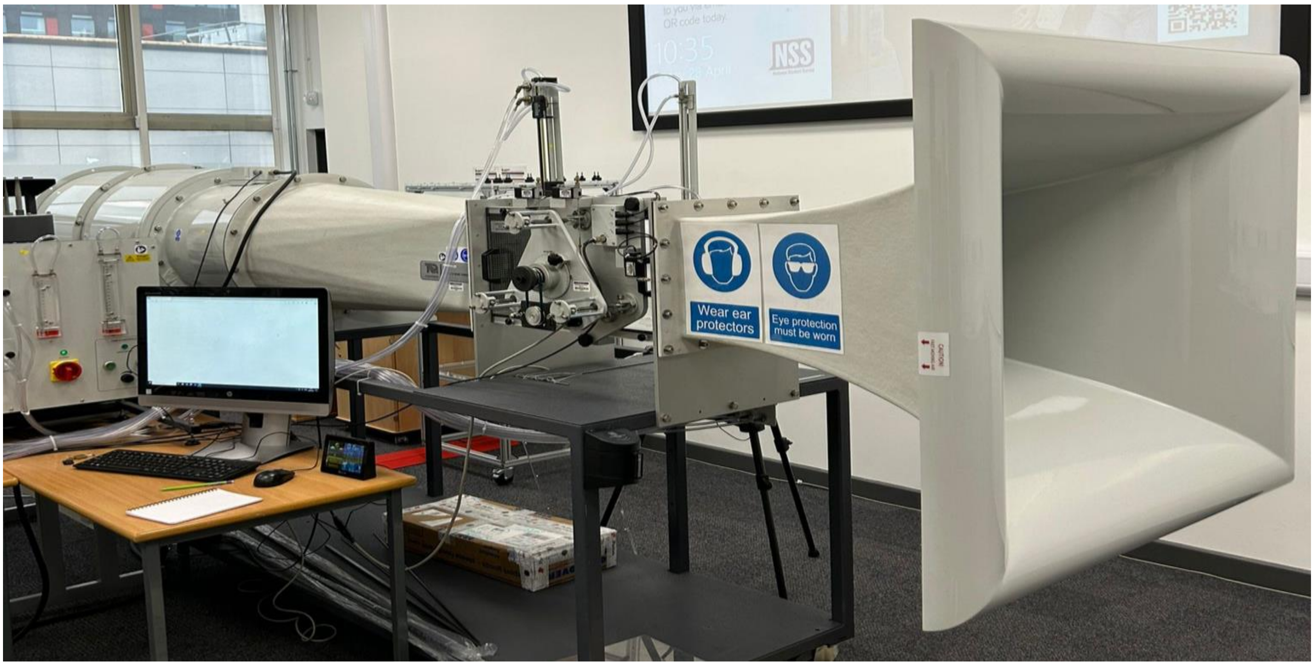


Figure 61 Wind tunnel setup before the test

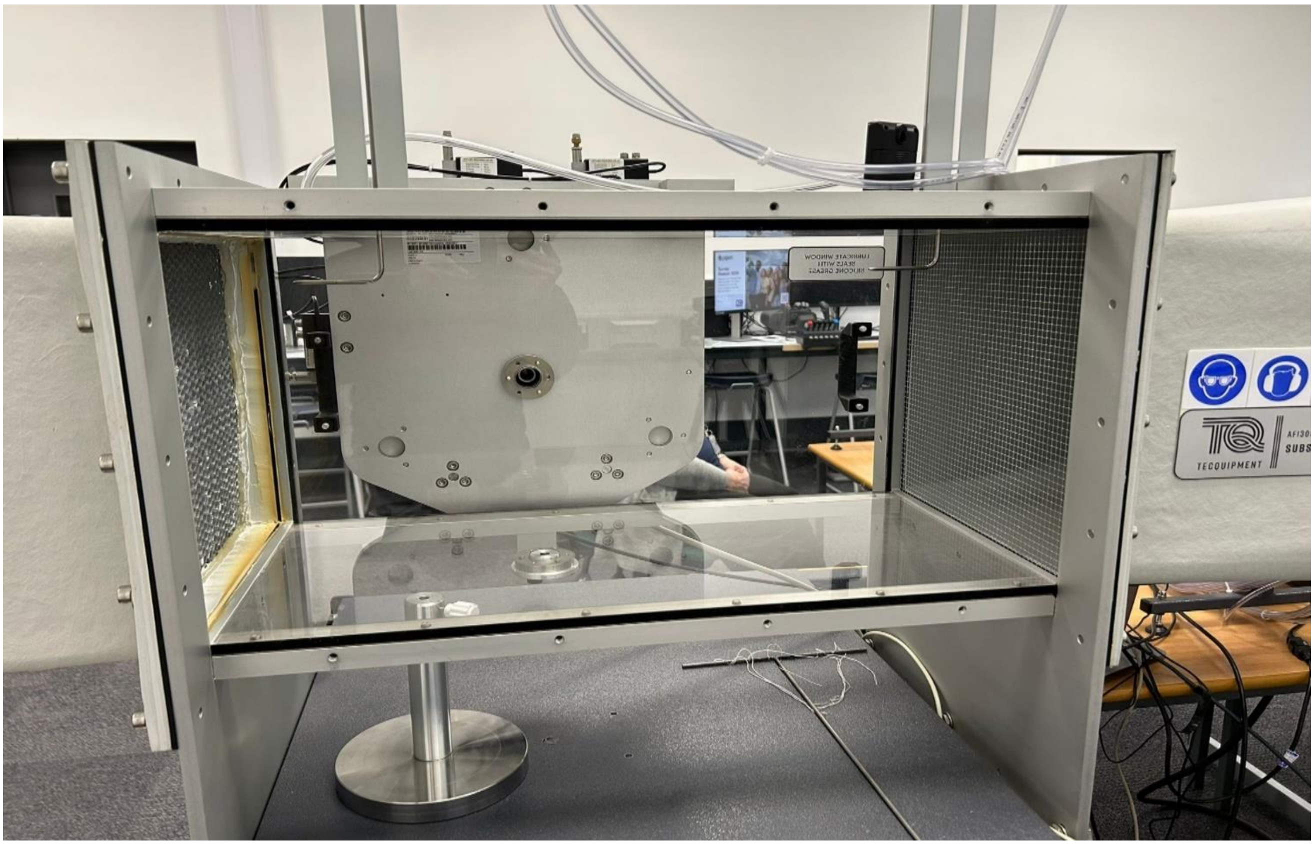

Figure 62 The operating portion of TecQuipment's subsonic wind tunnel (AF1300) can accommodate Three-Component Balance.

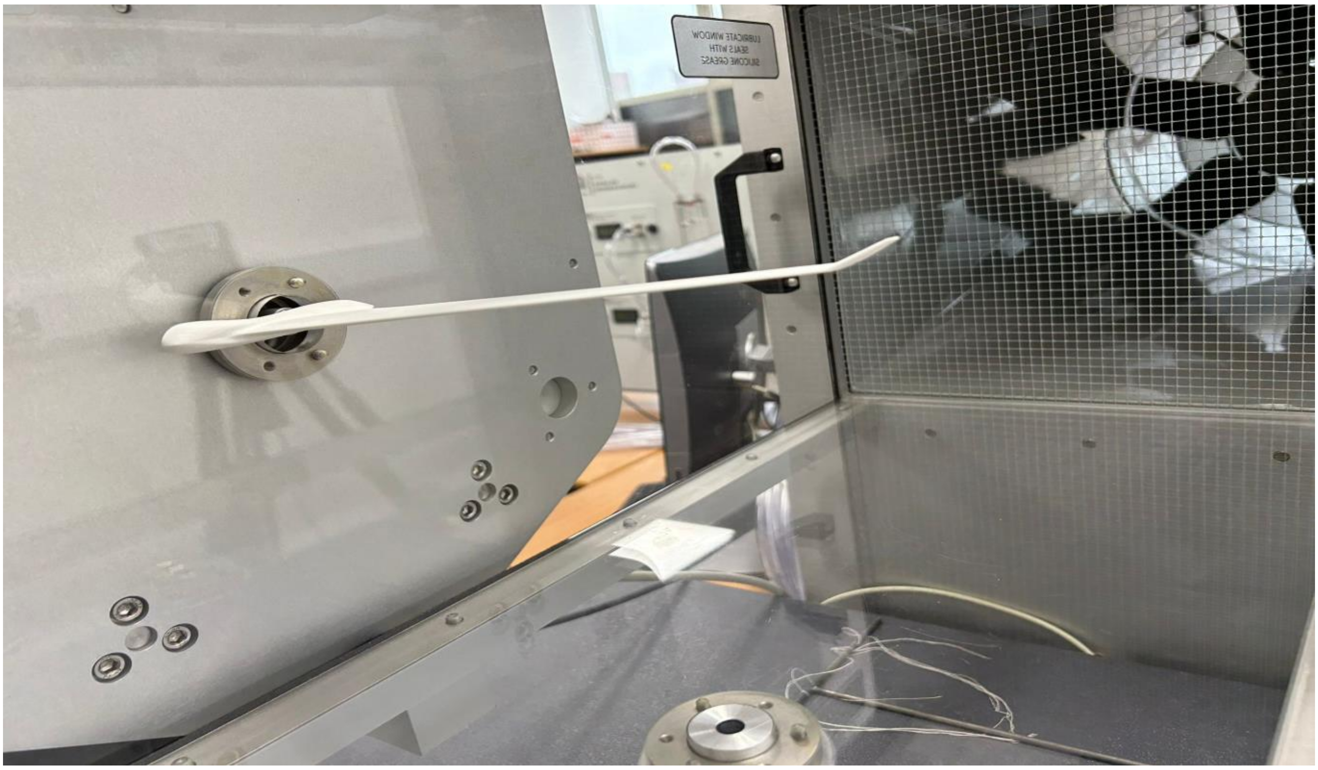

Figure 63 Aircraft fit for testing.


Figure 64 Atmospheric temperature detector

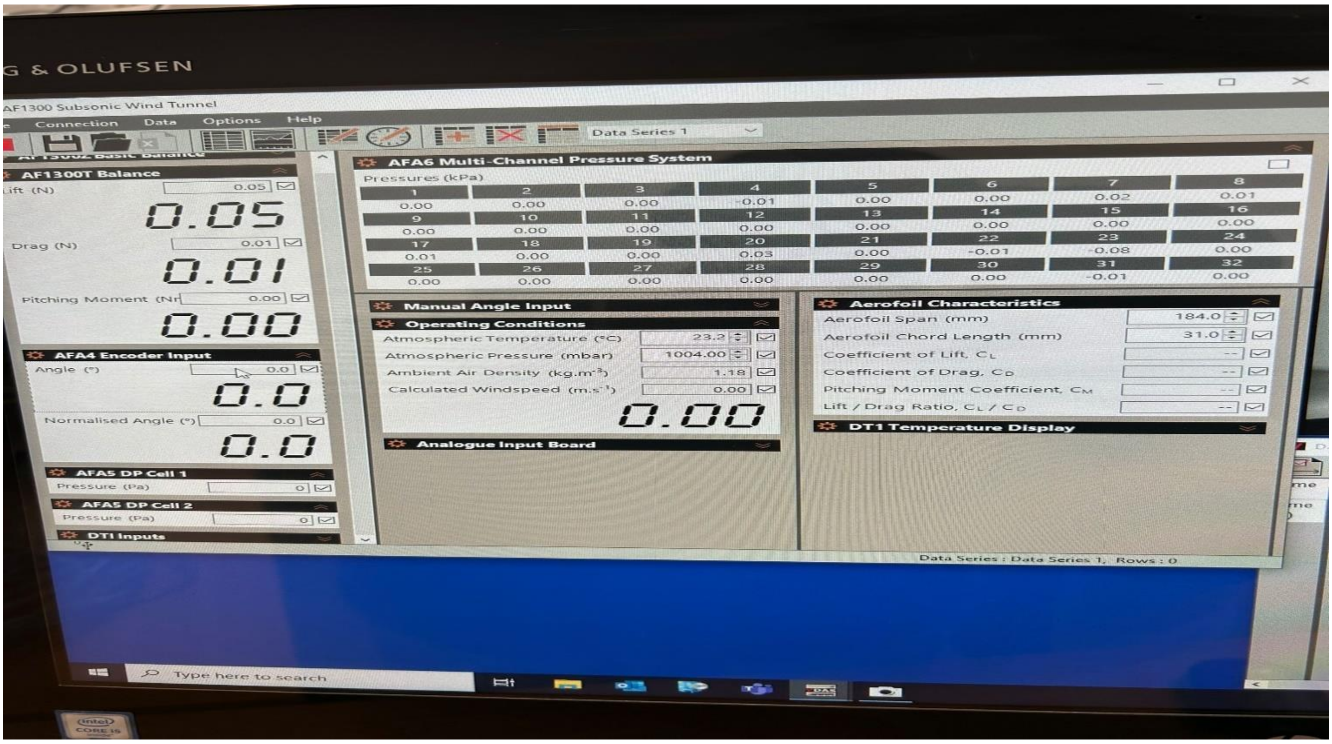


Figure 65 Initial setup before lift and drag.


Figure 66 Wind tunnel sensors are kept at zero before testing.

## 4.3 Data from Wind Tunnel

| Time | AF1300T Balance | | | AFA4 Encoder Input | | AFA5 DP Cell 1 | AFA5 DP Cell 2 |
|---|---|---|---|---|---|---|---|
| Time | Lift | Drag | Pitching Moment | Angle | Normalised Angle | Pressure | Pressure |
| (s) | (N) | (N) | (Nm) | (°) | (°) | (Pa) | (Pa) |
| 0 | **0.00** | **0.00** | 0.00 | 0.0 | 0.0 | 0 | 1 |
| 83.2 | **-0.02** | **0.08** | 0.00 | 0.0 | 0.0 | 215 | 248 |
| 118.3 | **-0.50** | **0.11** | 0.02 | 355.0 | 5.0 | 206 | 252 |
| 147 | **-0.92** | **0.23** | 0.02 | 350.0 | 10.0 | 219 | 247 |
| 178.2 | **-0.96** | **0.37** | 0.02 | 345.0 | 15.0 | 219 | 246 |
| 210.3 | **0.01** | **0.14** | 0.00 | 0.0 | 0.0 | 218 | 246 |
| 469.6 | **-0.05** | **0.08** | 0.00 | 0.0 | 0.0 | 220 | 246 |
| 499.5 | **0.52** | **0.09** | 0.01 | 5.0 | -5.0 | 220 | 249 |
| 544.9 | **0.92** | **0.14** | 0.01 | 10.0 | -10.0 | 213 | 246 |
| 576.1 | **0.99** | **0.28** | 0.02 | 15.0 | -15.0 | 207 | 248 |

Table 8 Data from testing of lift and drag.

| Operating Conditions | | | |
|---|---|---|---|
| **Atmospheric Temperature** | **Atmospheric Pressure** | **Ambient Air Density** | **Calculated Windspeed** |
| (°C) | **(mbar)** | (Kg.m$^{-3}$) | (m.s$^{-1}$) |
| | | | |
| 23.2 | 1004.00 | 1.18 | 0.00 |
| 23.2 | 1004.00 | 1.18 | 19.08 |
| 23.2 | 1004.00 | 1.18 | 18.68 |
| 23.2 | 1004.00 | 1.18 | 19.26 |
| 23.2 | 1004.00 | 1.18 | 19.26 |
| 23.2 | 1004.00 | 1.18 | 19.21 |
| 23.2 | 1004.00 | 1.18 | 19.30 |
| 23.2 | 1004.00 | 1.18 | 19.30 |
| 23.2 | 1004.00 | 1.18 | 18.99 |
| 23.2 | 1004.00 | 1.18 | 18.72 |

Table 9 Operating Conditions of the wind tunnel

| Aerofoil Characteristics | | | | | |
|---|---|---|---|---|---|
| **Aerofoil Span** | **Aerofoil Chord Length** | Coefficient of Lift, $C_L$ | Coefficient of Drag, $C_D$ | Pitching Moment Coefficient, $C_M$ | Lift / Drag Ratio, $C_L / C_D$ |
| **(mm)** | **(mm)** | | | | |
| 184.0 | 31.0 | -- | -- | -- | -- |
| | | | | | |
| 184.0 | 31.0 | -0.02 | 0.07 | 0.00 | -0.29 |
| 184.0 | 31.0 | -0.43 | 0.09 | 0.55 | -4.78 |
| 184.0 | 31.0 | -0.74 | 0.18 | 0.52 | -4.11 |
| 184.0 | 31.0 | -0.77 | 0.30 | 0.52 | -2.57 |
| 184.0 | 31.0 | 0.01 | 0.11 | 0.00 | 0.09 |
| 184.0 | 31.0 | -0.04 | 0.06 | 0.00 | -0.67 |
| 184.0 | 31.0 | 0.41 | 0.07 | 0.26 | 5.86 |
| 184.0 | 31.0 | 0.76 | 0.12 | 0.27 | 6.33 |
| 184.0 | 31.0 | 0.84 | 0.24 | 0.55 | 3.50 |
| | | | | | |

Table 10 Aerofoil Characteristics

## 4.4 Analysis

The right ambient pressure and temperature have been set for the wind tunnel. With the assistance of the rod depicted in the Figure (63), the aeroplane is secured into a three-Component balance. All the sensors are initially examined, and the lift drag is held at zero.

The aircraft should also be maintained at an angle of attack of $0^0$. The wind tunnel is turned on, the angle is adjusted based on the situation, and the results are noted. The values of lift and drag are recorded, and the coefficient of lift and drag is determined using the lift and drag values shown in the table.

It can be shown that the lift and drag on Skywalkers X8 are **-0.08** and **0.004** respectively and that the lift and drag on other models are equally **-0.05** and **0.08**. So, it follows that software testing and wind tunnel testing have similar values.

It has been demonstrated that the aircraft has plastic characteristics that could impact the results of wind tunnel tests.

# CHAPTER-5

## 5. DISCUSSION AND CRITICAL ANALYSIS

The report's primary goal is to understand Skywalkers X8's expertise. Here, the aircraft's 2.12 m wing is designed in Solidworks, and it is then imported into Ansys for engineering analysis. The aircraft is sent for 3D printing after the appropriate software examination. Following that, the workpiece is tested in a wind tunnel for additional analysis. The excellent performance of the aircraft is quantified in this study and aids in the development of better low-speed aircraft on the market. To develop the aircraft, a market analysis is also required. This investigation and study will be beneficial to those in the developing aeronautical field who are looking at the use of planes in the military and other scientific endeavours.

Many difficulties arise during the development of aircraft. Firstly, it is very difficult to design an aircraft with proper dimensions, the dimensions of the aircraft determine the weight of the aircraft. Since the weight is directly proportional to the force applied to the aircraft. The performance of an aeroplane is significantly influenced by the weight distribution. Your aircraft's fuel consumption, speed, rate of ascent, controllability, ceiling, and even structural integrity will all be impacted by the way it is loaded. [35]

Once the geometry has been decided upon, a 2L enclosure must be created. Because the geometry is not selected in the correct XY-plane, drawing the enclosure with the half model is very challenging. As a result, it was decided to draw up a winning plan to address the issue. Similarly, because Ansys 23 makes the choice automatically, selecting the body and face sizing elements during meshing is quite difficult. Less than the indicated elements should make up the meshing elements. It is challenging to select the appropriate reference value because the model is free drawing. According to the wind tunnel, which uses 305*305 mm working areas as the velocity limit of 31 m/s, the referencing value and speed of the aircraft are chosen. [36].

One of the PhD seniors during the study proposes adding BOI inside the enclosure for the correct results, as indicated in the figure (5). However, it can be difficult to obtain accurate results when computing results. [7]. Like how there are differences in the materials chosen for 3D printing, there are also differences in the attributes of aeroplanes in software. Aluminium is automatically picked in the software, but plastic is used while printing. The software has a density of 1.25 whereas plastic has a density of 1.118, resulting in significantly different outcomes.

In the report, a separate section, FEA analysis is carried out to determine whether the model is fit for flight or not. The model's fundamental flaw is that it lacks a clear value for the load it needs to be supplied to function properly. The aircraft's tension and strain are what define its stability. To calculate a load, a 100 N load is typically chosen. As illustrated in Figure (57), the FOS (Factor of Safety) is calculated to be 1.9, which is in the model's favour. The best FOS, in general, ranges between 1.5 to 3 [37] and the model shows that it can carry out its flight.

When conducting wind tunnel testing, the issue arises because the working area is only 305*305 mm and the wind tunnel's top speed is 31 m/s [36]. Our attention is therefore drawn to the fact that a test at a greater velocity cannot be conducted in a wind tunnel and that a tiny model should be used instead so the selected velocity is 19 m/s.

# CHAPTER-6

## 6. CONCLUSION

The Skywalker X8 aircraft has 2.12 m wings, can carry 1-3 kg of cargo, and weighs about 0.88 kg. The design is created in the Solidworks programme, after which it is loaded into the Ansys programme for pre-processing and wind tunnel test. The exact layout of the Skywalker X8 aircraft is presented in the article, along with a proper load and performance analysis carried out with software and a check of the aircraft's static and dynamic stability.

To prepare the model as accurate a demonstration as possible utilising numerical modelling supported by wind tunnel testing, this study has provided critical considerations to make, both in the experiment design and in the interpretation of the results.

The case study of the Skywalker X8 fixed-wing UAV shows several differences that require further research through validation using flight data, despite the numerical results and wind tunnel results generally matching each other reasonably well, especially in the lift. Notably, the computational modelling understates the drag, and the pitch moment from the wind tunnel testing exhibits sensitivity to the centre of gravity. Furthermore, since they weren't put to the test, the stability coefficients from the numerical modelling need to be verified with actual flight data indoors in a wind tunnel.

Learn about various software, such as Solidworks, that is used in the report to perform various FEA analyses and design work. One of this software's significant accomplishments is the FOS, which assesses the aircraft's operational state. Like this, Ansys software aids in the execution of numerous CAD stimulation studies like pressure contour and velocity contour which establish whether the aeroplane is simple to run in various environments. It was a challenging challenge for XFLR5 to choose the NACA profile for the aircraft, but it was accomplished with an accurate and simple analysis. After these analyses are all done correctly, the aircraft can be tested as a prototype with the appropriate electronic parts, such as a motor, propeller, etc., which aid in fatigue and drop tests, and then it can be released onto the market for use.

Working on this project ultimately proved to be interesting and educational as I learned more about many subjects and was able to practise using several software programmes like Solidworks, Ansys, and XFLR5. With this project, I was able to put all the knowledge I learned during my postgraduate teaching experience to use.

# CHAPTER-7

## 7. RECOMMENDATION

In the paper, a low-speed aircraft called the Skywalkers X8 is constructed and tested. In the beginning, I would like to suggest that an aircraft undergo a fatigue and drop test.

With the aid of university funds, the correct model can be produced once the wind tunnel testing is completed and is successful. The model will also be well-equipped with the batteries, motor, many electronic sensors, cameras, etc. that go into making a full UAV. The model can be tested in the ground for fatigue and drop test after it has been prepared with the help of the professor and the lab technician. This test provides information on the aircraft's marketability.

After the drop test, we advise testing the prototype aircraft since it already matched the FOS. Although it might be costly, working with a university can make it possible.

# 8. REFERENCE

**[1]** Anderson, Jr, J. (1997). A History of Aerodynamics: And Its Impact on Flying Machines (Cambridge Aerospace Series). Cambridge: Cambridge University Press. doi:10.1017/CBO9780511607158

**[2]** Imperial War Museums (2018). A Brief History of Drones. [online] Imperial War Museums. Available at: https://www.iwm.org.uk/history/a-brief-history-of-drones.

**[3]** Markets and Markets. (n.d.). *Unmanned Aerial Vehicle (UAV) Market Trends & Growth Driver MarketsandMarkets™*. [online] Available at: https://www.marketsandmarkets.com/Market-Reports/unmanned-aerial-vehicles-uav-market-66

**[4]** Barnhart, R., Hottman, S., Marshall, D. and Shappee, E. (n.d.). *INTRODUCTION TO UNMANNED AIRCRAFT SYSTEMS*

**[5]** Sam Daley (2022). What Is A Drone? What Are Uses For Drones? | Built In. [online] builtin.com. Available at: https://builtin.com/drones.

**[6]** ANSYS Innovation Courses. (n.d.). *What are BOIs and FOIs — Lesson 2*. [online] Available at: https://courses.ansys.com/index.php/courses/add-local-sizing/lessons/what-are-bois-and-fois-lesson-2/#:~:text=Among%20the%20different%20local%20sizings [Accessed 1 Apr. 2023].

**[7]** Schellenberg, B., Richardson, T., Watson, M., Greatwood, C., Clarke, R., Thomas, R., Wood, K., Freer, J., Thomas, H., Liu, E., Salama, F. and Chigna, G. (2019). Remote sensing and identification of volcanic plumes using fixed-wing UAVs over Volcán de Fuego, Guatemala. *Journal of Field Robotics*, 36(7), pp.1192–1211. doi: https://doi.org/10.1002/rob.21896.

**[8]** Reinhardt, D., Gryte, K. and Arne Johansen, T. (2022). Modeling of the Skywalker X8 Fixed-Wing UAV: Flight Tests and System Identification. *2022 International Conference on Unmanned Aircraft Systems (ICUAS)*. doi: https://doi.org/10.1109/icuas54217.2022.9836104.

**[9]** Nicolosi, F., Corcione, S., Trifari, V. and De Marco, A. (2021). Design and Optimization of a Large Turboprop Aircraft. *Aerospace*, 8(5), p.132.

**[10]** Mohammadi Farhadi, R., Kortunov, V., Molchanov, A. and Solianyk, T. (2018). ESTIMATION OF THE LATERAL AERODYNAMIC COEFFICIENTS FOR SKYWALKER X8 FLYING WING FROM REAL FLIGHT-TEST DATA. *Acta Polytechnica*, 58(2), p.77. doi: https://doi.org/10.14311/ap.2018.58.0077.

**[11]** Moe, A. and Pyone, A. (n.d.). *Design and Construction of Hand-Launched Flying Wing RC Aircraft peer-review under responsibility of International Journal of Research Publications (IJRP.ORG)*.

**[12]** Holla, S. and Jain, S. (2017). Design and CFD Analysis of a Fixed Wing for an Unmanned Aerial Vehicle. *International Journal of Latest Engineering Research and Applications (IJLERA)*, 02(07), pp.77–85.

**[13]** Gryte, K., Hann, R., Alam, M., Roháč, J., Johansen, A. and Fossen, T. (n.d.). *Aerodynamic modeling of the Skywalker X8 Fixed-Wing Unmanned Aerial Vehicle*.

**[14]** Feng, Z., Gan, T., Feng, K., Khouli, F., Elsayed, M. and Nitzsche, F. (n.d.). *Development and Optimization of Flight Dynamics, Control Laws and Avionics System for a UAV with a Multi-scale Optimized Blended Wing Body Configuration*.

**[15]** Castroviejo, D., Van Der Stichelen, M. and Hendrick, P. (n.d.). Distributed electric propulsion with blended wing-body for fixed-wing UAVs. doi: https://doi.org/10.13009/EUCASS2022-4724.

**[16]** M. Kozek and A. Schirrer, Modeling and Control for a Blended Wing Body Aircraft, New York: Springer, 2014.

**[17]** R. H. Liebeck, M. A. Page and B. K. Rawdon, "Blended-wing-body subsonic commercial transport," in 36th AIAA Aerospace Sciences Meeting & Exhibit, 1998.

**[18]** M. Saucez, "The Handling Qualities Resolution of a Flying Wing Configuration," Ph.D Thesis, University of Toulouse, Toulouse, France, 2013.

**[19]** Karthik M A , Srinivasan K , Srujan S , Subhash Holla H S , Suraj Jain M 5,. (n.d.). Design and CFD Analysis of a Fixed Wing for an Unmanned Aerial Vehicle, 2017

**[20]** K. Gryte, "High angle of attack landing of an unmanned aerial vehicle," Master's thesis, Department of Engineering Cybernetics, Norwegian University of Science and Technology, Trondheim, Norway, 2015

**[21]** Z. F. T. Gan, J. K. Feng, F. Khouli, M. S. ElSayed, and F. Nitzsche, "Development and optimization of flight dynamics, control laws and avionics system for a uav with a multi-scale optimized blended wing body configuration," CASI Aero'19, 2019

**[23]** G. Licitra, A. Burger, P. Williams, R. Ruiterkamp, and M. Diehl, ¨ "Aerodynamic model identification of an autonomous aircraft for airborne wind energy," Optimal Control Applications and Methods, 2019.

**[24]** B. M. Simmons, H. G. McClelland, and C. A. Woolsey, "Nonlinear model identification methodology for small, fixed-wing, unmanned aircraft," Journal of Aircraft, vol. 56, no. 3, pp. 1056–1067, 2019. [Online]. Available: https://doi.org/10.2514/1.C035160

**[25]** J. J. Matt, S. G. Hagerott, B. C. Svoboda, H. Chao, and H. P. Flanagan, "Frequency domain system identification of a small flying-wing uas," in AIAA SCITECH 2022 Forum, 2022, p. 2407.

**[26]** help.solidworks.com. (n.d.). *SolidWorks Web Help*. [online] Available at: https://help.solidworks.com/.

**[27]** Smith, J., Su, J., Liu, C. and Chen, W.-H. (2017). Disturbance Observer Based Control with Anti-Windup Applied to a Small Fixed Wing UAV for Disturbance Rejection. *Journal of Intelligent & Robotic Systems*, 88(2-4), pp.329–346. doi: https://doi.org/10.1007/s10846-017-0534-5.

**[28]** www.ansys.com. (n.d.). Engineering Simulation & 3D Design Software | Ansys. [online] Available at: https://www.ansys.com.

**[29]** Durmus, Seyhun, et al. "Investigation of Wing Forms through Mass and Wing Area Chart Experimental Investigation of Performance Enhancement on Cooling Channels by Using Turbulators View Project Designing and Producing an UAV Inspired from the Black-Headed

Gull with Biomimetic Ways View Project Investigation of Wing Forms through Mass and Wing Area Chart." *Cilt*, vol. 11, no. 2, 2022, pp. 107–112, https://doi.org/10.46810/tdfd.1084396. Accessed 27 Apr. 2023.

**[30]** Witcher, Kenneth, et al. "Aerodynamic Analysis of Low-Speed Wing Design Using Taguchi L9 Orthogonal Array." *MATEC Web of Conferences*, vol. 151, 2018, p. 04005, https://doi.org/10.1051/matecconf/201815104005. Accessed 27 Apr. 2023.

**[31]** Koyuncuoglu, H. and He, P. (n.d.). *CFD-Based Multi-Component Aerodynamic Optimization for Wing Propeller Coupling*.

**[32]** Muruga, J. and Jeyan, L. (2019). THE LOW-SPEED AERODYNAMIC ANALYSIS OF SEGMENTAL WING PROFILE. *Article in Proceedings of the Institution of Mechanical Engineers Part G Journal of Aerospace Engineering*. doi: https://doi.org/10.24247/ijmperdaug2019135.

**[33]** Smith, J., Su, J., Liu, C. and Chen, W.-H. (2017). Disturbance Observer Based Control with Anti-Windup Applied to a Small Fixed Wing UAV for Disturbance Rejection. *Journal of Intelligent & Robotic Systems*, 88(2-4), pp.329–346. doi: https://doi.org/10.1007/s10846-017-0534-5.

**[34]** Zhao, J., Fan, Z., Chang, M. and Wang, G. (2022a). Coupling Effects on Distributed Multi-Propeller Channel Wing at Low-Speed Condition. *Energies*, 15(15), p.5352. doi: https://doi.org/10.3390/en15155352.

**[35]** www.eaa.org. (n.d.). *Weight & Balance: Weighing and measuring your safety*. [online] Available at: https://www.eaa.org/eaa/aircraft-building/builderresources/while-youre-building/building-articles/weight-and-balance/weight-and-balance#:~:text=Weight%20and%20balance%20is%20so%20critical%20to%20the [Accessed 30 Apr. 2023].

**[36]** TecQuipment. (2018). *SUBSONIC WIND TUNNEL 305 mm - SUBSONIC WIND TUNNEL 305 mm*. [online] Available at: https://www.tecquipment.com/subsonic-wind-tunnel-300mm.

**[37]** SafetyCulture. (2023). *Factor of Safety*. [online] Available at: https://safetyculture.com/topics/factor-of-safety/.

[38] Blogs.nasa.gov. (n.d.). *Factors of Safety – Wayne Hale's Blog*. [online] Available at: https://blogs.nasa.gov/waynehalesblog/2008/12/16/post_1229459081779/.